공학박사학위논문

Evaluation of Chloride Penetration into Cementitious Materials Using Short-Term Ponding Test

단기 침지 실험(Short-Term Ponding Test)을 이용한 시멘트 계 재료 내부로의 염소이온 침투 평가

2014년 8월

서울대학교 대학원

건설환경공학부

박 병 선

Evaluation of Chloride Penetration into Cementitious Materials Using Short-Term Ponding Test

단기 침지 실험(**Short-Term Ponding Test**)을 이용한
시멘트 계 재료 내부로의 염소이온 침투 평가

지도 교수 조 재 열

이 논문을 공학박사 학위논문으로 제출함
2014 년 6 월

서울대학교 대학원
건설환경공학부
박 병 선

박병선의 공학박사 학위논문을 인준함
2014 년 6 월

위 원 장 _____ (인)

부위원장 _____ (인)

위 원 _____ (인)

위 원 _____ (인)

위 원 _____ (인)

ABSTRACT

Evaluation of Chloride Penetration into Cementitious Materials Using Short-Term Ponding Test

Park, Byoungsun
Department of Civil & Environmental Engineering
The Graduate School
Seoul National University

Many concrete structures have recently been constructed on the seashore. In structures exposed to seawater, chloride ion is transported through concrete by various mechanisms such as diffusion, and results in the corrosion of embedded steel in concrete structures. So, the chloride transport rate in concrete needs to be predicted, to prevent degradation of the durability of concrete structures in service life. The chloride ion diffusion coefficient is a crucial factor in evaluating the chloride transport rate in concrete. A number of test methods have been developed to measure the chloride ion diffusion coefficient of concrete. Most of these test methods require excessive test duration, or else represent a chloride ion penetration mechanism that does not adequately reflect chloride ion transport in real concrete structures.

This thesis proposes a new test method to determine the chloride ion

diffusion coefficient, while avoiding these deficiencies. The proposed method incorporates a new analytical approach that determines the diffusion coefficient from the change of chloride ion concentration in a source solution. The proposed method can be called a short-term ponding test, in comparison with traditional long-term immersion tests. Validation tests were performed to verify the developed test method and mathematical model. It was found that the proposed test method and analytical solution could estimate the chloride ion diffusion coefficient within two weeks. The short-term ponding test was validated by comparison with a long-term immersion test, and an electrical migration-diffusion test (CTH test). Both the long-term immersion test and the short-term ponding test produced similar results, but the CTH test results differed significantly. This indicates that the short-term ponding test is a time-efficient and realistic method that reflects the actual marine environment.

Numerical analysis was performed to verify assumptions in the mathematical model of the short-term ponding test. Pdepe function, one of the Matlab functions, was used to calculate the chloride concentration with time in the source solution, solving the governing equation of the mathematical model. The effects of concrete age and concentration change in the source solution on the diffusion coefficient in the short-term ponding test were verified. From numerical analysis, it can be concluded that in the short-term ponding test, the effect of concrete age and concentration change in the source solution can be neglected. The chloride binding isotherm of the short-term ponding test was also verified. Inverse analysis was adopted to estimate the effective diffusion coefficient, and Freundlich binding isotherm coefficients. It was found that the linear binding isotherm could be assumed in the short-term

ponding test.

Keywords : Chloride ion, Diffusion coefficient, Durability design, Numerical analysis, Short-term ponding test

Student Number : 2008-21030

TABLE OF CONTENTS

LIST OF TABLES

LIST OF FIGURES

NOTATIONS

Symbol	Description and definition	Unit
A	Cross-sectional area	
$A_{concrete}$	Cross-sectional area of concrete	m^2
c	Free chloride concentration in general, by volume of solution	$kg_{Cl}/m^3_{solution}$
c_0	A solvent concentration	$kg_{Cl}/m^3_{solution}$
c_1	Coefficient of general solution in Laplace Transform	
c_2	Coefficient of general solution in Laplace Transform	
c_{up}	Free chloride concentration in a bulk solution or an upstream diffusion cell	$kg_{Cl}/m^3_{solution}$
c_{down}	Free chloride concentration in a downstream diffusion cell	$kg_{Cl}/m^3_{solution}$
c_b	Bound chloride concentration by volume of material	kg_{Cl}/m^3
c_{cell}	Free chloride concentration in cell	$kg_{Cl}/m^3_{solution}$
c_i	Initial concentration of free chloride in pore solution	$kg_{Cl}/m^3_{solution}$
c_{ini}	Initial concentration of free chloride in	
c^s	Free chloride concentration in fully saturated solution	$kg_{Cl}/m^3_{solution}$
c_{sol}	Free chloride concentration in source solution	$kg_{Cl}/m^3_{solution}$

c_t	Total chloride concentration by volume of material	kg_{Cl}/m^3
C_b	Content of bound chloride by weight of material	$kg_{Cl}/kg_{material}$
C_{bm}	The monolayer adsorption capacity of bound chloride	$kg_{Cl}/kg_{material}$
C_t	Content of total chloride by weight of material	$kg_{Cl}/kg_{material}$
C_{ti}	Initial content of total chloride in concrete	$kg_{Cl}/kg_{material}$
C_{ts}	Content of total chloride at the surface of concrete	$kg_{Cl}/kg_{material}$
D	Diffusion coefficient	m^2/s
D_0	Intrinsic diffusion coefficient	m_x^2/s
D_{app}	Apparent diffusion coefficient	m_x^2/s
D_{ave}	Average diffusion coefficient	m_x^2/s
D_{con}	Diffusion coefficient varied by concentration	m_x^2/s
D_{ini}	Diffusion coefficient at initial concentration	m_x^2/s
D_{end}	Diffusion coefficient at end concentration	m_x^2/s
D_{LT}	Apparent diffusion coefficient obtained from long-term immersion test	m_x^2/s
D_{nssd}	Diffusion coefficient obtained from a non-steady-state diffusion test	m_x^2/s
D_{nssm}	Diffusion coefficient obtained from a non-steady-state migration test	m_x^2/s
D_{ssd}	Diffusion coefficient obtained from a steady-state diffusion test	m_x^2/s

D_{ssm}	Diffusion coefficient obtained from a steady-state migration test	m_x^2/s
D_{ST}	Apparent diffusion coefficient obtained from short-term ponding test	m_x^2/s
$D_{ref,c}$	A reference diffusion coefficient at reference concentration	m_x^2/s
$D_{ref,t}$	A reference diffusion coefficient at reference time	m_x^2/s
f	A friction coefficient	
$f_b(T)$	The temperature-dependent coefficient	
E_b	The activation energy for chloride binding	J/mol
F	Faraday constant, $F = 9.648 \times 10^4\ J/(V \cdot mol)$	$J/(V \cdot mol)$
h	The height of source solution	mm
J_c	Flux of chloride ions through a unit are of solution	$\frac{kg_{Cl}}{m_{solution}^2 \cdot s}$
$J_{concrete}$	Flux of chloride ions through a unit are of concrete	$\frac{kg_{Cl}}{m_{concrete}^2 \cdot s}$
K	Experimental constant	
K_b	The chloride binding factor in a non-steady state migration test	$m_{solution}^3/kg_{gel}$
L	Thickness of specimen	m
m	A coefficient that expresses the rate of change of the diffusion coefficient	
n	The number of specimens	
R	Gas constant, $R = 8.314\ J/(mol \cdot K)$	$J/(mol \cdot K)$

t	Time variable	s
T_0	Reference temperature	K
T	Absolute temperature	K
t_{eff}	Age of concrete	s
t_p	A coefficient of the confidence level	
t_{ref}	The reference time	s
U	Electrical potential difference	V
V_{cell}	Volume of cell	m^3
V_{cell1}	Volume of cell1	m^3
W_{gel}	The hydrate gel content in concrete	$kg_{gel}/m^3_{concrete}$
x	Distance variable	m
z	Ion valence	
z_-	The valence of anions	
α_{LN}	An experimental constant of linear isotherm	
α_{FD}	An experimental coefficient of Freundlich isotherm	
α_{BET}	Difference of adsorption energy between first layer and the higher layer	
β_{LN}	An experimental constant of linear isotherm	
β_{LM}	An experimental constant of Langmuir isotherm	
β_{FD}	An experimental coefficient of Freundlich isotherm	
β_{BET}	Difference of adsorption energy between second layer and the higher layers	

β_v	
μ	The mean value of diffusion coefficients
$\bar{\mu}$	The expectation value of the diffusion coefficient
σ	The standard deviation of diffusion coefficient
θ	Porosity
Ω	Domain
ψ_i	Shape function

1. Introduction

1.1 Research background

Although concrete is known to be a very durable material, degradation by physical and chemical factors is inevitable as time goes by. This deterioration may threaten the functionality and safety of concrete structures during their service lives. In particular, durability design against chloride ion penetration should be performed for concrete structures exposed to the marine environment, since steel corrosion caused by chloride ion penetration into concrete is a major cause of the degradation in durability of concrete structures. Fig. 1.1 shows steel corrosion in concrete structures by chloride ion penetration.

Figure 1.1 Deal pier, Kent: Corrosion protection of steel support structure and reinstatement of concrete encasement

Steel corrosion by chloride ion penetration degrades the performance of steel, and decreases the bearing capacity of concrete structures. Also, since the volume of corroded steel increases, cracks are induced surrounding the steel in concrete. In severe cases, concrete cover can delaminate from structures. Fig. 1.2 shows a schematic presentation of damage induced by steel corrosion.

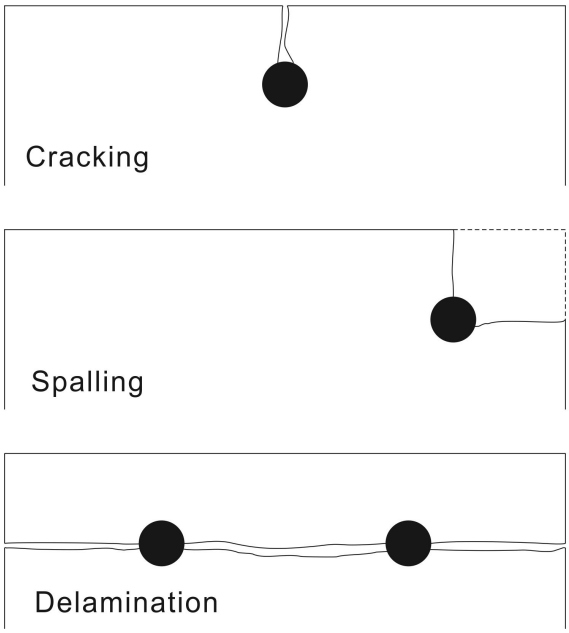

Figure 1.2 Schematic presentation damage to concrete structures induced by steel corrosion

Fig. 1.3 shows the collapse under its own weight, without warning, of Ynys-y-gwas bridge in Port Talbot, caused by the corrosion of prestressing steel strands. Because steel corrosion by chloride ion penetration occurs throughout the whole surface of structures exposed to seawater, once steel corrosion occurs, it is costly to repair. So, it is very important to predict the

chloride ion penetration through concrete, to prevent steel corrosion during the target lifetime of structures.

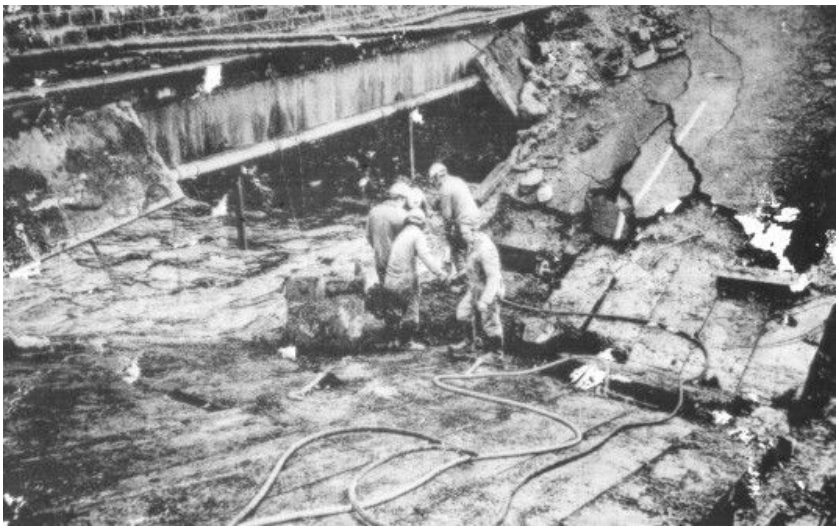

Figure 1.3 Collapse of Ynys-y-gwas bridge in Port Talbot

Chloride transport in concrete is a complicated mechanism that involves ion diffusion, capillary suction, and advection; but ion diffusion governs chloride transport in the case of fully saturated concrete pores. In this case, the chloride penetration rate can be evaluated using the chloride ion diffusion coefficient. For this reason, a number of methodologies based on mathematical models have been proposed to predict chloride ion penetration. In these methods, the diffusion coefficient is considered to be a major parameter affecting chloride ion transport in concrete. So, it is important to accurately evaluate the chloride ion diffusion coefficient, to predict the chloride ion penetration in concrete. Currently, two kinds of test methods, long-term immersion tests and electrical migration-diffusion tests, are the

most widely used means of determining the diffusion coefficient. Diffusion coefficients obtained from the long-term immersion test and CTH test are adopted in the durability design methods of ACI Life 365 and Duracrete, respectively. ACI Life 365 has been designated by ACI Committee 365 for durability design for chloride penetration into concrete. Duracrete is one of the study results from performance-based design performed in Europe. Eq. (1.1) and Eq. (1.2) show the relative chloride concentration in concrete represented by ACI Life 365 and Duracrete.

$$C(x,t) = \left(C_i + (C_s - C_i) \cdot \left[1 - \mathrm{erf}\left(\frac{x}{2\sqrt{D_{nss} \cdot t}} \right) \right] \right) \tag{1.1}$$

$$C(x,t) = \left(C_i + (C_{s,\Delta x} - C_i) \cdot \left[1 - \mathrm{erf}\left(\frac{x - \Delta x}{2\sqrt{D_{nssm} \cdot t}} \right) \right] \right) \tag{1.2}$$

However, a long-term immersion test requires such a long period of time to determine the chloride ion diffusion coefficient that it may have changed in the interim, due to the cement hydration process. The electrical migration-diffusion test can determine the chloride ion diffusion coefficient in a short period of time; nevertheless, the diffusion coefficient obtained by the electrical migration-diffusion test is not the same as the actual value, because the chloride ion penetration mechanism simulated in the electrical migration-diffusion test is different from that which occurs in real concrete structures. So, a new test method is developed in this study to determine the chloride ion diffusion coefficient, while avoiding those deficiencies. Verification was performed using validation tests and numerical analysis.

1.2 Objectives and Scope

The main objective of this study is to develop a novel test method to determine the chloride ion diffusion coefficient of cementitious materials. The new test method is a kind of rapid ponding test, in which the chloride ion diffusion coefficient can be obtained using only the known change in the chloride ion concentration of the source solution. To calculate the diffusion coefficient using the short-term ponding test proposed in this study, a new mathematical model is presented, in which the decrease in chloride ion concentration in the source solution during the test is considered a boundary condition. The validation test was performed for mortar and concrete specimens with two W/C ratios, and two different initial chloride ion concentrations. In addition, the diffusion coefficient determined using the proposed method was compared with those from the long-term immersion and electrical migration-diffusion tests. Finally, assumptions in developed the mathematical model were verified by numerical analysis. The validation of assumptions in the mathematical model was verified by investigating the effect of assumptions on the apparent diffusion coefficients obtained from the developed test.

1.3 Outline

Chapter 1 shows the introduction to this thesis, and includes a general description of the objectives, scope, and outline of the thesis.

Chapter 2 presents a literature review of the theoretical background. It includes the mechanisms of steel corrosion, and of chloride penetration, the theory of chloride ion binding, and a description of other test methods to determine the chloride ion diffusion coefficient.

Chapter 3 describes a novel test method that was developed in this thesis to determine the chloride ion diffusion coefficient. It includes a test set-up, and mathematical model of the new test method.

Chapter 4 discusses the validation test performed in this thesis. It includes the test program, test results, and discussions.

Chapter 5 presents the numerical analysis for verification of the mathematical model developed in this thesis. It includes verification of the assumptions in the mathematical model.

Chapter 6 summarizes the concluding remarks.

2. Theoretical Backgrounds

2.1 Mechanisms of steel corrosion

Embedded steel in concrete is surrounded with a thin passivity layer of oxide which strongly adheres to the underlying steel and gives it complete protection from corrosion. So, steel in concrete doesn't corrode when the passivity layer remains. However, when alkalinity and pH in concrete pore is decreased, the passivity layer begins to be destroyed. In this case, steel embedded in concrete begins to corrode. Fig 2.1 shows mechanisms of steel corrosion in concrete

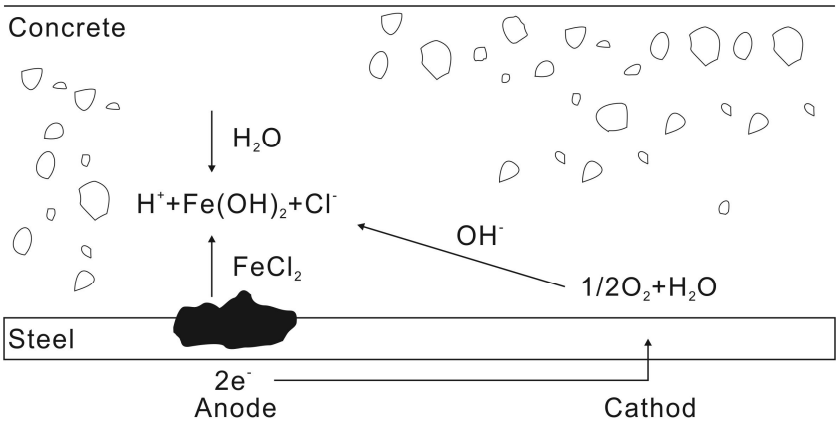

Figure 2.1 Electrochemical reaction after destruction of passivity layer in steel

From Fig 2.1, it can be shown that the steel corrosion is induced by electrochemical reaction after destruction of passivity layer. The mechanism is

described as follows.

Anodic reaction:

$$Fe \rightarrow Fe^{2+} + 2e^{-} \tag{2.1}$$

Cathodic reaction:

$$2e^{-} + H_2O + \frac{1}{2}O_2 \rightarrow 2\left(OH\right)^{-} \tag{2.2}$$

Overall reaction:

$$Fe + H_2O + \frac{1}{2}O_2 \rightarrow Fe\left(OH\right)_2 \tag{2.3}$$

In these mechanisms, steel and pore solution are act as a metallic conductor and an electrolyte each. The released electrons from anode move towards the cathode through steel and ferrous ions released from anode are dissolved in the pore solution. Dissolved ferrous ions are combined with hydroxyl ions released from cathode, and ferrous hydroxide is made in anode.

From Fig. 2.1, it is shown that steel corrosion occurs in anode, the detailed mechanisms of steel corrosion are represented as follows.

$$Fe \rightarrow Fe^{2+} + 2e^{-} \tag{2.4}$$

$$Fe^{2+} + 2Cl^{-} \rightarrow FeCl_2 \tag{2.5}$$

$$FeCl_2 + 2H_2O \rightarrow Fe\left(OH\right)_2 + 2H^{+} + 2Cl^{-} \tag{2.6}$$

In this process, chloride ions form ferrous chloride with ferrous, and released after forming ferrous hydroxide. Therefore chloride ions act as catalysts to form ferrous hydroxide in this process. Hydrogen ion released from anode decrease pH of anode, and this reaction makes pH in the vicinity of steel decreases. So, the released chloride ions continue to react with ferrous ions and breaks the passivity layer, which means that one the concentration of chloride ion exceeds thresholds level, the destructing of the passivity layer doesn't stop. So, it is needed to evaluate chloride penetration rate in concrete to predict initiation time of steel corrosion.

2.2 Chloride binding

2.2.1 Generals

Chloride ions penetrated into concrete are divided into two kinds of ions. Some are called as free chloride ions that move freely through pore solution in concrete. The others are called binding chloride ions that are captured by cement hydrate in concrete and remain precipitates in pore solution. Chloride ions in pore solution are bound with cement hydrate in concrete by two kinds of mechanisms. One is chemical reaction between chloride ion and cement hydrate, resulting in chloride containing compound. The compound is Friedel's salt ($Ca_3Al_2O_6 \bullet CaCl_2 \bullet 10H_2O$). The other mechanism is physical adsorption. Chloride ions in pore solution are adsorbed onto the Calcium silicate hydrate (CSH) gel, and remain stationary in gel. Since binding chloride ions are combined with cement hydrate in concrete, only free

chloride ions affect steel corrosion. In this reason, it is important to know binding chloride concentration in penetrated chloride ions into concrete for prediction of degradation of durability design of concrete structures exposed to marine environment. Binding isotherm is used to express the concentration relationship between binding chloride ions and free chloride ions. In next section, chloride binding isotherms presented by former researcher are represented.

2.2.2 Binding isotherms

2.2.2.1 Linear isotherm

In early research of chloride binding isotherm, chloride binding concentration was suggested as linear isotherm with free chloride concentration. Concentration of binding equation was expressed by Eq. (2.7)

$$C_b = \alpha_{LN} \cdot c \tag{2.7}$$

where, α_{LN} is an experimental constant of linear isotherm. Using this equation, concentration of binding concentration could be calculated easily, but, it has been shown that the equation suggested by Tuuti doesn't fit with test results by studies presented by other researchers. So, linear isotherm has been modified incorporating y-intercept as shown in Eq. (2.8).

$$C_b = \alpha_{LN} \cdot c + \beta_{LN} \tag{2.8}$$

The test results presented by former researchers were fit with Eq. (2.8) well, but there was a problem that it cannot explain the physical meaning of y-intercept(β_{LN}). According to Eq. (2.8), binding chloride ions are extent though there were no free chloride ions. So, to explain binding isotherm, non-linear binding isotherm was proposed by other researchers.

2.2.2.2 Langmuir isotherm

In most cases, the relationship between binding and free chloride ions is non-linear. To explain non-linear relationship between binding chloride ions and free chloride ions, Pereira and Hegedus have suggested Langmuir isotherm which is used to describe substance adsorption as shown in Eq. (2.9).

$$C_b = \frac{C_{bm}\beta_{LM}c}{1+\beta_{LM}c} \tag{2.9}$$

Where C_{bm} means the monolayer adsorption capacity and can be taken as constant. According to study reported by Tang, Langmuir isotherm fits with test results fairly well when free chloride concentrations are higher than 0.05 mol/l.

2.2.2.3 Freundlich isotherm

Tang has reported that Freundlich isotherm is suitable to explain relationship between binding chloride ion and free chloride ion in a range of free chloride concentrations from 0.01 to 1 mol/l. This range has covered the free chloride concentration in sea water. A Freundlich isotherm is expressed as Eq. (2.10).

$$C_b = \alpha_{FD} \cdot c^{\beta_{FD}} \tag{2.10}$$

where, α_{FD} and β_{FD} are experimental coefficients obtained from a regression analysis using test results. So, there are no physical meanings of coefficients.

2.2.2.4 BET isotherm

Xu has reported a modified Brunauer-Emmett-Teller (BET) isotherm to express relationship between binding chloride ion and free chloride ion. This model was proposed from BET theory that explains physical adsorption between solid and gas molecules. The BET isotherm is expressed as Eq. (2.11)

$$\frac{C_b}{C_{bm}} = \frac{\alpha_{BET}\dfrac{c}{c^s}\left[1-\left(1-\beta_{BET}\right)\left(1-\beta_{BET}\dfrac{c}{c^s}\right)^2\right]}{\beta_{BET}\left(1-\beta_{BET}\dfrac{c}{c^s}\right)\left[1-\beta_{BET}\dfrac{c}{c^s}+\alpha_{BET}\dfrac{c}{c^s}\left(1-\beta_{BET}\dfrac{c}{c^s}+\dfrac{c}{c^s}\right)\right]} \tag{2.11}$$

where, c^s is free chloride concentration in fully saturated solution. α_{BET} is difference of adsorption energy between first layer and the higher layers. β_{BET} is difference of adsorption energy between second layer and the higher layers.

2.2.3 Factors affecting chloride binding

Chloride binding is affected by combined influences of several factors such as composition substance of concrete and external environmental conditions. So, many studies have been reported to explain effect of factors on chloride binding. The main parameters influencing chloride binding are W/C ratio, cement contents, cement and binder type, temperature, ageing source solution type. In this thesis, the effect of cement and binder type, temperature, seawater has been represented.

2.2.3.1 Effect of binder

The quantity of C_3A and C_4AF, the compositions of cement hydrate, affect chloride binding, since chloride ion in pore solution is reacted with C_3A and C_4AF to form Friedels salts. So, if quantity of C_3A and C_4AF in binder increases, quantity of chloride binding increases. Fly Ash contains pozzolanic materials differently from OPC. Containing pozzolanic materials can increase the binding ability of chloride according to former studies. Also some researchers have reported that hydrate of slag cement reveals the formation of finer hydrated products resulting in a higher physical binding capacity.

2.2.3.2 Effect of temperature

Some researchers have reported that quantity of chloride binding decrease with increase of temperature. The relationship between temperature and quantity of binding chloride can be expressed as shown in Eq. (2.12) incorporating the Arrhenius law.

$$f_b(T) = \frac{C_b}{C_b\big|_{T_0}} = e^{\frac{E_b}{R}\left(\frac{1}{T}-\frac{1}{T_0}\right)} \tag{2.12}$$

where, $f_b(T)$ and E_b can be called the temperature-dependent coefficient and the activation energy for chloride binding, respectively. This phenomenon can be explained by physical and chemical mechanisms. For a physical mechanism, increase of temperature results in increasing the thermal vibration of chloride ions, so adsorption between chloride ions and cement hydrate is disrupted. For a chemical reaction, although an increase of temperature increases the rate of the reaction, it may also increase the solubility of the Friedel's salt, resulting in more chloride ions free at the equilibrium.

2.2.3.3 Effect of variety ions existed in seawater

Seawater contains a total of approximately 35.5 g/L dissolved salts. Due to the variety ions included in the seawater such as, sulfate ions, magnesium ions and carbonate ions, complicated reactions between ions in seawater and

cement hydrate of concrete occur in pore solution. So, the effect of variety ions in seawater except Na^+ and Cl^- on chloride binding is needed to consider. Because these ions react with cement hydrate to produce precipitate and change the pore structures, effect of these reactions have to be considered to predict chloride binding in concrete. Weerdt (2012) has investigated effect of these ions to changes in the phase assemblage of concrete.

Sulfate ions penetrated into concrete react with calcium hydroxide in pore solution to produce gypsum. This process is described as Eq. (2.13).

$$SO_4^{2-} + Ca(OH)_2 \rightarrow CaSO_4 + 2OH^- \tag{2.13}$$

Gypsum produced by Eq. (2.13) reacts with C_3A and H_2O to produce ettringite formation. Some researchers have reported that the formation of ettringite leads to an increase in the solid volume which might lead to expansion and cracking. However, Mehta has reported that the increase of volume by sulfate in seawater is limited, since the concentration in seawater is not enough to lead to cracks.

$$C_3A + CaSO_4 + 32H_2O \rightarrow C_3A \cdot 3CaSO_4 \cdot 32H_2O \tag{2.14}$$

At temperatures below 15 ^oC, sulphate attack by seawater on concrete containing calcium carbonate for example as limestone filler, or combined sulphate carbonate attack by seawater on concrete can result in thaumasite formation. Thaumasite is non-cementing reaction product which can result in disintegration of the cement hydrate. The reaction is expressed as Eq. (2.15).

$$CaCO_3 + CaSO_4 + C-S-H + H \rightarrow$$
$$CaCO_3 \cdot CaSO_4 \cdot CaSiO_3 \cdot 15H_2O \quad (thaumatsite) \tag{2.15}$$

In the normal pH range seawater is under saturated with respect to brucite ($Mg(OH)_2$), but brucite will precipitate when seawater meets a high pH, such as one of the pore silution of concrete typical concrete (pH 12.5-13.5). Eq. (2.16) shows the reaction of Mg^{2+} with calcium hydroxide causing the precipitation of brucite.

$$Mg^{2+} + Ca(OH)_2 \rightarrow Mg(OH)_2 + Ca^{2+} \tag{2.16}$$

Bruenfeld and Newman have reported that 30 μm depth of brucite has been produced at concrete surface exposed to seawater for four days. This precipitate can act as insoluble film to prevent from penetrating chloride ion. But the film can be easily destructed by various effect since the thickness of the film is thin and might be produced incomplete due to low concentration of $Ca(OH)_2$.

Figs. 2.2 and 2.3 show diagram of compound produced by seawater and NaCl solution. This result was represented by Weerdts research (2012). In Fig. 2.2, it can be shown that thaumasite, brucite are produced by seawater differently with NaCl solution. Also, Friedel's salts is decreased in seawater compared to that of NaCl solution and ettringite increases when concrete was exposed to seawater by comparing with that of NaCl solution. So, in case of chloride ion penetration from seawater, reactions between ions in seawater

such as SO^{2+} and cement hydrate are needed to be considered to predict quantity of binding chloride ion.

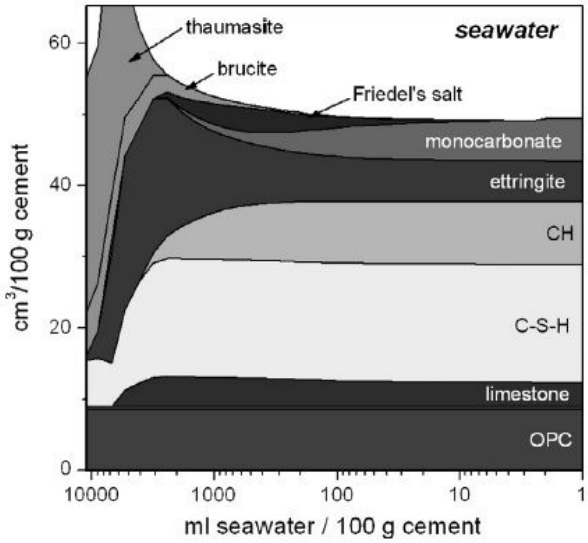

Figure 2.2 GEMS results for 100g coment (OPC + limestone) in contact with an increasing amount of sea water (Weerdt, 2012)

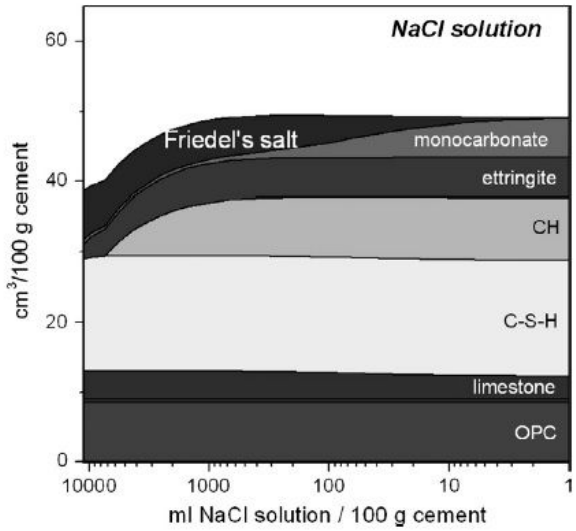

Figure 2.3 GEMS results for 100 g cement (OPC + limestone) in contact with

an increasing amount of NaCl solution (165 g NaCl/l) (Weerdt, 2012)

2.3 Chloride ion diffusion in concrete

2.3.1 General

Chloride ion transport in concrete is very complicated mechanism containing such as capillary suction, advection and ion diffusion. But, if concrete pore is fully saturated, chloride ion transport is governed by ion diffusion. Diffusion means phenomenon that substance moves from high concentration to low concentration by concentration gradient. In concrete, only free chloride ion moves by diffusion and concentration gradient means concentration gradient of free chloride ion.

2.3.2 Diffusion in concrete

Generally, diffusion is expressed by Fick's 1st law. Assuming x-direction penetration, Fick's 1st law is described as Eq. (2.17).

$$J = -D_{ssd} \frac{\partial c}{\partial x} \tag{2.17}$$

where, J is chloride ion flux, D_{ssd} is diffusion coefficient, c is chloride concentration, x is distance. Fick's 1st law can be adopted to explain in steady-state condition diffusion which concentration gradient is

constant with time and distance. But concentration gradient is changed with time and distance in concrete due to effects of chloride binding and variety chemical reactions. This is called non-steady-state condition, and non-steady-state diffusion can be expressed by Fick's 2nd law. Fick's 2nd law can be expressed by Eq. (2.18).

$$\frac{\partial c}{\partial t} = -\frac{\partial}{\partial x}(J) = -\frac{\partial}{\partial x}\left(-D_{ssd}\frac{\partial c}{\partial x}\right) \tag{2.18}$$

In Eq. (2.18), if diffusion coefficient (D) is constant, Eq. (2.18) can be rewritten by Eq. (2.19).

$$\frac{\partial c}{\partial t} = D_{ssd}\frac{\partial^2 c}{\partial x^2} \tag{2.19}$$

In non-steady-state conditions, concentration gradient is changed by time (t) and distance (x). Eq. (2.19) can be rewritten as Eq. (2.20) by dividing chloride concentration into free chloride ion and binding chloride ion.

$$\frac{\partial c_t}{\partial t} = \frac{\partial(\theta c + c_b)}{\partial t} = \left(\theta + \frac{\partial c_b}{\partial c}\right)\frac{\partial c}{\partial t} = D_{ssd}\frac{\partial^2 c}{\partial x^2} \tag{2.20}$$

Eq. (2.20) can be expressed by Eq. (2.21), expressing the formation of Fick's 2nd law.

$$\frac{\partial c}{\partial t} = \frac{D_{ssd}}{\left(\theta + \frac{\partial c_b}{\partial c}\right)} \frac{\partial^2 c}{\partial x^2} = D_{app} \frac{\partial^2 c}{\partial x^2} \tag{2.21}$$

In Eq. (2.21), $\partial c_b / \partial c$ is concentration ratio between free chloride ion and binding chloride ion and is changed in non-steady-state condition. So, apparent diffusion coefficient (D_{app}) is changed by free chloride concentration. It is needed assumption that apparent diffusion coefficient (D_{app}) is constant during test to calculate apparent diffusion coefficient by analytical solution.

2.4 Existing test methods

2.4.1 Long-term immersion test (Conventional immersion test)

The long-term immersion test is a fundamental and widely-used method to determine the chloride ion diffusion coefficient in concrete. In this test, a concrete specimen is immersed in a chloride ion solution for 35-90 days, and the diffusion coefficient is calculated from the chloride ion concentration measured along the depth of the immersed specimen. The long-term immersion test is standardized as AASHTO T 259 and NT Build 443. NT Build 443 is used in the Life-365 Service Life Prediction Model for predicting the service life and life-cycle costs of reinforced concrete exposed to chlorides.

Fig. 2.4 shows the experimental arrangement of AASHTO T 259. The side of concrete specimen is sealed by epoxy to prevent a chloride leak. 3 %

NaCl solution is used as source solution of test. In this test, diffusion coefficient is determined using chloride ion concentration profile in concrete after 90 days immersion.

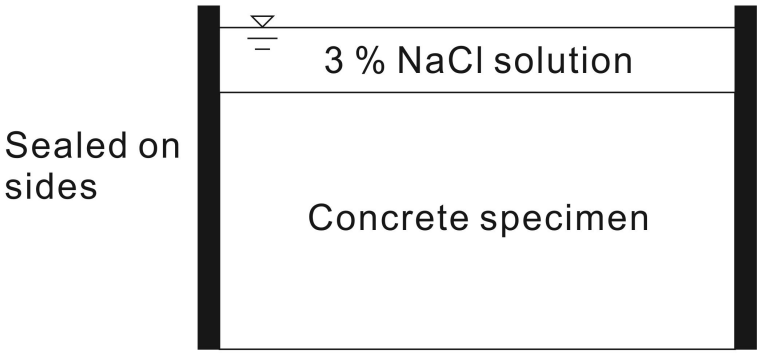

Figure 2.4 Experimental arrangement of AASHTO T 259

NT Build 443 was developed to overcome shortcomings of AASHTO T 259. Fig. 2.5 shows the experimental arrangement of NT build 443. In NT Build 443, the concrete specimen is immersed in 18 % chloride concentration solution after sealing all surfaces except one surface. Chloride ion concentration profile is measured from immersed specimen by depth.

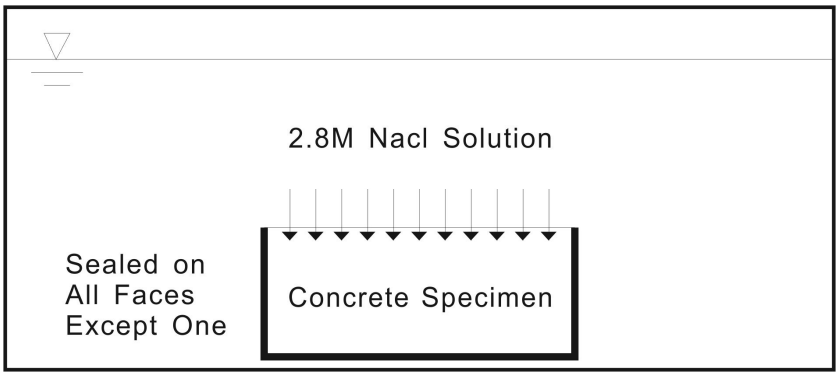

Figure 2.5 Experimental arrangement of NT Build 443

The chloride ion penetration mechanism in the long-term immersion test can be explained using Fick's 2nd law as follows.

$$\frac{\partial C_t}{\partial t} = D_{LT} \frac{\partial^2 C_t}{\partial x^2} \tag{2.22}$$

where, C_t is the total chloride ion concentration (mass% of sample), t is time (s), x is distance (m), D_{LT} is the apparent diffusion coefficient determined during the long-term immersion test and is defined as Eq. (2.23).

$$D_{LT} = \frac{D_{ssd}}{\theta + \frac{\partial C_b}{\partial c}} \tag{2.23}$$

where D_{ssd}, θ, C_b, and c are the steady-state diffusion coefficient , porosity, concentration of binding chloride ion, and concentration of free chloride ion, respectively. Assuming that the concentration ratio between the free chloride ion and the binding chloride ion, the surface chloride ion concentration and the diffusion coefficient are constant, the chloride ion diffusion coefficient can be calculated using Eq. (2.24).

$$C_t = C_{ts} - \left(C_{ts} - C_{ti}\right) \cdot erf\left(\frac{x}{2\sqrt{D_{LT} \cdot t}}\right) \tag{2.24}$$

where C_{ts} is the surface chloride ion concentration (mass% of sample) and C_{ti} is the initial chloride ion concentration (mass% of sample) in concrete. Finally, the diffusion coefficient is obtained by curve-fitting between the total concentration profile measured along the depth of the immersed concrete and the concentration profile estimated by Eq. (2.24).

Although the long-term immersion test simulates the real chloride ion penetration mechanism, it requires a long immersion time of at least 35-90 days. Because the pore structure of the concrete varies during the hydration process, the long test period affects the diffusion coefficient. Therefore, the assumption, employed in the derivation of Eq. (2.24), that the diffusion coefficient is constant throughout the test is not in accord with the actual test conditions. Besides, the complicated procedure to measure the chloride ion concentration in concrete, consisting of collecting concrete powder along the depth and extracting chloride ions from the powder, is a deficiency of the long-term immersion test. So, a new test method to determine the chloride ion diffusion coefficient while avoiding these deficiencies is needed.

2.4.2 Diffusion cell test

In the diffusion cell test, a thin concrete specimen is subjected to two kinds of cell, upstream cell and downstream cell. Upstream cell contains chloride solution and downstream cell contains distilled water. In this test, chloride ion transports from upstream cell to downstream cell through concrete specimen by concentration gradient as time passed. Fig. 2.6 shows the experimental arrangement of diffusion cell test.

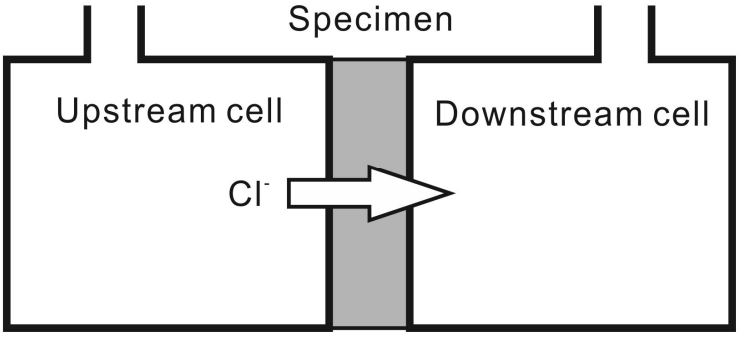

Figure 2.6 Experimental arrangement of diffusion cell test

Chloride concentration gradient in downstream cell becomes constant after reaching steady-state condition. Diffusion coefficient can be estimated by Eq. (2.25) substituting concentration change measured by time in cells.

$$D_{ssd} = J_{concrete} \cdot \frac{L}{c_{up} - c_{down}} = \frac{V_{cell\,1} \cdot \Delta c_{down}}{A_{concrete} \cdot \Delta t} \cdot \frac{L}{c_{up} - c_{down}} \tag{2.25}$$

In diffusion cell test, chloride ion penetration is described by Fick's 1st law. So, diffusion coefficient obtained from diffusion cell test is effective diffusion coefficient that doesn't consider effect of chloride binding. So, diffusion coefficient obtained from diffusion cell test has different mathematical meaning with that of long-term immersion test such as NT Build 443. Also, since it is needed to wait to reach steady-state condition in diffusion cell test, it takes long time to determine diffusion coefficient. Since only a thin specimen can be used in diffusion cell test, it is difficult to

estimate diffusion coefficient of concrete specimen containing coarse aggregate

2.4.3 Rapid Chloride Permeability Test (RCPT)

In the RCPT, 50 × 100 mm concrete specimen is subjected to two kinds of reservoir. And a 60 V DC voltage for 6 hours is applied on two reservoirs to accelerate chloride ion penetration during test as shown in Fig. 2.7. RCPT is adopted by ASTM and standardized as AASHTO T 277(ASTM C1202).

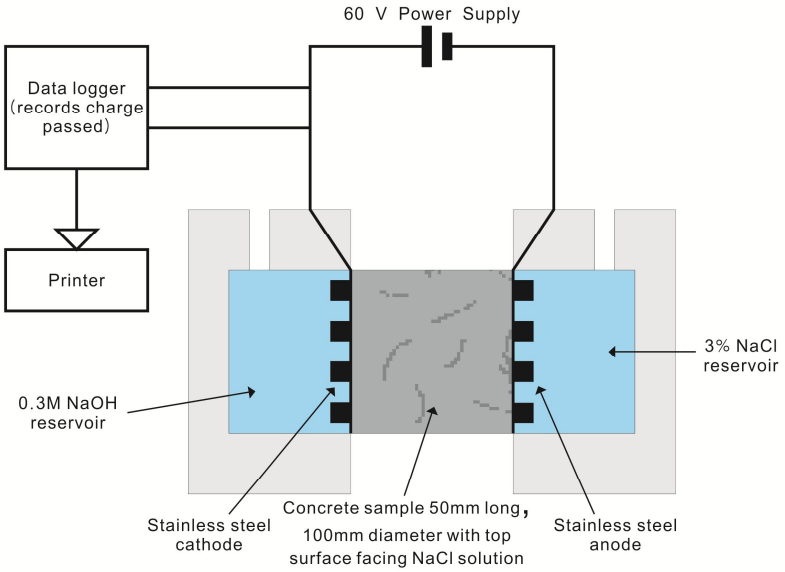

Figure 2.7 Experimental arrangement of RCPT

One reservoir contains a 0.3M NaOH solution and the other reservoir

contains 3 % NaCl solution. The total charge passed through concrete specimen is measured during test, and this is used to evaluate diffusivity of specimen using Table 2.1. Using RCPT, it can just be known chloride penetrability of concrete, but diffusion coefficient can't be estimated.

Table 2.1 RCPT ratings for chloride ion penetration (ASTM C1202)

Charge Passed (Coulombs)	Chloride Ion Penetrability
> 4,000	High
2,000 – 4,000	Moderate
1,000 – 2,000	Low
100 – 1,000	Very Low
< 100	Negligible

2.4.4 Electrical-migration test (NT Build 355)

Electrical-migration test has similar experimental arrangement with diffusion cell test. But, since an electrical field is applied to accelerate chloride ion penetration in electrical-migration test, diffusion coefficient can be determined shorter than diffusion cell test. The experimental arrangement is shown as Fig. 2.8.

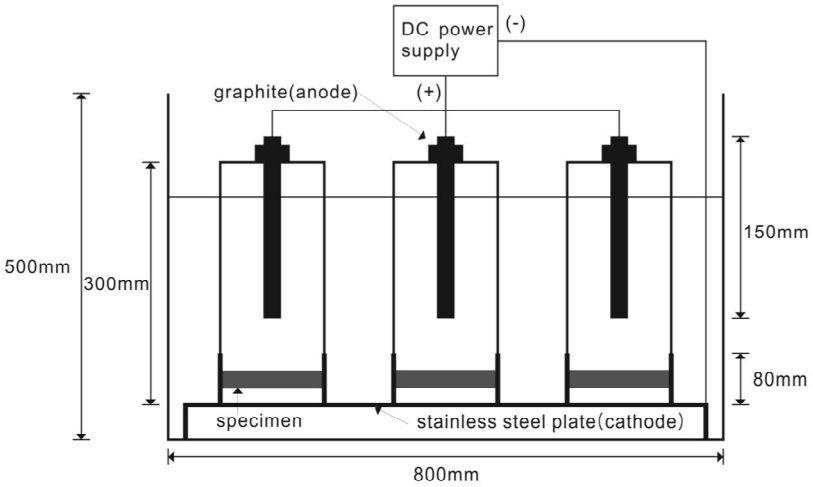

Figure 2.8 Typical experimental arrangement of electrical-migration test

Chloride ion is transported from cathode solution to anode solution in electrical-migration test. So, the chloride concentration in anode solution increases by time. Likewise diffusion cell test, to determine diffusion coefficient, chloride concentration change in anode solution is measured by time after reaching steady-state conditions. In electrical-migration test, chloride ion transport is governed by Nernst-Planck equation. (See Eq. (2.26))

$$J = -D_{ssm}\left(\frac{\partial c}{\partial x} - \frac{zFU}{RTL}c\right) \tag{2.26}$$

When voltage is applied, chloride ion penetration is governed by migration. So, diffusion term of Nernst-Planck equation can be neglected and the equation can be rewritten as Eq. (2.27).

$$J = -D_{ssm} \frac{zFU}{RTL} c \tag{2.27}$$

Eq. (2.27) can be rearranged by Eq. (2.28) and diffusion coefficient can be estimated by Eq. (2.28) using chloride ion concentration change in anode solution.

$$D_{ssm} = -J \cdot \frac{RTL}{zFUc_0} \cdot \frac{V_{cell} \cdot \Delta c_{cell}}{A_{concrete} \cdot \Delta t} \tag{2.28}$$

Because chloride ion penetration mechanism in electrical-migration test is different from that of real structure exposed to seawater, diffusion coefficient obtained from electrical-migration test has different meaning from that of real structures. So, diffusion coefficient obtained from electrical migration test can only be used to evaluate diffusivity of concrete and is difficult to be applied to design of structure.

2.4.5 Chalmers Tekniska Hogskola (CTH) test

CTH test proposed by Tang and Nilsson is most widely used to estimate diffusion coefficient among migration tests. The experimental arrangement is shown as Fig. 2.9.

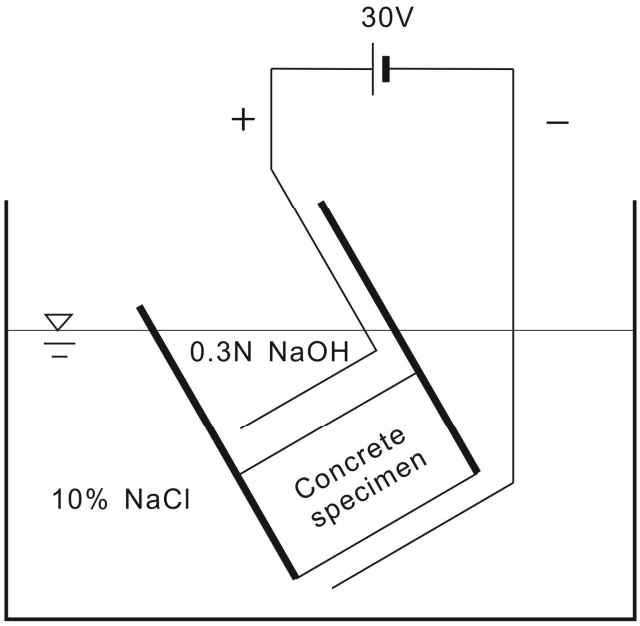

Figure 2.9 Experimental arrangement of CTH test

The chloride ion diffusion coefficient can be obtained within 6-96 hours using the CTH test. The CTH test is standardized as NT Build 492, and is used as a standard test method in the European durability test specifications, Duracrete. Because chloride ions are transported by ion migration as well as by diffusion in the CTH test, chloride ion transport is represented by the Nernst-Plank equation.

$$\frac{\partial c}{\partial t} = D_{nssm}\left(\frac{\partial^2 c}{\partial x^2} - \frac{zFU}{RTL}\cdot\frac{\partial c}{\partial x}\right) \tag{2.29}$$

where z is ion valence, F is Faraday constant, U is electrical

potential difference, R is gas constant, T is temperature, and L is thickness of the specimen. The parameter D_{nssm} is the apparent diffusion coefficient determined by the CTH test and is defined as in Eq. (2.30).

$$D_{nssm} = \frac{D_{ssm}}{\theta + K_b \cdot W_{gel}} \tag{2.30}$$

where D_{ssm} is the steady-state migration coefficient, θ is porosity, K_b is the chloride binding factor in a non-steady state migration test, and W_{gel} is the hydrate gel content in concrete. The value $K_b \cdot W_{gel}$ represents the quantity of chloride ion binding and is assumed to be a constant determined by the cement hydration ratio and the chloride ion concentration in the source solution, irrespective of the chloride ion concentration in concrete.

Although the CTH test is the most widely used due to its short test duration and relatively simple test procedure, some researchers have pointed out deficiencies of the test caused by its reliance on electrical equipment. Chloride ion transport in concrete is affected by electrochemical reactions between various ions in the pore solution. When the chloride ions are accelerated by an electrical field, the resulting electrochemical reactions, such as ion interactions and ion binding, might be different from those in an actual marine environment. This phenomenon might lead to an incorrect estimation of the chloride ion diffusion coefficient.

Some research also indicates that the mathematical model for chloride

ion binding in the CTH test is problematic. In mathematical model of CTH test, chloride concentration profile by CTH test has been presented as Fig. 2.10. But, some specimens had different chloride concentration profiles from proposed profile by the mathematical model of the CTH test like Fig. 2.11.

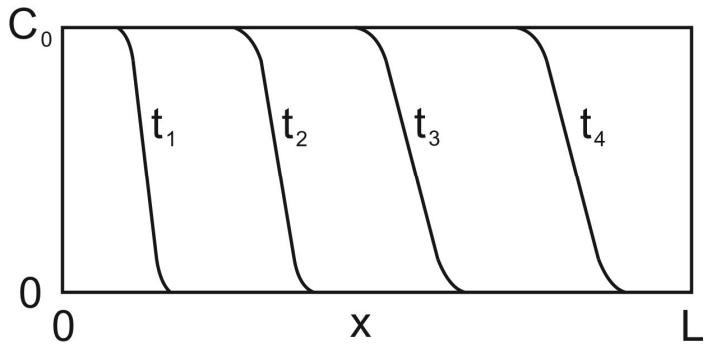

Figure 2.10 Theoretical concentration profiles of chloride ions under the action of an external electrical field (Tang, 1996)

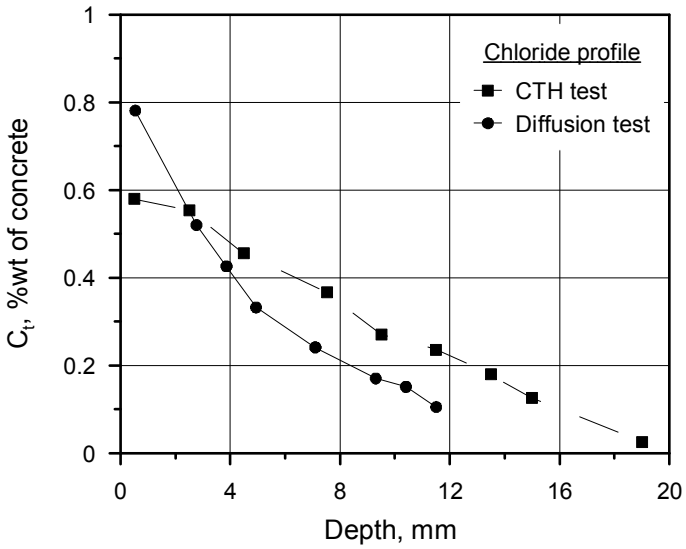

Figure 2.11 Experimental total chloride profile in concrete after the migration and diffusion tests for concrete (Spiesz, 2012)

Spiesz proposed that this phenomenon is due to the non-equilibrium caused by the limited mass transfer between the pore solution and the cement hydrate. While the binding reaction between the chloride ions and the cement hydrate is sustained for 7-14 days, the CTH test is commonly completed within 24 hours. This time difference means that chloride ion transport occurs with imperfect binding reactions. Consequently, the chloride ion penetration mechanism in the mathematical model used in CTH would be different from reality. This deficiency may cause error in the estimation of the diffusion coefficient.

2.4.6 Resistivity Technique

To determine diffusivity of chloride ion in concrete using conductivity of concrete specimen, resistivity technique is developed. Resistivity is the electrical resistance of a substance and the inverse of conductivity. Formation Factor is used to determine the conductivity of a concrete specimen. The Formation Factor (FF) can be expressed as shown in Eq. (2.31)

$$FF = \frac{\sigma}{\sigma_0} \tag{2.31}$$

where, σ is the conductivity of the concrete specimen and σ_0 is the conductivity of the pore solution in concrete. In resistivity technique, the diffusion coefficient in concrete is determined using Formation Factor incorporating the pore structures in concrete as shown in Eq. (2.32)

$$FF = \frac{D}{D_0} \tag{2.32}$$

where, D is the diffusion coefficient of concrete and D_0 is the diffusion coefficient of chloride in the pore solution.

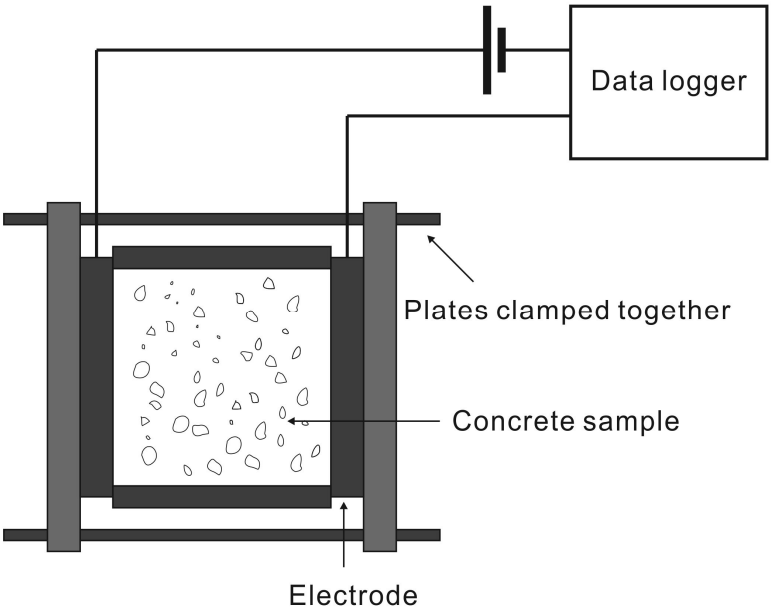

Figure 2.12 DC resistivity measuring test

Fig. 2.12 shows the experimental arrangement of direct current (DC) resistivity measuring test. In this test, the determination of DC resistance is calculated from the Eq. (2.33), in case of constant polarization at different applied voltages.

$$R_{RT} = \frac{E_{a1}I_2 - E_{a2}I_1}{I_1 - I_2} \tag{2.33}$$

where, R_{RT} is the resistance, E_{a1} and E_{a2} are the two applied voltages and I_1 and I_2 are the relevant currents. Resistivity can be calculated by Eq. (2.34).

$$\rho = R_{RT}\frac{A}{L} \tag{2.34}$$

where, ρ is the resistivity, A is the area and L is the length.

2.4.7 Pressure penetration techniques

Pressure penetration technique is one of accelerated test methods to evaluate chloride penetration in concrete. In this method, chloride ions in source solution are penetrated into concrete by pressure. In this method, chloride ion is penetrated into concrete by convection and diffusion. So, governing equation can be expressed by the Eq. (2.35)

$$\frac{\partial c}{\partial t} = D\frac{\partial^2 c}{\partial x^2} - \bar{v}\frac{\partial c}{\partial x} \tag{2.35}$$

In Eq. (2.35), $\bar{v}$ is the average flow transport rate and can be expressed as Eq. (2.36).

$$\bar{v} = -\frac{k_{HP}}{\theta}\frac{\partial h_{presure}}{\partial x} \tag{2.36}$$

where, k_{HP} is the hydraulic permeability, θ is the porosity and $h_{pressure}$ is the applied pressure head. The experimental arrangement of pressure penetration is technique is similar with that of water permeability test using pressure cell. The experimental arrangement is expressed as Fig. 2.13.

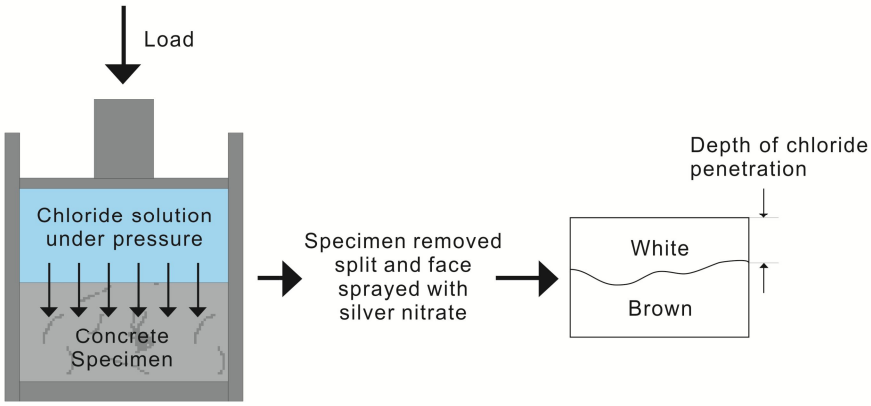

Figure 2.13 The experimental arrangement of pressure penetration technique

After setting of saturated concrete in cell, a source solution is poured and a pressure is applied on source solution to penetrate chloride ion into concrete. Applied pressure is maintained during test period. After test, chloride penetration depth is measured using colorimetric method incorporating $AgNO_3$. From test k_{HP}, hydraulic permeability, is determined by Eq. (2.37).

$$k_{HP} = \frac{\theta \cdot L \cdot x_d}{t \cdot h_{pressure}} \tag{2.37}$$

Table 2.2 Summary of test methods to determine diffusion coefficient

Method	Penetration mechanisms	Meaning of diffusion coefficient	Test duration	Standardization	Remarks
Long-term immersion test	Non-steady-state Diffusion	$D_{LT} = \frac{D_{ssd}}{\theta + \frac{\partial C_b}{\partial c}}$	35 ~ 90 days	AASHTO T 259 NT Build 443	- requires long testing period - difficult to measure chloride profile in concrete - adopted in ACI Life 365
Diffusion cell test	Steady-state Diffusion	D_{ssd}	Depends on specimen	-	- requires long testing period - applicable to very thin specimens
RCPT	Non-steady-state Migration	-	6 hours	AASHTO T 277 ASTM C1202	- penetration occurs due to migration - not useful for determination of diffusion coefficient
Electrical migration test	Non-steady-state Migration	D_{ssm}	Depends on specimen and voltage	NT Build 355	- requires relatively short testing period - penetration occurs due to migration - diffusion coefficient varies with specimen thickness and voltage
CTH test	Non-steady-state Migration	$D_{nssm} = \frac{D_{ssm}}{\theta + K_b \cdot W_{gel}}$	6 ~ 96 hours	NT Build 492	- penetration occurs due to migration - adopted in Duracrete
Resistivity technique	Non-steady-state Migration	-	30 Minutes	-	- requires very short testing period - specific conductivity depends on solution concentration - not easy to measure conductivity
Pressure penetration technique	Non-steady-state Convention and Diffusion	-	Depends on specimen and pressure	-	- requires relatively long testing period - not useful for determination of diffusion coefficient

3. Short-Term Ponding Test

3.1 Experimental set-up

Fig. 3.1 shows the test setup for the short-term ponding test proposed in this study. In the long-term immersion test, it is assumed that the concentration of the source solution in which a specimen is totally immersed remains constant during the test. On the other hand, in the short-term ponding test proposed in this study, a small container filled with solution is placed on the surface of a specimen disc (Fig. 3.2). This scheme allows the chloride ions to penetrate into the specimen in one direction, and the concentration of the solution in the container continuously decreases

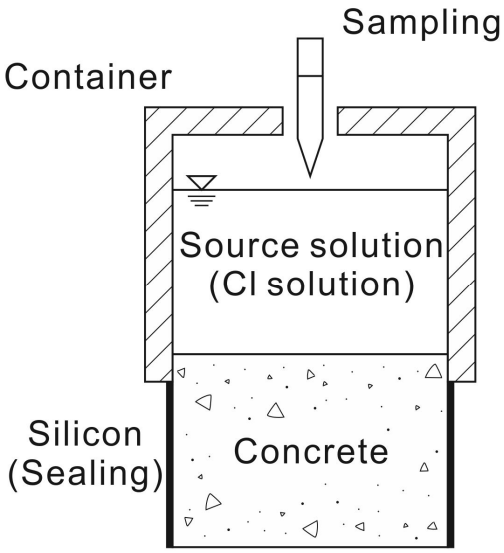

Figure 3.1 Test setup for short-term ponding test

Figure 3.2 The photo of the test setup

Fig. 3.3 shows the transport mechanism of chloride ions in the short-term ponding test. As seen in Fig. 3.3(a), the actual test configuration uses a specimen of finite height, but for the purposes of the mathematical modeling, the specimen height is assumed to be infinite (Fig. 3.3(b)). In this method, chloride ion in source solution penetrates into concrete during test, so chloride concentration in source solution. Chloride penetrates into concrete by one-dimension. Consequently, diffusion coefficient can be estimated by mathematical model applying chloride concentration change in source solution.

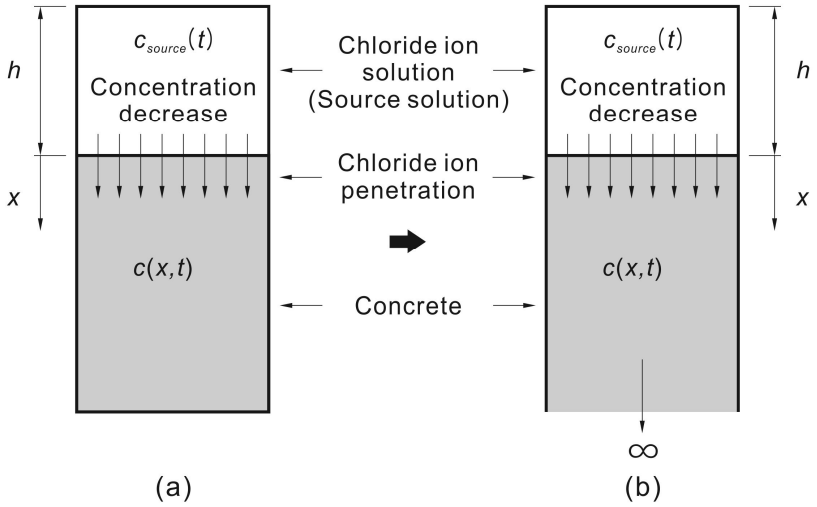

Figure 3.3 Conceptual diagram of mathematical models: (a) finite-depth model, (b) infinite-depth model

In this mathematical model, some assumptions have been used to determine diffusion coefficient simply by analytical solution. First, total volume of source solution is constant during test. To maintain total volume of solution, vaporization of source solution was prevented using a lid as shown in Fig 3.2. Second, concrete pore is fully saturated. So, the test was performed using fully saturated specimen by guideline of NT Build 443. Third, specimen must have enough depth that chloride ion can't reach during test. This assumption was verified in Chapter 5 by numerical analysis.

3.2 Mathematical model

3.2.1 Governing equation

Chloride ions are transported by a complicated mechanism: combined diffusion and advection by capillary water transport. However, if a concrete pore is fully saturated, chloride penetration can be expressed solely as non-steady state diffusion. Hence, in this ponding test, chloride ion transport can also be expressed by Fick's 2nd law.

$$\frac{\partial(\theta c)}{\partial t}+\frac{\partial c_b}{\partial t}=\frac{\partial}{\partial x}\left(D_{ssd}\frac{\partial c}{\partial x}\right) \tag{3.1}$$

The second term on the right side of Eq. (3.1) denotes the sink term of chloride ions due to chloride ion binding. If θ and the diffusion coefficient in Eq. (3.1) are assumed to be constant in concrete (or mortar) and at a certain time, respectively, Eq. (3.1) can be rewritten as:

$$\frac{\partial c}{\partial t}\left(\theta+\frac{\partial c_b}{\partial c}\right)=D_{ssd}\frac{\partial^2 c}{\partial x^2} \tag{3.2}$$

Eq. (3.2) is rewritten in the form of Fick's 2nd law, incorporating the apparent diffusion coefficient (D_{ST}), and becomes a governing equation of the mathematical model presented in this study.

$$\frac{\partial c}{\partial t} = \frac{D_{ssd}}{\theta + \frac{\partial c_b}{\partial c}} \frac{\partial^2 c}{\partial x^2} = D_{ST} \frac{\partial^2 c}{\partial x^2} \tag{3.3}$$

where

$$D_{ST} = \frac{D_{ssd}}{\theta + \frac{\partial c_b}{\partial c}} \tag{3.4}$$

In Eq. (3.4), $\partial c_b / \partial c$ is the concentration ratio between the free and the binding chloride ion. Generally, binding chloride concentration has non-linear relationship with free chloride concentration, but, in this mathematical model, linear binding isotherm was assumed. And diffusion coefficient of specimen was assumed to be constant during test irrespective of change of concrete age and change of concentration in source solution. These assumptions were verified in Chapter 5. In our mathematical model, the chloride ion concentration in concrete is expressed in terms of its concentration in the pore solution because the chloride ion concentration change in the source solution is intended to be the main variable used to calculate the diffusion coefficient. Note that the apparent diffusion coefficient D_{ST} in Eq. (3.3) has the same meaning as D_{LT} in Eq. (2.3) for the long-term immersion test since Fick's 2nd law was employed in both mathematical models to explain the chloride ion transport.

3.2.2 Initial and Boundary conditions

Because chloride binding is non-linear and occurs in non-equilibrium conditions for a long period of time, the term $\partial C_b / \partial c$ in Eq. (3.4), the concentration ratio of free-to-binding chloride ion, can hardly be considered to be constant. In the short-term ponding test, however, the chloride ion concentration of the external solution is relatively lower than it is in other tests, such as NT Build 492 and 443 tests. Tuutti reported that the relationship between free and binding chlorides in his experiment, which involved a chloride concentration lower than 20 g/l, was linear compared with the relationship measured in higher concentrations. So, linear and equilibrium condition binding is assumed to be linear for the simplification of the calculation in this study. Under this assumption, the governing equation expressed in Eq. (3.3) can be solved for the following initial and boundary conditions.

The initial condition is

$$c(x,0) = 0 \qquad 0 < x < \infty \tag{3.5}$$

In Fig. 3.3(b), if the total volume of the source solution is constant and chloride ions are only transported through concrete, the chloride ion concentration change in the source solution can be expressed as Eqs. (3.6) and (3.7).

$$c(0,t) = c_{sol}(t) \tag{3.6}$$

$$c_{sol}(t) = c_{sol}(0) - \frac{A}{V}\int_0^t \left[J_{concrete}\right]_{x=0} dx \qquad 0 < t \tag{3.7}$$

where c_{sol} is the chloride ion concentration in the source solution ($kg_{Cl}/m^3_{solution}$), is the contact area between the source solution and the concrete (m^2), V is the total volume of the source solution (m^3), and J is the flux of chloride ions in concrete ($kg_{Cl}/m^2_{concrete} \cdot s$).

A decreased chloride ion concentration in the source solution can be expressed as a function of flux into the concrete surface and exposure time to the solution. Flux at concrete surface can be defined as a product of the diffusion coefficient and concentration gradient at concrete surface (Eq. (3.8)).

$$J_{concrete}\Big|_{x=0} = -D_{ST}\frac{\partial c}{\partial x}\Big|_{x=0} \tag{3.8}$$

In this mathematical model, Eq. (3.7) was employed as a boundary condition. The infinite-point condition is

$$c(\infty, t) = 0 \qquad 0 < t \tag{3.9}$$

In this equation, it is difficult to assume that the diffusion coefficient remains constant during the short-term ponding test because the test takes 14 days to determine the chloride diffusion coefficient; however, this duration is still shorter than that of the long-term immersion test. Thus, for practical

reasons, it is assumed that the diffusion coefficient is constant during the short-term ponding test in this study.

3.2.3 Analytical solution

In this section, mathematical formulation of analytical solution is presented. Governing equation(Eq. (3.3)) can be expressed as following equation applying the Laplace transform and initial condition Eq. (3.5). The chloride diffusion coefficient is assumed to be constant with time.

$$L\left(c\left(x,t\right)\right)=\bar{c}\left(x,s\right) \tag{3.10}$$

$$L\left(\frac{\partial c}{\partial t}\right)=s\cdot L\left(c\right)-c\left(x,0\right)=s\cdot\bar{c} \tag{3.11}$$

$$s\cdot\bar{c}=D_{ST}\cdot\frac{\partial^2\bar{c}}{\partial x^2} \tag{3.12}$$

The general solution of Laplace transform expression can be expressed as follow.

$$\bar{c}=c_1\cdot exp\left(\sqrt{\frac{s}{D_{ST}}}\cdot x\right)+c_2\cdot exp\left(-\sqrt{\frac{s}{D_{ST}}}\cdot x\right) \tag{3.13}$$

Initial and boundary conditions can be expressed as following equation applying the Laplace transform.

$$L\left(c\left(x,0\right)\right)=\bar{c}\left(x,0\right)=0 \qquad 0<x<\infty \tag{3.14}$$

$$L\left(c\left(\infty,t\right)\right)=\bar{c}\left(\infty,s\right)=0 \qquad 0<s \tag{3.15}$$

$$L\left(c\left(0,t\right)\right)=L\left(c_{sol}\left(t\right)\right)=\overline{c_{sol}}\left(s\right) \qquad 0<s \tag{3.16}$$

General solution (Eq. (3.13)) is expressed simply as Eq. (3.17) incorporating infinite-point condition (3.15).

$$\bar{c}=c_2\cdot exp\left(-\sqrt{\frac{s}{D_{ST}}}\cdot x\right);c_1=0 \tag{3.17}$$

Eq. (3.17) can be rewritten as Eq. (3.18) by inserting Eq. (3.16).

$$\bar{c}=\overline{c_{sol}}\left(s\right)\cdot exp\left(-\sqrt{\frac{s}{D_{ST}}}\cdot x\right);c_2=\overline{c_{sol}}\left(s\right) \tag{3.18}$$

Eq. (3.18) for the distance (x) derivative is as Eq. (3.19).

$$\frac{d\bar{c}}{dx}=-\sqrt{\frac{s}{D_{ST}}}\cdot\overline{c_{sol}}\left(s\right)\cdot exp\left(-\sqrt{\frac{s}{D_{ST}}}\cdot x\right) \tag{3.19}$$

Eq. (3.19) is rewritten as Eq. (3.20) at $x=0$.

$$\left.\frac{d\overline{c}}{dx}\right|_{x=0} = -\sqrt{\frac{s}{D_{ST}}} \cdot \overline{c_{sol}}(s) \tag{3.20}$$

Boundary condition (Eq. (3.7)) for the time derivative is as follow.

$$\frac{dc_{sol}(t)}{dt} = \frac{D_{ST}}{h} \cdot \left.\frac{dc}{dx}\right|_{x=0} \tag{3.21}$$

Eq. (3.21) can be expressed as follow applying the Laplace transform.

$$L\left(\frac{\partial c_{sol}}{\partial t}\right) = s \cdot \overline{c_{sol}}(s) - c_{sol}(0) \tag{3.22}$$

$$L\left(\frac{A \cdot D_{ST}}{V} \cdot \left.\frac{dc}{dx}\right|_{x=0}\right) = \frac{A \cdot D_{ST}}{V} \cdot \left.\frac{d\overline{c}}{dx}\right|_{x=0} \tag{3.23}$$

$$s \cdot \overline{c_{sol}}(s) - c_{sol}(0) = \frac{A \cdot D_{ST}}{V} \cdot \left.\frac{d\overline{c}}{dx}\right|_{x=0} \tag{3.24}$$

Eq. (3.24) can be rearranged as Eq. (3.25) by inserting Eq. (3.21).

$$\overline{c_{sol}}(s) = \frac{c_{sol}(0)}{\left(s + \frac{D_{ST}}{h} \cdot \sqrt{\frac{s}{D_{ST}}}\right)} = \frac{c_{sol}(0)}{\left(s + \frac{\sqrt{D_{ST} \cdot s}}{h}\right)} \tag{3.25}$$

Consequently, Applying Laplace transform to Eq. (3.25), an analytical solution of the mathematical model can be obtained as Eq. (3.26).

$$c_{sol}(t) = c_{sol}(0) \cdot \exp\left[D_{ST} \cdot \frac{t}{h^2} \right] \cdot erfc\left[\left(D_{ST} \cdot \frac{t}{h^2} \right)^{\frac{1}{2}} \right] \tag{3.26}$$

where h is the height of source solution. In the analytical solution, the concentration change in the source solution is affected by the diffusion coefficient and time. Fig. 3.4 shows the concentration change in the source solution calculated with the analytical solution for several diffusion coefficients. This shows that the chloride ion diffusion coefficient can be calculated by curve-fitting to minimize the difference between the measured and analytically obtained variations of chloride ion concentrations in the source solution.

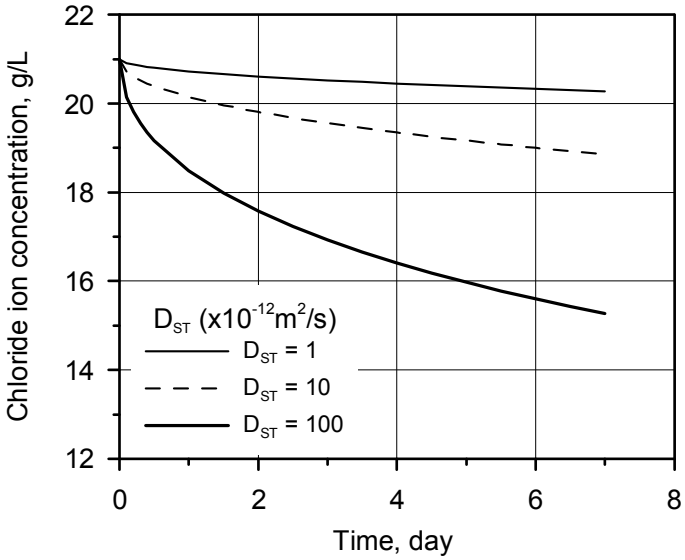

Figure 3.4 Concentration change in source solution calculated using analytical solution

From Fig. 3.4, it can be shown that chloride concentration in source solution is changed rapidly within 7 days. So, using this method, diffusion coefficient can be determined for short duration. And, in short-term ponding test, chloride concentration in marine environments can be used as concentration in source solution to determine diffusion coefficient differently from other tests such as CTH test and long-term immersion test. Because chloride concentration in source solution affects chloride penetration mechanisms and chloride binding, it can be very strong point of short-term ponding test that chloride concentration of seawater can be used as concentration in source solution to penetrate into concrete.

4. Validation Tests and Discussions

4.1 Experimental conditions

A series of tests was performed to validate the mathematical model and test method proposed in this study. The total volume of source solution, test duration and number of measurement has been determined using test results.

4.1.1 Materials and mixture proportions

The test equipment consisted of a mold, concentration measurement instrument, source solution, and cement-based specimen. A cylindrical container with a lid was made of acryl to maintain the source solution at a constant total volume. A 50 mm-thick cement-based specimen was assembled with the acrylic container using silicon to prevent leakage of the source solution. After curing for 28 days, all surfaces were sealed with silicon to isolate them from the surrounding environment, except for the top surface which was exposed to the solution (See Fig. 3.2).

In this test, mortar and concrete specimens were used. Two kinds of mortar (cement:sand = 1:2) in which the water-cement ratios were 0.45 and 0.6 were used. The mix proportion of concrete is shown in Table 4.1. OPC and river sand were used as a binder and fine aggregate, respectively. And 13 mm gravel was used as coarse aggregate. In HC specimen, high range water reducing admixture and Silica Fume were used. The test specimens, cast in a

100 mm by 200 mm cylinder mold for mortar and cast in a 150 mm by 300 mm cylinder mold for concrete, were cured in air at 20 ˚C for 24 hours and were demolded then cured in saturated lime water at 20 ˚C for 28 days. To eliminate the effects of bleeding or aggregate segregation, three 50 mm-thick cylindrical disc specimens were taken from the middle part of the cylinder after cutting both sides away.

Table 4.1 The mix proportion of concrete

	Water (kg/m^3)	Cement (kg/m^3)	Silica Fume (kg/m^3)	Sand (kg/m^3)	Gravel (kg/m^3)	Adx (kg/m^3)	Strength (Mpa)
NC	204	509	-	756	803	-	40
HC	160	590	51.3	604	868	6.41	80

In this study, for saturation of the specimens, the samples used in the short-term ponding test, NT Build 443, and NT Build 492 were immersed in $Ca(OH)_2$ solution until the mass stabilizes under surface-dry conditions, following the guidelines of NT Build 443.

4.1.2 Source solution

The validation test considered source solutions of NaCl with two chloride ion concentrations. The chloride ion concentration in common seawater was represented by 21 g/L, while 2.1 g/L was used to confirm the effect of chloride ion concentration on estimating the diffusion coefficient. The height of the source solution was determined to be 15 mm, and the volume of the source solution was approximately 106 ml for mortar and 177

ml for concrete to acquire a distinct change in concentration. The atmospheric temperature was maintained at 20 ˚C.

4.1.3 Measurement of chloride concentration in source solution

To measure the chloride ion concentration in solution, samples were collected at 0, 1, 2, 3, 4, 5, 7, 10, and 14 days. To minimize the total volume change of the source solution, the sampling size was chosen to be 0.5 ml, which was as small as possible. Because the sample volume was very small, the sample was diluted with distilled water to increase the quantity ten-fold. The chloride ion concentration was measured by an ion-selective electrode using a potential difference in samples. Ion-selective electrode used in this study was made by Thermo Scientific. The model name is Orion 9617 BNWP. This ion selective electrode can measure concentration 1 M to 5×10^{-5} M of range, 2 to 12 of pH range, 10 to 100 ^{o}C of temperature range. Reproducibility of measurement is ± 2 % and minimum 3 mL sample in 50 mL beaker is needed to measure chloride concentration.

Chloride concentration was measured by concentration slope that is determined using 100 ppm and 1,000 ppm reference solutions. Fig. 4.1 shows method of concentration measurement in source solution.

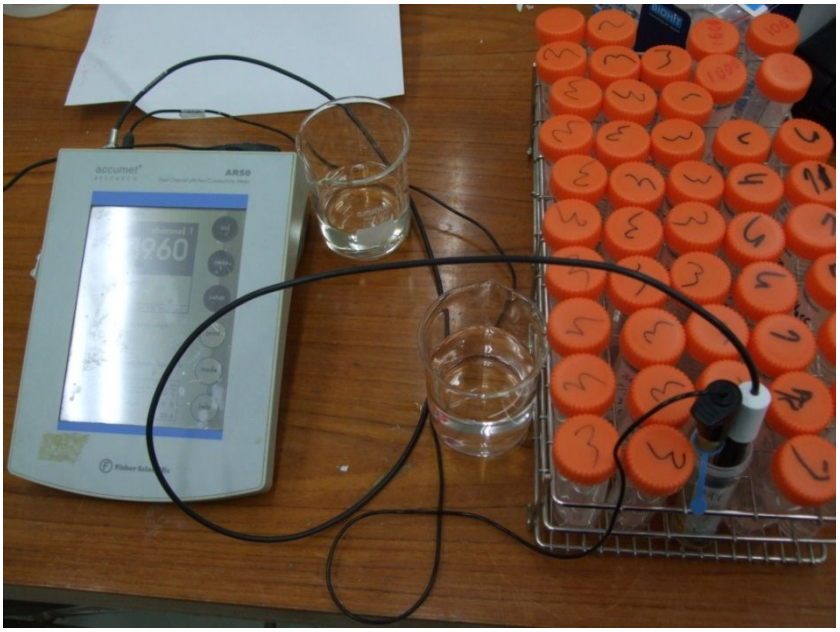

Figure 4.1 Concentration measurement from sample by ion-selective electrode using a potential difference

4.1.4 Other tests performed in this thesis

The long-term immersion test (NT Build 443) and the CTH test (NT Build 492) were simultaneously performed for comparison to the short-term ponding test on specimens fabricated at the same time. The concentrations of source solution, 165 g/L for NT Build 443 and 100 g/L for NT Build 492, were used following each guideline. Figs. 4.2 and 4.3 show experimental arrangements of NT Build 443 and NT Build 492, relatively.

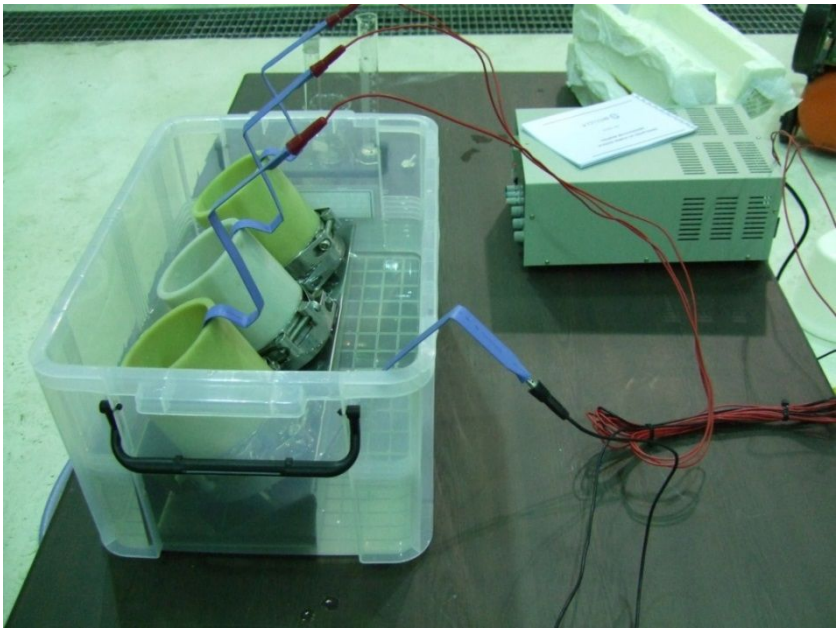

Figure 4.2 Experimental arrangement of NT Build 492 performed in thesis

Figure 4.3 Experimental arrangement of NT Build 443 performed in thesis

4.2 Chloride concentration in source solution

4.2.1 Concentration change in source solution

Figs. 4.4-4.9 show chloride ion concentrations in the source solution measured with time. Figs. 4.4 and 4.6 include the measurements from each of twelve mortar (W/C = 0.45) specimens that were simultaneously fabricated. And Figs. 4.5 and 4.7 show the measurements from each of eleven mortar (W/C = 0.60) specimens. Fig. 4.8 shows the measurements from each of eleven NC specimens and Fig. 4.9 shows the measurements from each of twelve HC specimens. All graphs show that the chloride ion concentration changed rapidly initially, and the rate of concentration change decreased with time. This tendency is similar with the graph of concentration change calculated from the analytical solution in Fig. 3.4. In Figs. 4.4-4.9, the initial concentrations measured from the source solutions differed slightly, although the source solutions were made from the same solution batch. In particular, Specimen 6 with W/C =0.60 and a target concentration of 2.1 g/L showed a larger difference than the other specimens. This difference might have arisen during the sample dilution process for concentration measurement and be due to the resolution limit of the ion-selective electrode.

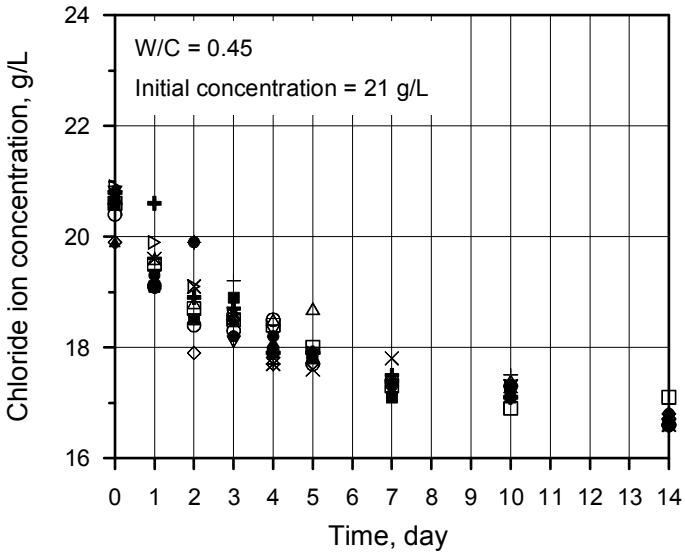

Figure 4.4 Chloride ion concentration change in 21 g/L source solution for mortar (W/C = 0.45)

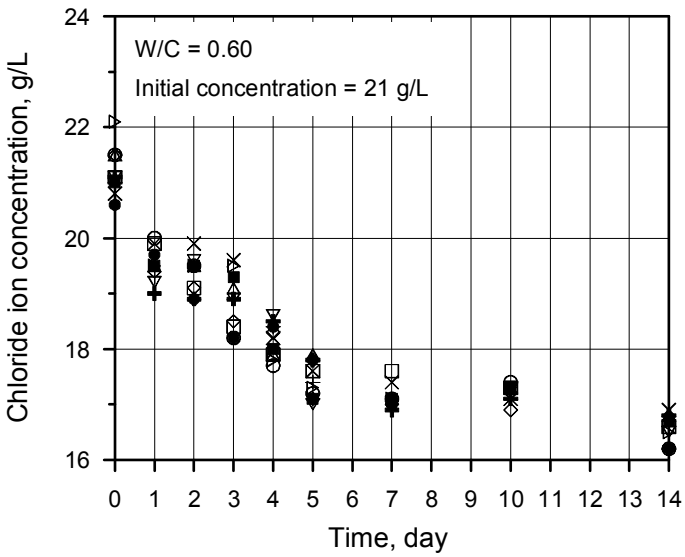

Figure 4.5 Chloride ion concentration change in 21 g/L source solution for mortar (W/C = 0.60)

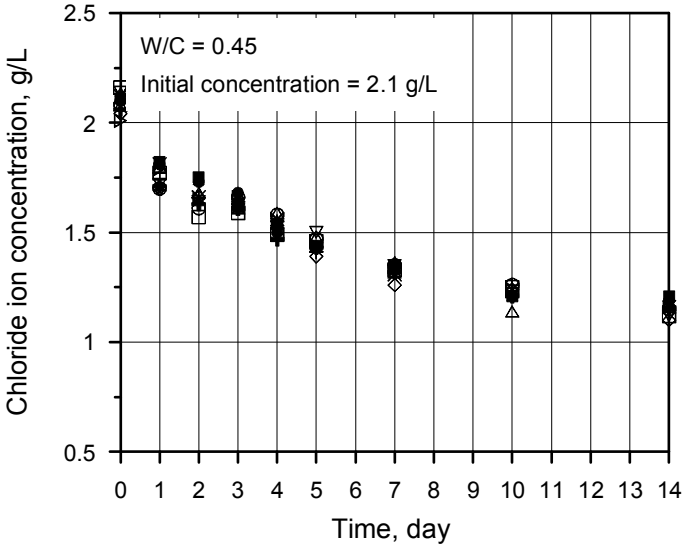

Figure 4.6 Chloride ion concentration change in 2.1 g/L source solution for mortar (W/C = 0.45)

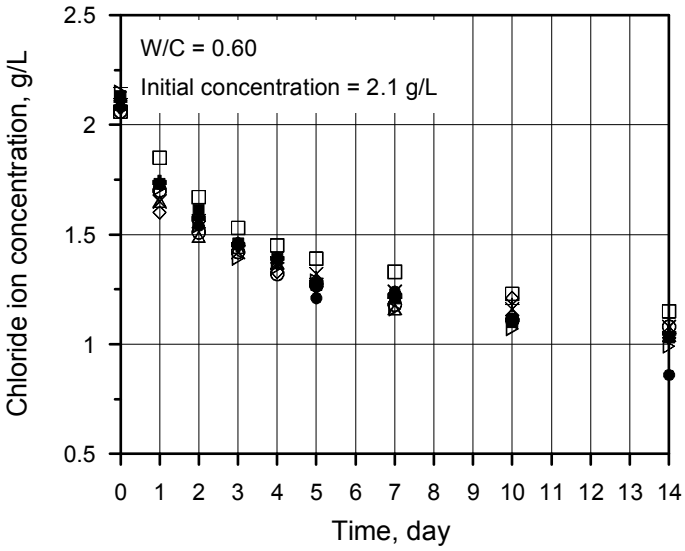

Figure 4.7 Chloride ion concentration change in 2.1 g/L source solution for mortar (W/C = 0.60)

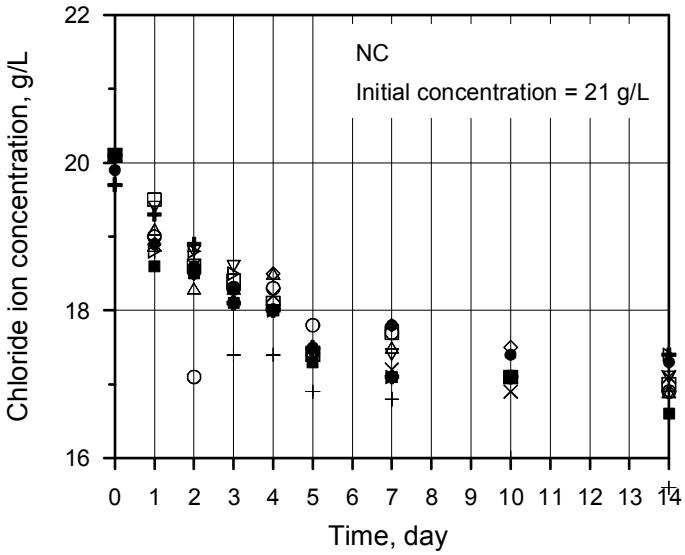

Figure 4.8 Chloride ion concentration change in 21 g/L source solution for NC

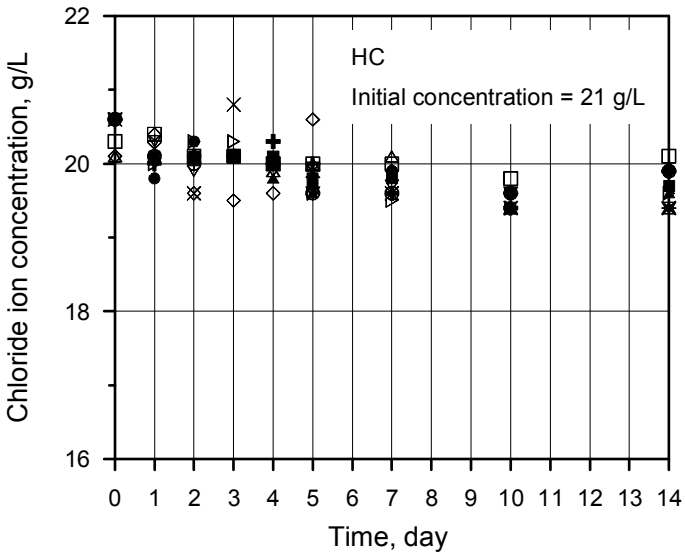

Figure 4.9 Chloride ion concentration change in 21 g/L source solution for HC

4.2.2 Effect of W/C

In Figs. 4.4-4.9, it can also be seen that the chloride ion concentration change in the source solution increased as the water-cement ratio increased. An increase in the W/C ratio commonly leads to an extension of concrete porosity, resulting in an increase in chloride flux in concrete. Consequently, it can be concluded that the short-term ponding test reflects this phenomenon well.

4.2.3 Effect of compression strength

Fig. 4.8 and Fig. 4.9 show that the chloride ion concentration change in the source solution decreased as the compressive strength of concrete increased. In general, increase of compressive strength results in decrease of porosity due to low content of water and air, resulting in decrease of diffusivity in concrete. So, concentration change of in source solution for HC was very small compared with that of other specimens. Especially, since compressive strength of HC used in this thesis was very high (80 Mpa), chloride concentration in source solution was seldom changed shown in Fig. 4.9. In this reason, diffusion coefficient of HC was anticipated to be very smaller than diffusion coefficient of NC.

4.2.4 Effect of concentration in source solution

In the comparison of the test results using two different concentrations, it was shown that the chloride ion concentration in the 2.1g/L solution changed

more rapidly than that in the 21g/L solution. This phenomenon results from the electrochemical reactions between ions in the concrete pore solution. In general, the pore structure of concrete is known to be a main factor affecting ion diffusivity in concrete, but a variety of electrochemical reactions, such as ionic interactions, ion-solvent interactions, and ion binding between ions and cement hydrate, also affect ion diffusivity. Hence, a concentration change in the source solution induces a change in ion flux caused by the difference in electrochemical reaction. Particularly, since the ionic interaction force is influenced by the distance between ions, if the concentration increases, the ion distance becomes smaller and ionic interaction increases, eventually resulting in lower ion diffusivity. For this reason, the concentration of the 2.1 g/L solution changed more rapidly than the concentration of the 21 g/L solution. The difference in the rate of decrease between the two solutions affects the calculation of the diffusion coefficient.

4.2.5 Cautions for measurement using ion selective electrode

In short-term immersion test, since diffusion coefficient is determine by measured concentration change in source solution, it is very important to measure chloride concentration in source solution exactly. So, in this section, cautions for measurement using ion-selective electrode used in this thesis is presented.

The life-time of ion-selective electrode used in this experiment is approximately one year. So, it is needed to confirm that the electrode is working ordinarily before tests. Concentration slope which is determined using two reference solutions was changed after 3 - 4 days from setting

concentration slope. So measurements of samples have to be performed within 2 - 3 days after determination of concentration slope. In this thesis, concentration in samples was measured at once after test. It was long time taken to measure concentration of samples, almost 30 seconds ~ 1 minute per one sample, so too much time is needed to measure concentration of all samples at once.

4.3 Diffusion coefficient

4.3.1 Determination method of diffusion coefficient

The diffusion coefficient can be calculated using the measured chloride ion concentration change and the analytical solution developed in this study. The chloride ion concentration change with time as estimated by the presented analytical solution varies according to the diffusion coefficient as shown in Fig. 3.4. The diffusion coefficient can be determined by curve-fitting to minimize the difference between the measured chloride ion concentrations and the profiles calculated by the analytical solution. The least squares method was employed to obtain a diffusion coefficient, i.e., a curve minimizing the difference between the measurements and the calculations. Fig. 4.10 shows a sample of the measured concentration and the optimized concentration profile using the analytical solution through curve fitting. In this saturation method, chloride ion penetration could conceivably be affected by surface capillary suction; however, the effect of capillary suction is likely negligible, because the measured chloride ion concentration-time curves for

the source solution are quite similar to the analytically derived curves shown in Fig 4.10.

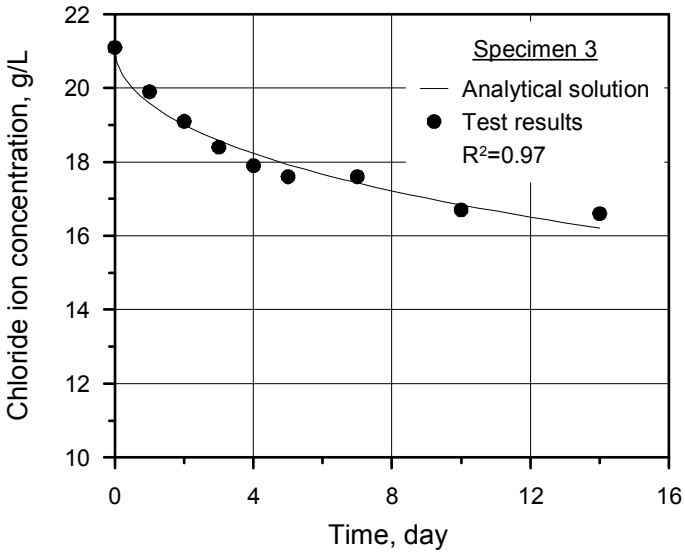

Figure 4.10 Calculation of diffusion coefficient in 21g/L solution for mortar (W/C =0.60)

4.3.2 Diffusion coefficient and coefficient of determination (R-square)

Table 4.2 shows the chloride ion diffusion coefficients and the coefficient of determination (R-square) of all specimens obtained by the above procedure. As seen in the table, R-squares were calculated by range of 0.89 ~1.00 in mortar specimens, this results show that analytical solution proposed in this method can determine diffusion coefficient fairly well. When diffusion coefficients were calculated in NC, R-squares were calculated larger than 0.87 except specimen 4 that R-square is 0.73. So, except specimen 4, it can be shown that diffusion coefficient can be determined by analytical solution and

measured data from test fairly well similar with results of mortar specimens. These results demonstrate that the diffusion coefficient can be determined within 14 days for mortar and NC specimens by the short-term ponding test. But, in HC specimens, R-squares were shown at low range of 0.16 ~ 0.94. This result indicated that the test concentration change in source solution for HC didn't fit with analytical solution in mathematical model of short-term ponding test. In HC specimen, chloride concentration in source solution hardly changed during 14 days. Since high strength concrete has very small porosity and very fineness pore structures, diffusion coefficient of high strength concrete is very small. So, concentration change in source solution for HC is changed slowly than that of NC. To determine diffusion coefficient of high strength specimen, it is needed to use ion-selective electrode of high resolution and to perform test longer period than normal strength concrete. NT build 443 and NT Build 492 show similar phenomenon which HC specimen took long time to estimate diffusion coefficient than NC specimen to determine diffusion coefficient. In this reason, the test results of HC were excluded in discussion for consistency of diffusion coefficient and numerical analysis performed in Chapter 5.

Short-term ponding test proposed in this study was shown to determine diffusion coefficient fairly well within 14 days except HC specimen. Also, complicated procedures such as grinding, sample preparation, and chloride extraction are not needed, because only the chloride ion concentration change in the source solution is used in the estimation of the diffusion coefficient in the short-term ponding test. Consequently, the short-term ponding test is shorter, less laborious and cheaper than the long-term immersion test.

Table 4.2 Diffusion coefficient (R-square) from the short-term ponding test (10^{-12} m^2/s)

W/C	0.45		0.60		NC	HC
Initial concentration (g/L)	21	2.1	21	2.1	21	21
Specimen 1	7.0 (0.89)	75.1 (0.99)	11.3 (0.96)	133.2 (0.99)	8.7 (0.95)	0.56 (0.94)
Specimen 2	5.4 (0.93)	68.1 (0.97)	17.0 (0.97)	123.3 (0.98)	5.3 (0.92)	0.04 (0.16)
Specimen 3	7.8 (0.96)	90.6 (0.99)	11.9 (0.97)	69.5 (0.97)	5.6 (0.94)	0.06 (0.56)
Specimen 4	7.4 (0.96)	64.6 (0.97)	16.4 (0.95)	115.8 (0.99)	6.2 (0.73)	0.49 (0.60)
Specimen 5	7.3 (0.96)	67.1 (0.96)	13.3 (0.94)	136.8 (0.99)	5.9 (0.94)	0.07 (0.52)
Specimen 6	9.8 (0.97)	80.4 (0.98)	12.0 (0.91)	-	5.6 (0.94)	0.62 (0.91)
Specimen 7	9.6 (0.95)	51.7 (0.96)	19.5 (0.93)	151.1 (1.00)	5.8 (0.87)	0.58 (0.77)
Specimen 8	8.6 (0.92)	73.5 (0.98)	8.5 (0.87)	111 (0.99)	6.3 (0.93)	0.56 (0.60)
Specimen 9	8.9 (0.92)	69.9 (0.99)	12.0 (0.93)	110.3 (0.99)	4.0 (0.87)	0.42 (0.59)
Specimen 10	9.0 (0.96)	67.4 (0.97)	11.6 (0.91)	125.7 (0.99)	7.2 (0.95)	0.49 (0.83)
Specimen 11	8.7 (0.92)	66.5 (0.97)	9.6 (0.97)	127.3 (0.95)	4.3 (0.92)	0.41 (0.45)
Specimen 12	5.2 (0.97)	79.5 (0.98)	-	-	-	0.58 (0.81)
Average	7.9	71.2	13.0	120.3	5.9	0.41
Standard deviation	1.5	9.7	3.3	21.7	1.3	0.22

4.3.3 Discussions

As previously described, specimen 6 with W/C = 0.60 and a target initial concentration of 2.1g/L was excluded from the data analysis, since its initial concentration showed an inexplicably large difference from the target. As anticipated from the chloride ion concentration changes measured in the test, the specimen with the larger W/C ratio had the greater diffusion coefficient due to the increase in the number and size of pores. It is shown that diffusion coefficient obtained from NC specimen is larger than that of HC specimen. This result came from that pore structure of high strength concrete is more sophisticated than that of low strength concrete. In addition, the diffusion coefficient calculated using the 2.1 g/L solution was approximately ten times larger than that from the 21 g/L solution. This result could also be predicted from the concentration measurement because the change in concentration with time was steeper in the 2.1 g/L solution (See Figs. 4.4-4.9 and note the axis scale).

Several studies support this result. Zhang investigated the diffusion coefficient according to the concentration change in the source solution using a steady-state migration test. As shown in Fig. 4.11, the chloride ion diffusion coefficient increased by 7.4 - 10.0 times when the concentration in the source solution decreased by ten times. Tang mathematically explained the change in diffusion and migration with concentration in the source solution by employing the concept of counter-electrical fields and the friction coefficient. Thus, it can be concluded that the diffusion coefficient varies with chloride concentration in source solution.

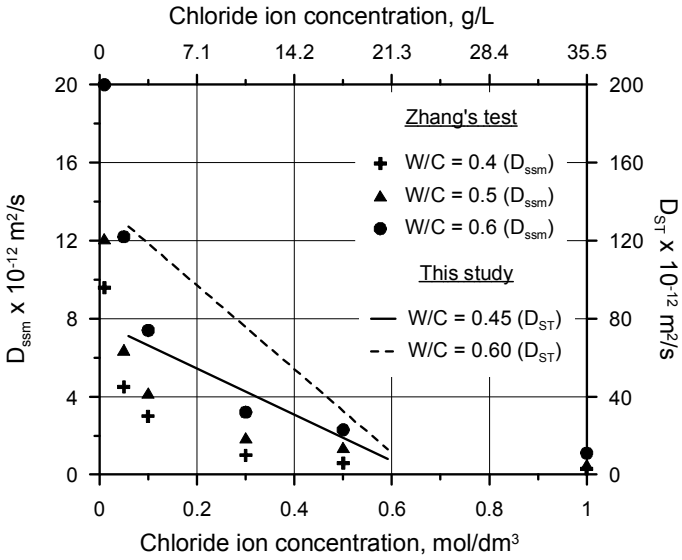

Figure 4.11 Diffusion coefficient according to concentration in source solution

In short-term ponding test, diffusion coefficient is determined from concentration change in source solution. But the change was small in range of 0.3 ~ 0.5 mol chloride concentration in source solution of Zhang's research as shown in Fig. 4.11. The range of concentration change in short-term ponding test was shown as 16 ~ 21 g/L, 0.45 ~ 0.59 mol. So, it can be expected that the change of diffusion coefficient during short-term ponding test is very small. The change of diffusion coefficient in source solution was verified in Chapter 5 using numerical analysis.

4.3.4 Reproducibility of short-term ponding test

As can be seen Figs. 4.4-4.9, there were systematic errors in measurements of chloride concentration in samples. Diffusion coefficient obtained from short-term ponding test can be affected by these errors. So, it is needed to verify the effect of these errors on determination of diffusion coefficient in short-term ponding test. Table 4.3 shows initial concentrations in solutions, average concentration, standard deviation and coefficient of variation (CoV) of initial concentrations. The average CoV of samples was calculated as 1.9 %.

Table 4.3 Initial concentration measured in source solution and CoV of initial concentration

	M(0.45)		M(0.60)		NC	HC
Con	21 g/L	2.1 g/L	21 g/L	2.1 g/L	21 g/L	21 g/L
Sp1	20.6	2.13	21	2.17	19.7	20.6
Sp2	19.9	2.04	21.5	2.11	20.1	20.1
Sp3	20.6	2.16	21.1	2.06	20.1	20.3
Sp4	20.4	2.08	21.5	2.06	20.1	20.6
Sp5	20.7	2.08	21.5	2.13	20.1	20.1
Sp6	20.8	2.14	21.1	2.35	20.1	20.6
Sp7	20.9	2.01	22.1	2.15	20.1	20.6
Sp8	20.7	2.12	20.8	2.09	20.1	20.6
Sp9	20.8	2.06	21.1	2.08	19.7	20.6
Sp10	20.6	2.11	21	2.13	20.1	20.6
Sp11	20.8	2.1	20.6	2.08	19.9	20.6
Sp12	19.9	2.14	-	-	-	20.6
Ave	20.6	2.1	21.2	2.1	20	20.5
SD	0.33	0.045	0.41	0.082	0.16	0.2
COV	0.016	0.021	0.019	0.039	0.008	0.01

CoV was used to verify reproducibility of diffusion coefficient by systematic error of measurements obtained from short-term ponding test. Verification process was performed as follows. First, chloride concentration curve in source solution was calculated by analytical solution incorporating arbitrary diffusion coefficient. Second, arbitrary errors were generated on

chloride concentration curve by CoV calculated from Table 4.3, the errors were expressed by normalized distribution. The errors were shown as Fig 4.12. Third, diffusion coefficient was determined by analytical solution incorporating concentration curve which was made in second step.

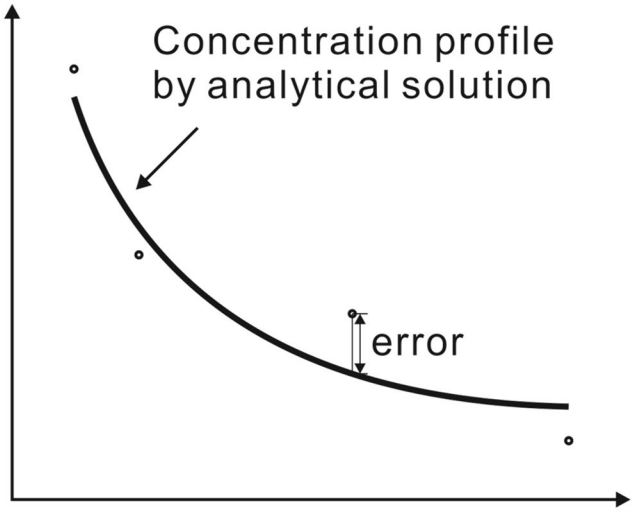

Figure 4.12 Errors inserted in concentration curve by analytical solution

In this analysis, three kinds of reference diffusion coefficients, D = 5, 10, 20 × 10^{-12} m^2/s, were used. The errors were inserted in concentration profiles in source solution adopting 1.9 % CoV. 1 set contained 10 diffusion coefficient and 1000 sets of average diffusion coefficient and standard deviation were calculated. Table 4.4 shows average diffusion coefficient and standard deviation obtained from analytical solution incorporating chloride concentration profiles inserting errors. From Table, it can be shown that CoV was increased with decrease of reference diffusion coefficient.

Table 4.4 Average diffusion coefficient and standard deviation obtained from analytical solution incorporating chloride concentration profiles inserting errors

Reference diffusion coefficient	Average diffusion coefficient	Standard deviation	CoV
5×10^{-12} m^2/s	5.14×10^{-12} m^2/s	0.57×10^{-12} m^2/s	0.11
10×10^{-12} m^2/s	10.13×10^{-12} m^2/s	0.81×10^{-12} m^2/s	0.08
20×10^{-12} m^2/s	20.13×10^{-12} m^2/s	1.23×10^{-12} m^2/s	0.06

Diffusion coefficient of HC was determined 0.41×10^{-12} m^2/s. This is smaller than 5×10^{-12} m^2/s, so it is needed to high resolution ion-selective electrode to determine diffusion coefficient of HC exactly. To propose minimum resolution of ion-selective electrode to determine diffusion coefficient, average diffusion coefficient and standard deviation were calculated using chloride concentration curve containing errors by CoV.

Table 4.5 shows diffusion coefficient and standard deviation of reference diffusion coefficient, 0.41×10^{-12} m^2/s, by resolution of ion-selective electrode. From the table, it can be shown the more reproducibility of ion-selective electrode decrease, the more diffusion coefficient of HC become closer 0.41×10^{-12} m^2/s. CoV of diffusion coefficient was decreased with decrease of reproducibility. So, it can be concluded that 0.5 % reproducibility of ion-selective electrode is needed to determine diffusion coefficient of HC.

Table 4.5 Diffusion coefficient and standard deviation of HC obtained from statistical analysis by resolution of ion-selective electrode

Reproducibility	2 %	1 %	0.5 %	0.1 %
Diffusion coefficient ($\times 10^{-12}$ m^2/s)	0.538	0.45	0.418	0.41
Standard deviation ($\times 10^{-12}$ m^2/s)	0.154	0.082	0.039	0.008
CoV	0.29	0.18	0.09	0.02

4.3.5 Standard for curve-fitting

In determination of diffusion coefficient for HC, the range of R^2 was shown 0.16 ~ 0.94. So, it is difficult to conclude that measured data fit analytical solution well. It is needed to present R^2 which it can be concluded to fit between measured data and concentration profiles of analytical solution well. Correlation analysis was performed to present minimum R^2 which expressed well fitted. Eq. (4.1) shows sample correlation coefficient.

$$r = \frac{\sum_{i=1}^{n}\left(x_i - \bar{x}\right)\left(y_i - \bar{y}\right)}{\sqrt{\sum_{i=1}^{n}\left(x_i - \bar{x}\right)}\sqrt{\sum_{i=1}^{n}\left(y_i - \bar{y}\right)}} \tag{4.1}$$

Test statistic was calculated using Eq. (4.2) adopting Eq. (4.1).

$$T = \sqrt{n-2}\,\frac{r}{\sqrt{1-r^2}} \tag{4.2}$$

The correlation between measured data and concentration profiles obtained from analytical solution was verified using test data of HC. Table 4.6 shows test statistic obtained from Eq. (4.2) using measured data of HC. In the table, $t_{0.005}$ shows t-distribution value in 1 % level of significance From the Table, it can be shown that increasing of R^2 results in increasing of test statistic generally. When R^2 was larger than 0.60, test statistic was larger than $t_{0.005}$ excluding some cases. So, it can be concluded that measured data are well fitted with concentration profiles obtained from analytical solution when R^2 is larger than 0.60.

Table 4.6 R^2 of HC and Test statistic by Eq. (4.2) using results of HC

	R^2	r	Test statistic	$t_{0.005}$
Specimen 1	0.94	0.98	12.6	3.106
Specimen 2	0.16	0.23	0.62	3.106
Specimen 3	0.56	0.71	2.69	3.106
Specimen 4	0.60	0.80	3.48	3.106
Specimen 5	0.52	0.76	3.13	3.106
Specimen 6	0.91	0.95	8.07	3.106
Specimen 7	0.77	0.86	4.45	3.106
Specimen 8	0.60	0.74	2.91	3.106
Specimen 9	0.59	0.76	3.05	3.106
Specimen 10	0.83	0.91	5.72	3.106
Specimen 11	0.45	0.71	2.65	3.106
Specimen 12	0.81	0.90	5.47	3.106

4.3.6 Consistency of apparent diffusion coefficient

In this study, the consistency of the diffusion coefficient was examined to determine the minimum test period and number of measurements. Figs. 4.13-4.17 show the diffusion coefficients calculated from the measured chloride ion concentrations given in Figs. 4.4-4.9.

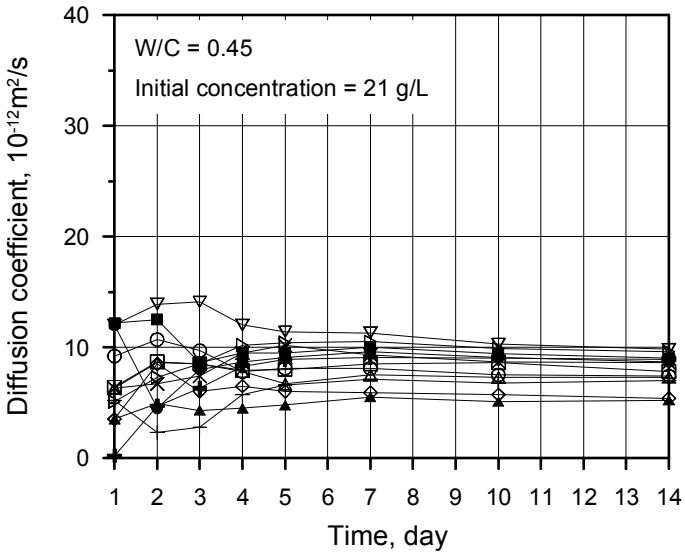

Figure 4.13 Diffusion coefficient for mortar (W/C = 0.45) in 21 g/L source solution

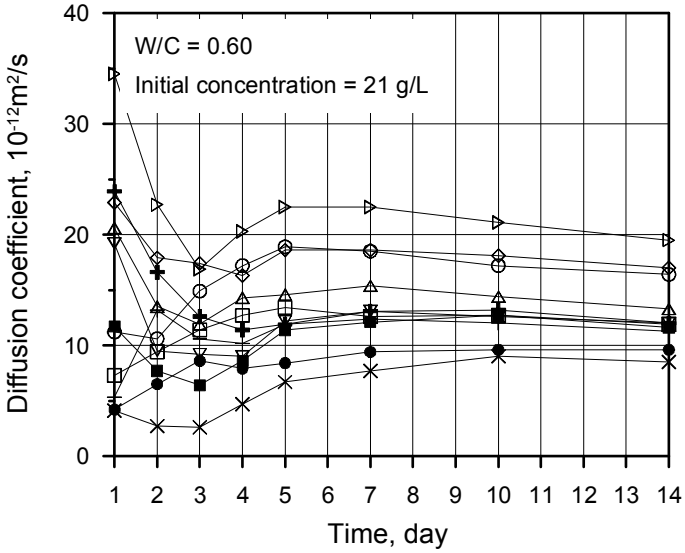

Figure 4.14 Diffusion coefficient for mortar (W/C = 0.60) in 21g/L source solution

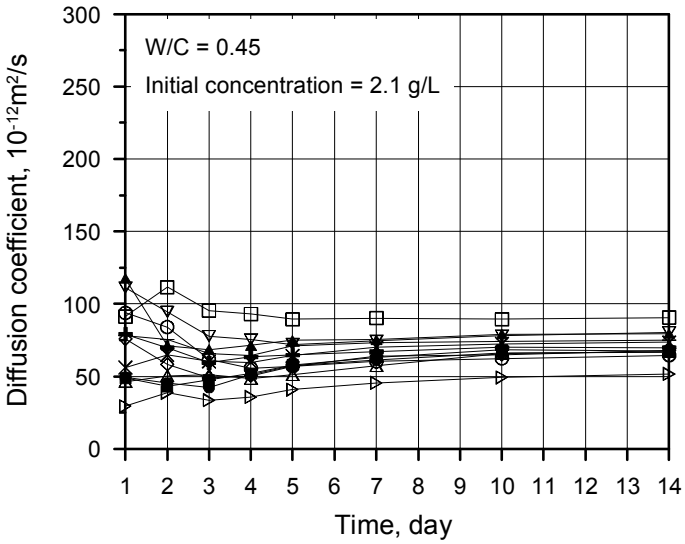

Figure 4.15 Diffusion coefficient for mortar (W/C = 0.45) in 2.1g/L source solution

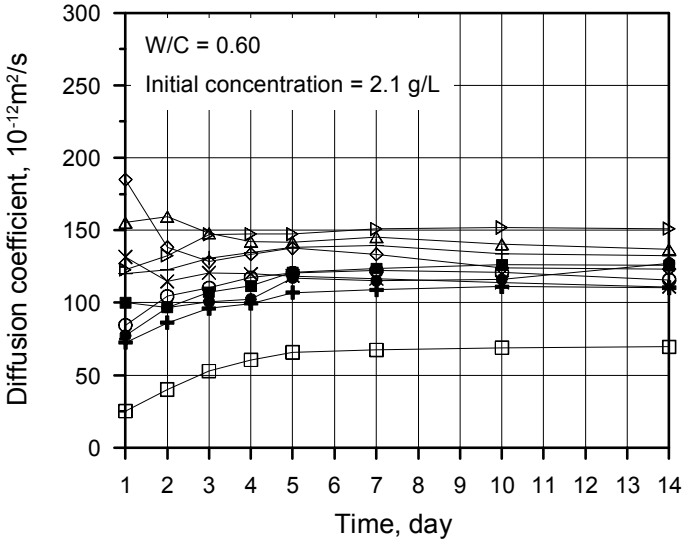

Figure 4.16 Diffusion coefficient for mortar (W/C = 0.60) in 2.1g/L source solution

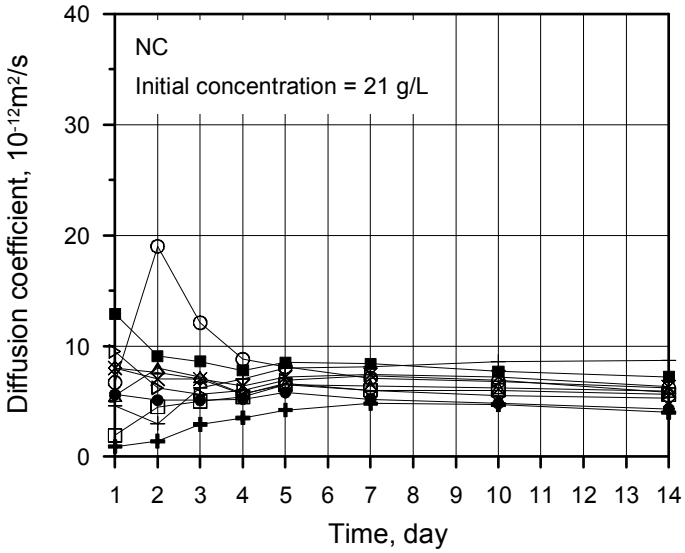

Figure 4.17 Diffusion coefficient for NC in 2.1g/L source solution

The diffusion coefficients fluctuated, especially in the early period. This

phenomenon results from the scarcity of test data required for curve-fitting. So, it is needed statistical analysis to determine test duration and number of measurement for evaluation of diffusion coefficient using short-term ponding test. In statistical analysis, correlation analysis and CoV analysis were performed. Table 4.7 shows results of correlation analysis obtained from Eq. (4.2) between diffusion coefficients at each day and 14 days. When level of significance is 1 %, $t_{0.005}$ is 3.106. So, if test statistic is larger than 3.106, it can be concluded that the diffusion coefficient at certain time is same with diffusion coefficient at 14 days. From Table 4.7, it can be shown that it takes four days to determine same diffusion coefficient with diffusion coefficient at 14 days for W/C = 0.45 mortar incorporating 21 g/L and takes five days to determine same diffusion coefficient with diffusion coefficient at 14 days for NC. In case of other specimens, only one day was needed to determine same diffusion coefficient with diffusion coefficient at 14 days.

Table 4.7 Test statistic of correlation analysis obtained from Eq. (4.2) between diffusion coefficients at each test period and 14 days

Specimen	Mortar (W/C=0.45)		Mortar (W/C=0.60)		NC
Concentration	21 g/L	2.1 g/L	21 g/L	2.1 g/L	21 g/L
1 day	1.56	3.12	3.49	3.69	1.22
2 day	1.08	4.37	4.25	6.14	0.52
3 day	2.56	7.98	5.86	9.55	1.46
4 day	6.82	11.2	10.0	9.97	2.92
5 day	9.86	12.9	22.3	14.1	4.69
7 day	17.6	17.1	27.6	15.3	6.45
10 day	20.3	27.1	36.7	22.5	11.5

Table 4.8 shows CoV of specimens by each day. From Table 4.8, it can be shown that CoV of each specimen converged after 7 days. From correlation analysis and CoV analysis, it can be concluded that seven days and 5 data are needed to determine diffusion coefficient using short-term ponding test. Similarly, the long-term immersion test (NT Build 443) requires more than six measurements for reliable curve fitting.

Table 4.8 CoV of specimens at each test period

Specimen	Mortar (W/C=0.45)		Mortar (W/C=0.60)		NC
Concentration	21 g/L	2.1 g/L	21 g/L	2.1 g/L	21 g/L
1 day	0.56	0.38	0.66	0.45	0.59
2 day	0.44	0.33	0.48	0.34	0.68
3 day	0.37	0.28	0.40	0.31	0.38
4 day	0.25	0.25	0.38	0.30	0.24
5 day	0.24	0.20	0.34	0.27	0.18
7 day	0.21	0.17	0.31	0.26	0.17
10 day	0.20	0.14	0.26	0.25	0.18
14 day	0.19	0.14	0.25	0.24	0.22

4.4 Specimen numbers for target uncertainty

To assess target uncertainty of the diffusion coefficient determined using the short-term ponding test, a reliability analysis was performed using the average and standard deviations of the diffusion coefficients for each variable (Table 4.2). Specimen numbers to reach target uncertainty can be calculated using Eq. (4.3)

$$n = \left(\frac{1.96 \cdot \sigma}{u \cdot \bar{x}} \right) \tag{4.3}$$

where $\bar{x}$ is the average diffusion coefficients, σ is the standard deviation of diffusion coefficients, and n is the number of specimens. Assuming a confidence level of 95%, specimen number required for target uncertainty was calculated using Eq. (4.3) for each variable. The target uncertainty was 10 %, 20 %, 30 % of average diffusion coefficient. Table 4.6 shows the minimum number of specimens for target uncertainty. When target uncertainty was 10 % of average diffusion coefficient, 14 ~ 25 specimens were needed to determine diffusion coefficient. When target uncertainty was 20 %, only 4 ~ 7 number of specimens were needed. From this table, it can be concluded that target uncertainty is between 10 % and 20 % when 10 ~ 12 specimens are used to determine diffusion coefficient in short-term ponding test.

Table 4.9 The minimum number of specimens for target uncertainty

Target uncertainty	Mortar (W/C = 0.45)	Mortar (W/C = 0.60)	NC
10 %	14	25	19
20 %	4	7	5
30 %	2	3	3

4.5 Comparison with existing tests

4.5.1 Test results obtained from NT Build 492 and NT Build 443

To validate the mathematical model and the test method developed in this study, the long-term immersion test (NT Build 443) and CTH test (NT

Build 492), which are currently widely used, were performed on three mortar specimens with W/C = 0.45, three mortar specimens with W/C = 0.60, three NC specimens and two HC specimens for NT Build 443, two mortar specimens with W/C = 0.45, three mortar specimens with W/C = 0.60, three NC specimens and three HC specimens for NT Build 492. Concentrations of the source solution, 165 g/L for NT Build 443 and 100 g/L for NT Build 492, were used following each guideline. The diffusion coefficients obtained from these tests were compared with the results of the short-term ponding test. Figs. 4.18-4.21 show the total chloride ion concentration profile in the concrete specimen obtained from the NT Build 443 test.

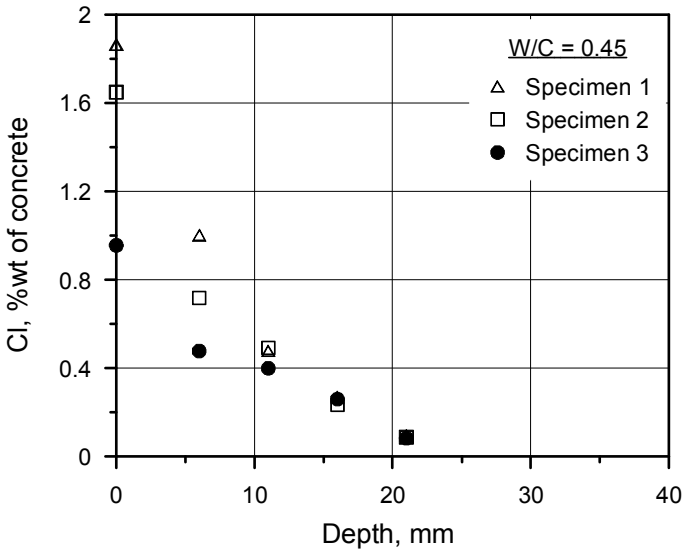

Figure 4.18 Concentration profiles of chloride ions in long-term immersion test with mortar (W/C = 0.45)

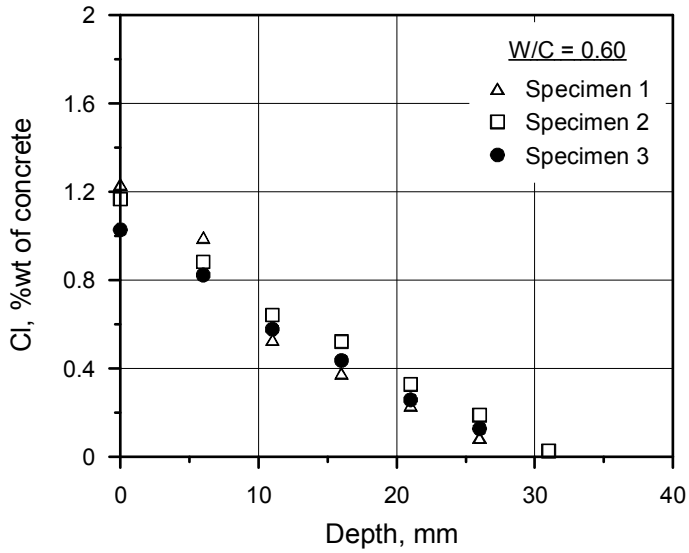

Figure 4.19 Concentration profiles of chloride ions in long-term immersion test with mortar (W/C = 0.60)

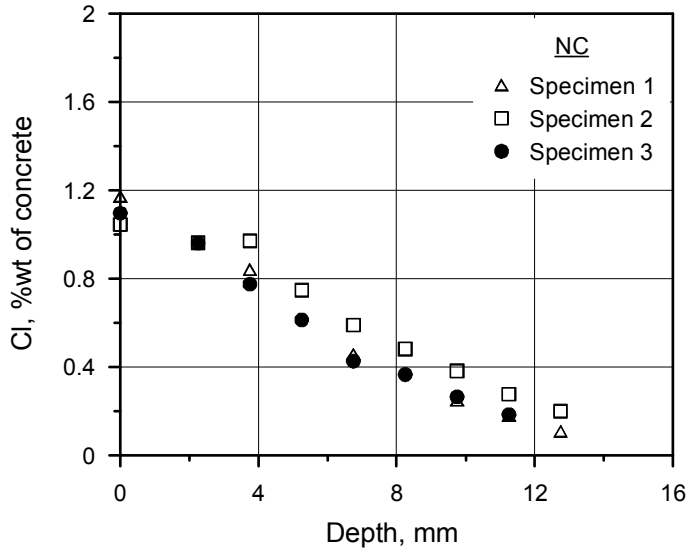

Figure 4.20 Concentration profiles of chloride ions in long-term immersion test with NC

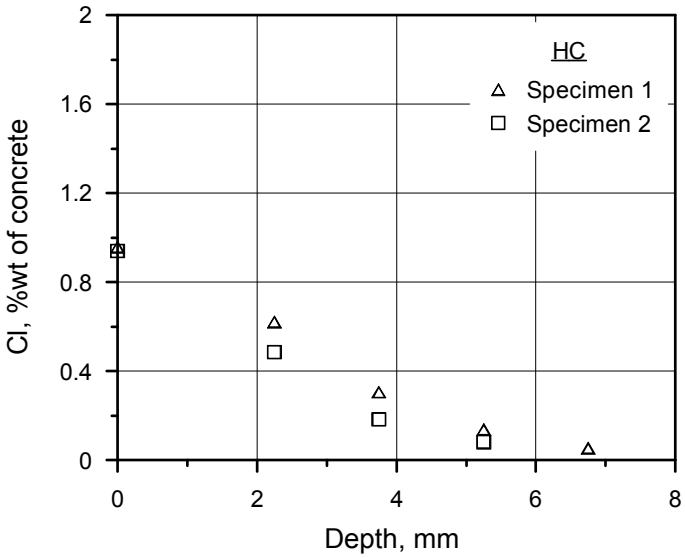

Figure 4.21 Concentration profiles of chloride ions in long-term immersion test with HC

In this test, the chloride ion concentration was measured from a 2 mm-thick ground sample at every 5 mm of depth in mortar specimen and a 2 mm-thick ground sample at every 2 mm of depth in concrete specimen. Table 4.10 shows the chloride ion penetration depth in concrete obtained by the NT Build 492 test manual. The measuring point of the penetration depth is shown in Fig. 4.22. Based on the manual, the test was performed by applying 15 volts for 24 hours, and 10 volts for 6 hours to mortar with W/C = 0.45 and mortar with W/C = 0.60, respectively. In concrete, the test was performed by applying 20 volts for 24 hours, and 60 volts for 48 hours to NC and HC, respectively.

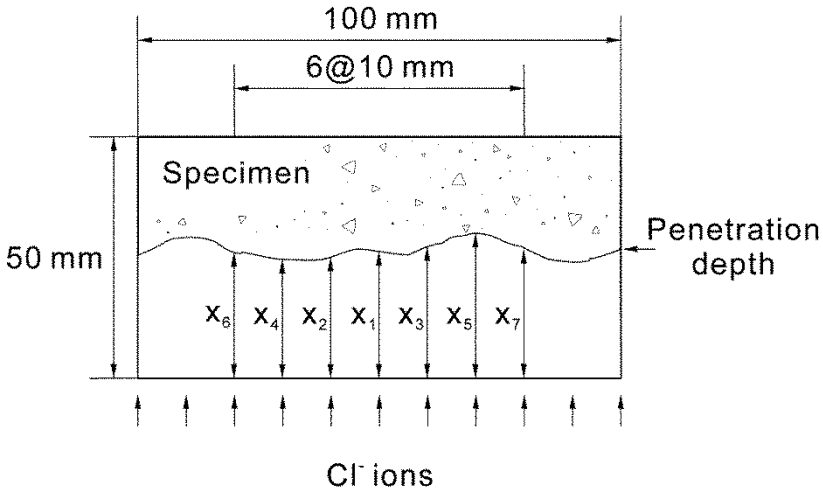

Figure 4.22 Measuring point in NT Build 492

Table 4.10 Penetration depth of chloride ion in CTH test (mm)

	Mortar W/C = 0.45		Mortar W/C = 0.60			NC			HC		
Location	Sp 1	Sp 2	Sp 1	Sp 2	Sp 3	Sp 1	Sp 2	Sp 3	Sp 1	Sp 2	Sp 3
X_1	17.2	16.2	8.1	8.1	7.7	15	16	16	3.8	3.4	3.4
X_2	17.1	17.7	8.4	7.9	7.3	16	17	16	5	3.5	4.6
X_3	17.0	18.1	8.9	8.3	7.3	15	17	17	4.7	4	4.3
X_4	16.9	18.2	7.6	7.7	8.4	16	16	15	4.4	4.1	4.4
X_5	17.7	16.1	9.4	8.9	6.7	17	17	17	3.4	3.6	3.7
X_6	17.1	18.2	8.1	7.6	9.0	14	15	15	5.1	6	2.9
X_7	17.8	18.0	10.0	9.4	7.2	16	17	18	4.8	3.8	5.7
Average	17.3	17.5	8.6	8.3	7.7	15.6	16.4	16.3	4.5	3.7	4.2

The diffusion coefficients were calculated using each test result (Fig. 4.18-4.21 and Table 4.10), incorporating the analytical solutions presented in each test standard. Table 4.11 and Fig. 4.23 show a comparison of the diffusion coefficients obtained from each test. Short-term ponding test and long-term immersion tests showed similar results, but the CTH test provided results that were considerably different from the diffusion tests. To compare diffusion coefficients obtained from short-term ponding test and long-term immersion test, t-test was performed. Table 4.12 shows results of t-test between diffusion coefficients of short-term ponding test and diffusion coefficients of long-term immersion test. 10 % level of significance was used to compare two diffusion coefficients. From the t-test, it can be concluded that the diffusion coefficients obtained from short-term ponding test and long-term immersion test were same. The diffusion coefficient of HC specimens obtained from short-term ponding test showed similar results with other test results in spite of coefficients of determination (R^2) were low. This result indicated that short-term ponding test can determine diffusion coefficient fairly well in spite of measuring errors occurred due to low resolution of ion-selective electrode.

Table 4.11 Average diffusion coefficient from each test method (10^{-12} m^2/s)

	Short-term Ponding test (This study)	Long-term Immersion test (NT Build 443)	CTH test (NT Build 492)
Mortar (W/C=0.45)	7.9	5.7	14.8
Mortar (W/C=0.60)	13.0	17.7	39.9
NC	5.9	6.5	11.1
HC	0.41	0.73	0.41

Table 4.12 Results of t-test between diffusion coefficients obtained from short-term ponding test and long-term immersion test

	W/C = 0.45		W/C = 0.60		NC		HC	
	ST	LT	ST	LT	ST	LT	ST	LT
Sp 1	7	4.9	11.3	13.7	8.7	4.7	0.56	0.89
Sp 2	5.4	4.5	17	19.8	5.3	9.5	0.04	0.57
Sp 3	7.8	7.6	11.9	19.8	5.6	5.3	0.06	
Sp 4	7.4		16.4		6.2		0.49	
Sp 5	7.3		13.3		5.9		0.07	
Sp 6	9.8		12		5.6		0.62	
Sp 7	9.6		19.5		5.8		0.58	
Sp 8	8.6		8.5		6.3		0.56	
Sp 9	8.9		12		4.0		0.42	
Sp 10	9		11.6		7.2		0.49	
Sp 11	8.7		9.6		4.3		0.41	
Sp 12	5.2						0.58	
Ave	7.89	5.67	13.0	17.7	5.9	6.5	0.41	0.73
SD	1.50	1.69	3.31	3.52	1.28	2.62	0.22	0.23
t-test	2.09		-2.10		-0.38		-1.88	
df	2.31		2.37		2.10		1.14	
$t_{0.05}$	2.74		2.71		2.86		5.84	

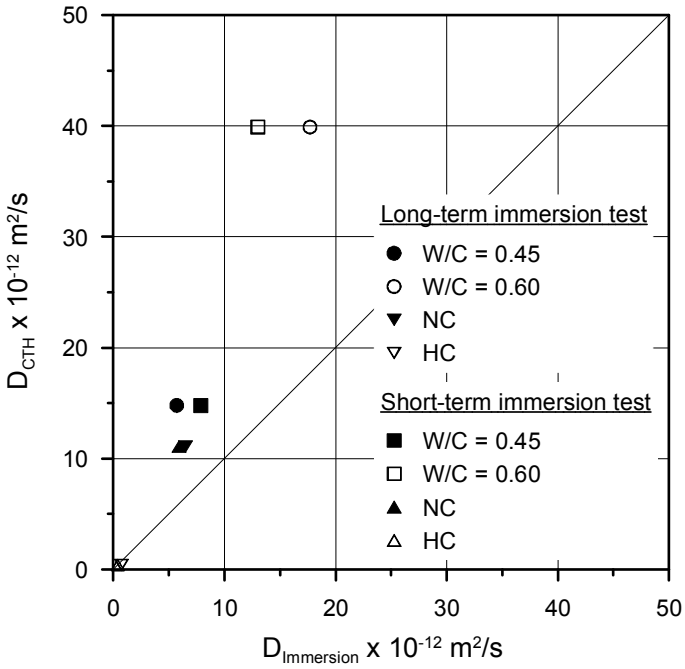

Figure 4.23 Comparison of the test results of NT Build 443 (long-term immersion test), NT Build 492 (CTH test) and this study

4.5.2 Discussions

In Section 4.3.3, it was demonstrated that the diffusion coefficient decreased with an increase in the concentration of the source solution. However, the diffusion coefficients obtained from both immersion tests were similar, although the concentration in the source solution of NT Build 443 is eight times higher than that of the short-term immersion test. MacDonald reported that concentration had no significant effect on the diffusion coefficient in a high concentration solution (higher than 0.5 M). Presumably this is why the diffusion coefficients are similar in spite of the large difference

in concentration.

The difference between immersion tests and CTH test had two sources. The first is related to the difference in chloride ion binding reaction between the immersion tests and the CTH method as explained in Section 2.4.5. Tang also observed a similar tendency in that the difference between the diffusion coefficients from the CTH test and the long-term immersion test increased with W/C, and suggested that this results from the different chloride ion binding mechanisms of the two tests. The short-term immersion test presented in this study was also performed for 14 days, which is enough to reflect a realistic chloride ion binding effect.

The second source is the difference in the chloride ion penetration mechanism. As described in Section 2.4.5, chloride ions are transported by ion migration as well as by diffusion in the CTH test, and Tang defined the difference between the steady-state diffusion coefficient (D_{ssd}) and the steady-state migration coefficient (D_{ssm}) in Eq. (4.4),

$$\frac{D_{ssd}}{D_{ssm}} = \left(1 - z\_K_{\tau 0} - z\_K_{\tau m}\right)\left(1 + \frac{\partial \ln \gamma}{\partial \ln c_{ext}}\right) \cdot \frac{f\left(1 + \left|\beta_v\right|\right)c_{ext} + c_0}{f\left(1 - \left|\beta_v\right|\right)c_{ext} + c_0} \quad (4.4)$$

where

$$\beta_v = \frac{1 + K_{\tau 0} + K_{\tau m}}{1 - K_{\tau 0} - K_{\tau m}} \quad (4.5)$$

where z_- is the valence of anions, c_0 is the solvent concentration, $K_{\tau m}$ and f reflect characteristics of the pore solution in concrete, while the parameters c_{ext}, $K_{\tau 0}$, and γ reflect the characteristics of the external source solution, especially in a steady state. After all, Eq. (4.4) implies that the ratio of the two diffusion coefficients varies according to pore characteristics. For this reason, the difference in the diffusion coefficient between the immersion tests and the CTH test was greater for mortar with W/C = 0.60 than for mortar with W/C = 0.45.

5. Numerical analysis

In this study, to determine diffusion coefficient simply using analytical solution and concentration change in source solution, diffusion coefficient is assumed to be constant during test irrespective of effects of aging and concentration change in source solution. And chloride binding isotherm was assumed to be linear for calculating analytical solution from governing equation. But, the diffusion coefficient is changed by concentration change in source solution and aging of concrete in real concrete structures. Also, chloride binding isotherm was represented as non-linear isotherm by former researches. So, it is needed to verify whether these assumptions are reasonable. In this chapter, the assumptions have been verified using numerical analysis. Also, the assumption of infinite specimen depth that was incorporated as boundary condition was verified.

5.1 Numerical formulation

5.1.1 General

In this section, the numerical analysis was performed to verify the assumptions in mathematical model. The finite element analysis procedure was incorporated for analysis of 1-direction diffusion. The governing equation of the numerical analysis is expressed as Eq. (5.1).

$$\frac{\partial c}{\partial t} = \frac{D_{ssd}}{\left(\theta + \frac{\partial c_b}{\partial c}\right)} \cdot \frac{\partial^2 c}{\partial x^2} = D_{ST} \frac{\partial^2 c}{\partial x^2} \tag{5.1}$$

The Galerkin's method was used in finite element analysis. The governing equation is multiplied with shape function ψ_i and integrated over domain Ω as Eq. (5.2).

$$\int_{\Omega} \psi_i \left(\frac{\partial c}{\partial t} - D_{ST} \frac{\partial^2 c}{\partial x^2} \right) d\Omega = 0 \tag{5.2}$$

The domain was composed with source solution and concrete and discretized into finite elements considering time efficiency as shown in Fig. 5.1. In short-term ponding test, chloride ion transport was assumed to be one-direction diffusion. Nearby contacted area between source solution and concrete, 1 mm of source solution and 1 mm concrete specimen was divided into 0.1 mm each. And the rest part was divided into 1 mm each. The time step was determined as one day in numerical analysis.

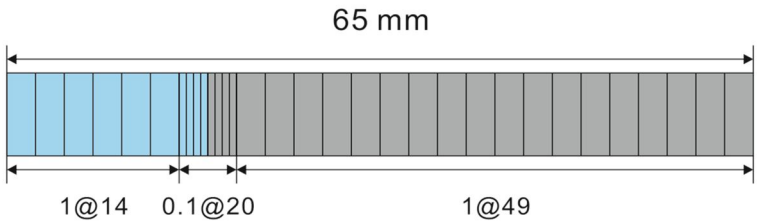

Figure 5.1Discretized model of source solution and concrete specimen in numerical analysis

5.1.2 Pdepe function

In this study, pdepe function, one of the Matlab function, was adopted to solve the one-direction partial differential problem. In pdepe function, the governing equation is expressed by Eq. (5.3).

$$c\left(x,t,u,\frac{\partial u}{\partial x}\right)\frac{\partial u}{\partial t}=\frac{\partial}{\partial x}\left(f\left(x,t,u,\frac{\partial u}{\partial x}\right)\right)+s\left(x,t,u,\frac{\partial u}{\partial x}\right) \tag{5.3}$$

where, $c\left(x,t,u,\frac{\partial u}{\partial x}\right)$ means relationship between partial derivatives, $f\left(x,t,u,\frac{\partial u}{\partial x}\right)$ means flux term, $s\left(x,t,u,\frac{\partial u}{\partial x}\right)$ means sink term. This function can solve the one-direction partial differential problem such as heat transfer and ion diffusion with time and distance. In this equation, chloride binding can be expressed by $c\left(x,t,u,\frac{\partial u}{\partial x}\right)$ and diffusion flux can be expressed by $f\left(x,t,u,\frac{\partial u}{\partial x}\right)$. Sink term $s\left(x,t,u,\frac{\partial u}{\partial x}\right)$ is zero in this mathematical model. So, each term of governing equation can be expressed as below.

$$c\left(x,t,u,\frac{\partial u}{\partial x}\right)=\left(\theta+\frac{\partial c_b}{\partial c}\right) \tag{5.4}$$

$$f\left(x,t,u,\frac{\partial u}{\partial x}\right)=D_{ssd}\frac{\partial c}{\partial x} \tag{5.5}$$

$$s\left(x,t,u,\frac{\partial u}{\partial x}\right)=0 \tag{5.6}$$

So, Eq. (5.3) is rewritten by Eq. (5.7) applying above equations.

$$\left(\theta+\frac{\partial c_b}{\partial c}\right)\frac{\partial c}{\partial t}=\frac{\partial}{\partial x}\left(D_{ssd}\frac{\partial c}{\partial x}\right) \tag{5.7}$$

where, c means free chloride concentration. In the analysis incorporating apparent diffusion coefficient, the governing equation was rewritten as Eq. (5.8) incorporating apparent diffusion coefficient D_{app}.

$$\frac{\partial c}{\partial t}=D_{ST}\frac{\partial^2 c}{\partial x^2} \tag{5.8}$$

In this case, $f\left(x,t,u,\frac{\partial u}{\partial x}\right)$ was $D_{ST}\frac{\partial c}{\partial x}$, $c\left(x,t,u,\frac{\partial u}{\partial x}\right)$ was zero. Initial condition was expressed by Eq. (5.9).

$$u\left(x,t_0\right)=u_0\left(x\right) \tag{5.9}$$

where, t_0 is initial time, x is distance. u_0 is initial concentration. Boundary condition can be expressed by Eq. (5.10).

$$p(x,t,u)+q(x,t)\cdot f\left(x,t,u,\frac{\partial u}{\partial x}\right)=0 \tag{5.10}$$

Using Eq. (5.10), the concentration and the concentration gradient can be applied at boundary of specimen and source solution.

5.2 Verification of results of numerical analysis

To verify the validity of numerical analysis, the concentration change in source solution calculated using numerical analysis was compared with that of analytical solution. The governing equation is expressed as Eq. (5.11).

$$\frac{\partial c}{\partial t}=D_{ST}\frac{\partial^2 c}{\partial x^2} \tag{5.11}$$

where, D_{ST} is the apparent diffusion coefficient obtained from short-term ponding test. The concentration change in source solution was calculated to compare with concentration change obtained from analytical solution.

The initial condition was same like Eqs. (5.12) and (5.13). The initial concentration in concrete is zero and initial concentration measure in tests is incorporated as the initial concentration in source solution in mathematical model.

$$c = c_{ini} \qquad in\ NaCl\ solution, \quad t = 0 \tag{5.12}$$

$$c = 0 \qquad in\ concrete, \qquad t = 0 \tag{5.13}$$

The boundary conditions were same like Eqs. (5.14) and (5.15). Concentration gradients at the boundary of source solution(x=0) and specimen(x=end) were zero.

$$\left.\frac{\partial c}{\partial x}\right|_{x=0} = 0 \tag{5.14}$$

$$\left.\frac{\partial c}{\partial x}\right|_{x=end} = 0 \tag{5.15}$$

Figs. 5.2 and 5.3 show concentration change in source solution obtained from numerical analysis and analytical solution.

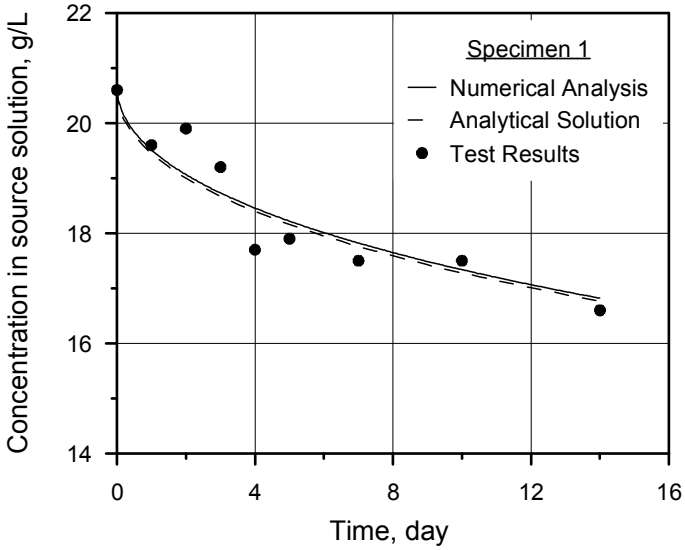

Figure 5.2 Concentration change in source solution of W/C=0.45 mortar specimen 1 obtained from numerical analysis and analytical solution

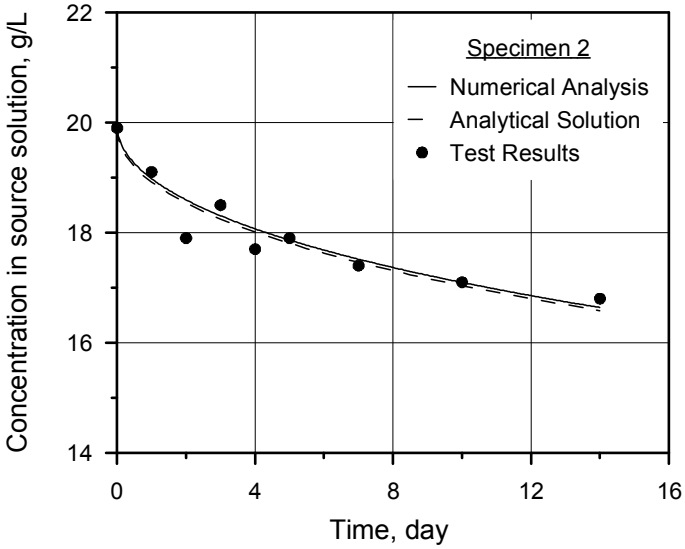

Figure 5.3 Concentration change in source solution of W/C=0.45 mortar specimen 2 obtained from numerical analysis and analytical solution

From graph, it can be shown that the concentration change obtained from numerical analysis was almost same with the concentration change obtained from analytical solution. So, it can be concluded that the numerical analysis could be used to verify assumptions in mathematical model.

5.3 Verification of assuming infinite specimen depth

In the mathematical model, infinite-point condition, Eq. (3.9), was incorporated as boundary condition. To adopt this condition in mathematical model, specimen must have enough depth that chloride ion can't reach during test. In validation test, 50 mm depth specimen was used to determine diffusion coefficient. Chloride penetration depth during test was calculated by numerical analysis. In numerical analysis, 20×10^{-12} m^2/s, larger than 13×10^{-12} m^2/s of W/C = 0.60 mortar, was used as diffusion coefficient. Test duration was 14 days. Initial chloride concentration in source solution and initial chloride concentration in concrete were 21 g/L and 0 g/L each. Fig 5.4 shows chloride concentration in concrete by numerical analysis. From figure, it can be shown that chloride penetration depth during short-term ponding test was approximately 21 mm. This result has indicated that the specimen depth can be assumed to be infinite during short-term ponding test.

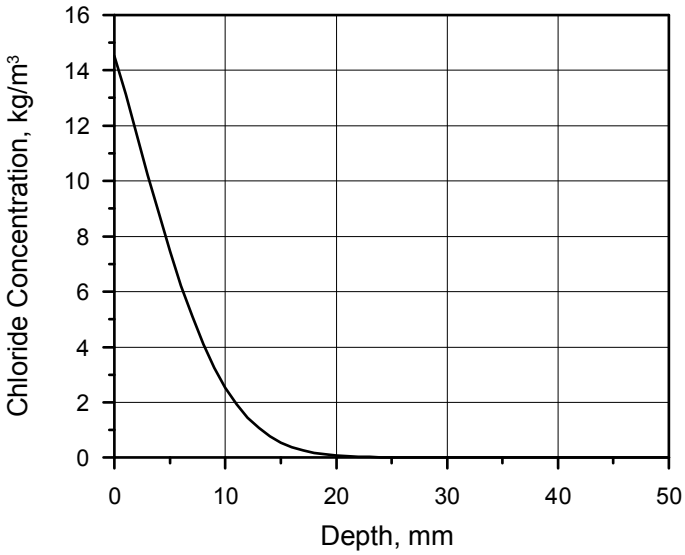

Figure 5.4 Chloride concentration in concrete obtained from numerical analysis

5.4 Effect of age on diffusion coefficient

5.4.1 General

Because the concrete is time-dependent material, the diffusivity of concrete has changed with time. Stanish and Tang have reported that the diffusion coefficient decreased by increase of concrete age. Fig. 5.16 shows diffusion coefficient change with time.

$$D(t) = D_{ref,t}\left(\frac{t_{ref}}{t_{eff}}\right)^{m} \tag{5.16}$$

where, $D_{ref,t}$ is a reference diffusion coefficient at reference time t_{ref}, t_{eff} is age of concrete, m is a coefficient that expresses the rate of change of the diffusion coefficient. Fig. 5.5 shows change of diffusion coefficient with time.

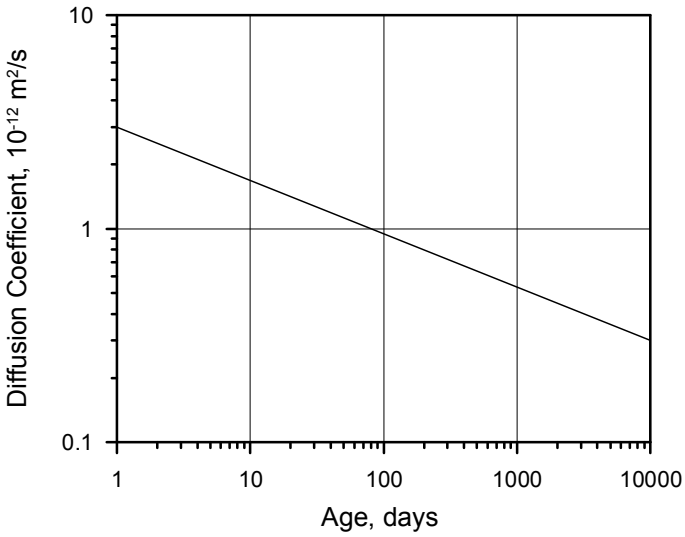

Figure 5.5 Change of diffusion coefficient with time

Short-term ponding test developed in this study takes 14 days to determine diffusion coefficient, so diffusion coefficient can be changed during test. Effect of age on apparent diffusion coefficient during short-term ponding test was verified using numerical analysis.

5.4.2 Diffusion coefficient model

ACI 365 Committee has suggested diffusion coefficient model that

expresses change of diffusion coefficient with time same like Eq. (5.17).

$$D(t) = D_{ref,t}\left(\frac{t_{ref}}{t}\right)^{m} \tag{5.17}$$

where, $D(t)$ is diffusion coefficient at time(t), D_{ref} is a reference diffusion coefficient at reference time (t_{ref}), m is a coefficient that expresses the rate of change of the diffusion coefficient. In ACI 365 Committee, m , a coefficient that expresses the rate of change of the diffusion coefficient, was suggested for Eq. (5.18).

$$m = 0.2 + 0.4\left(\%FA/50 + \%SG/70\right) \tag{5.18}$$

where, FA is content of fly ash, SG is content of slag. Fly ash is allowed to be replaced by 50 % of total content of binder and slag is allowed to be replaced by 70% of total content of binder. In this equation, m is limited by 0.60. To verify effect of aging on diffusion coefficient during short-term ponding test, the diffusion coefficient at initiation of short-term ponding test (28 day) was estimated by Eq. (5.17) and Eq. (5.18) incorporating trial-error method using test results.

To verify effect of various binder on diffusion coefficient, four kinds of m were considered in this numerical analysis, only cement, 30 % substituted by fly ash, 30 % substituted by slag, substituted by 30 % fly ash and slag each. The average diffusion coefficient during test was calculated by numerical

analysis, and was compared with apparent diffusion coefficient obtained from short-term ponding test.

5.4.3 Numerical analysis

The governing equation was expressed as Eq. (5.19).

$$\frac{\partial c}{\partial t} = \frac{\partial c}{\partial t}\left(D_{ref,t} \left(\frac{t_{ref}}{t} \right)^{m} \frac{\partial c}{\partial x} \right) \tag{5.19}$$

The initial conditions were expressed as Eqs. (5.20) and (5.21). The initial concentration in concrete was zero and the initial concentration in source solution was adopted by the initial concentration measured in test.

$$c = c_{ini} \qquad in\ NaCl\ solution, \quad t = 0 \tag{5.20}$$

$$c = 0 \qquad in\ concrete, \qquad t = 0 \tag{5.21}$$

The boundary conditions were same like Eqs. (5.22) and (5.23). The concentration gradients at the end of source solution and specimen each were zero.

$$\left. \frac{\partial c}{\partial x} \right|_{x=0} = 0 \tag{5.22}$$

$$\left. \frac{\partial c}{\partial x} \right|_{x=end} = 0 \tag{5.23}$$

The trial-error method was used to determine reference diffusion coefficient ($D_{ref,t}$) at minimum error.

5.4.4 Results and discussion

Fig. 5.6 shows concentration changes obtained from numerical analysis considering effect of age and analytical solution. From the figure, it can be shown that chloride concentration change obtained from numerical analysis was similar with that of analytical solution. The reference diffusion coefficients (28 days) were calculated from numerical analysis and were shown in Table 5.1 - 5.3 The results have indicated that the reference diffusion coefficients obtained from numerical analysis were 4 ~ 5 % larger than apparent diffusion coefficient obtained from short-term ponding test.

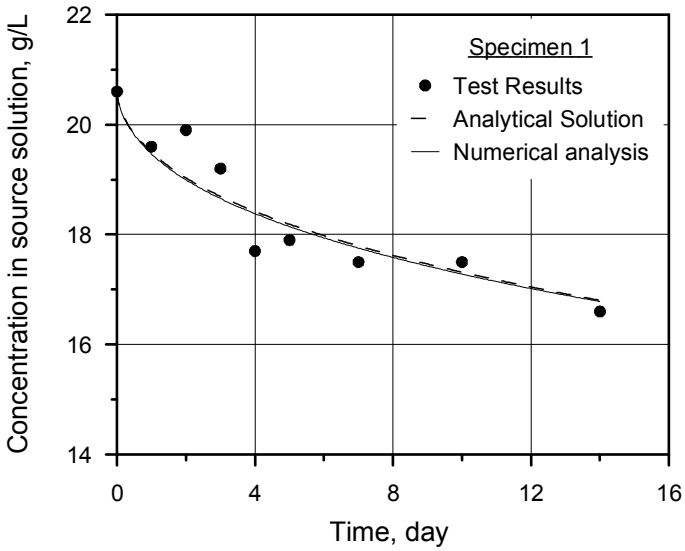

Figure 5.6 Concentration changes obtained from numerical analysis considering effect of age

Table 5.1 Diffusion coefficient of mortar(W/C=0.45) obtained from numerical analysis

	D_{ST}	D_{ref}
Specimen 1	7.0	7.4
Specimen 2	5.4	5.7
Specimen 3	7.8	8.2
Specimen 4	7.4	7.8
Specimen 5	7.3	7.7
Specimen 6	9.8	10.3
Specimen 7	9.6	10.1
Specimen 8	8.6	9.0
Specimen 9	8.9	9.3
Specimen 10	9.0	9.4
Specimen 11	8.7	9.2
Specimen 12	5.2	5.5
Average	7.9	8.3

Table 5.2 Diffusion coefficient of mortar(W/C=0.60) obtained from numerical analysis

	D_{ST}	D_{ref}
Specimen 1	11.3	11.9
Specimen 2	17.0	17.9
Specimen 3	11.9	12.5
Specimen 4	16.4	17.3
Specimen 5	13.3	14.0
Specimen 6	12.0	12.6
Specimen 7	19.5	20.8
Specimen 8	8.5	8.9
Specimen 9	12.0	12.6
Specimen 10	11.6	12.2
Specimen 11	9.6	10.1
Average	13.0	13.7

Table 5.3 Diffusion coefficient of NC obtained from numerical analysis

	D_{ST}	D_{ref}
Specimen 1	8.7	9.1
Specimen 2	5.3	5.6
Specimen 3	5.6	5.9
Specimen 4	6.2	6.6
Specimen 5	5.9	6.2
Specimen 6	5.6	5.9
Specimen 7	5.8	6.1
Specimen 8	6.3	6.7
Specimen 9	4.0	4.2
Specimen 10	7.2	7.6
Specimen 11	4.3	4.6
Average	5.9	6.2

The average diffusion coefficients were calculated to compare with apparent diffusion coefficient obtained from short-term ponding test. The arithmetic mean diffusion coefficients were calculated as average diffusion coefficient, and this diffusion coefficient was expressed in Fig. 5.7. Table 5.4 shows the average diffusion coefficient obtained from numerical analysis and apparent diffusion coefficient obtained from short-term ponding test and reference diffusion coefficient (28 days).

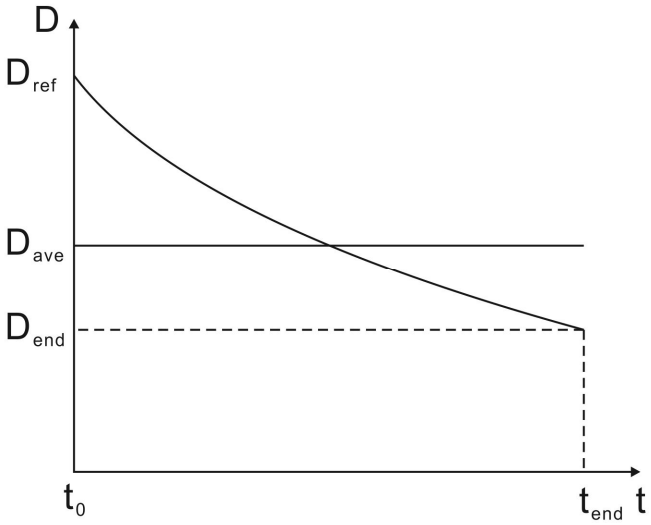

Figure 5.7 Calculation method of average diffusion coefficient with age

Table 5.4 Average diffusion coefficient obtained from numerical analysis

	Mortar W/C = 0.45	Mortar W/C = 0.60	NC
D_{ST}	7.9	13.0	5.9
$D_{ref,t}$	8.3	13.7	6.2
D_{ave}	8.0	13.1	6.0

From Table 5.4, it can be shown that the difference between average diffusion coefficients obtained from numerical analysis and those of the test was very small within 1 %. It can be shown that the effect of age on chloride diffusion coefficient can be neglected when only cement is used as binder.

Fig. 5.8 shows chloride concentration changes obtained from numerical analysis applying $D_{ref,t} = 10 \times 10^{-12}\ m^2/s$ in Eq. (5.19). The reference time was 28 days. From the figure, it can be shown that concentration change rate decreased with increase of m. This result indicated that substitution by the large amount of admixture lead to increase effect of age on diffusion coefficient. Table 5.5 and Fig. 5.9 show diffusion coefficient obtained from analytical solution incorporating concentration in Fig. 5.8. As anticipated, the more content of admixture increased, the more diffusion coefficient decreased. Diffusion coefficient of specimen containing only cement was calculated 3 % smaller than reference diffusion coefficient ($D_{ref} = 10 \times 10^{-12}\ m^2/s$). This result was similar with results expressed in Table 5.1-5.3. But, diffusion coefficients of specimen containing admixture were calculated 5 ~ 9 % smaller than reference diffusion coefficient. This result indicated that the diffusion coefficient have to be modified applying effect of age, if large amount of admixture is used as binder.

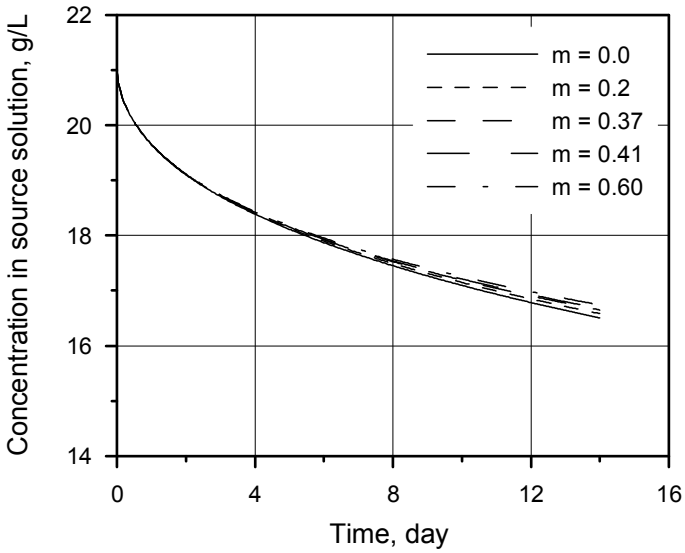

Figure 5.8 Concentration changes obtained from numerical analysis applying various m

Table 5.5 Diffusion coefficient obtained from analytical solution using concentration data by numerical analysis (Fig. 5.7)

binder	m	D_{ST} ($\times 10^{-12}$ m^2/s)
Cement	0.2	9.7
30 % SG	0.37	9.5
30 % FA	0.44	9.4
30 % SG + 30 % FA	0.60	9.1

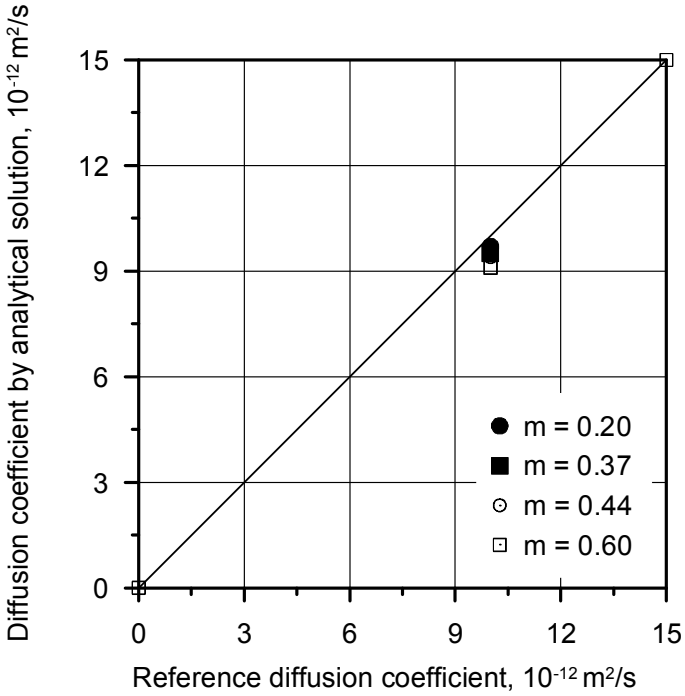

Figure 5.9 Diffusion coefficient obtained from analytical solution using concentration data by numerical analysis (Fig. 5.7)

5.5 Effect of concentration change in source solution

5.5.1 General

From the validation test performed in this study, it can be known that the diffusion coefficient increases with decrease of concentration in source solution. The diffusion coefficient increased 7 ~ 10 times when concentration in source solution decreased 10 times. Zhang had reported that the diffusion coefficient increases with concentration decrease in source solution from test results. In short-term ponding test, since diffusion coefficient is determined

using concentration change in source solution, the diffusion coefficient can be changed during test due to concentration change in source solution. The mathematical model of short-term ponding test doesn't consider this effect, so it is needed to verify that effect of concentration change on diffusion coefficient in short-term ponding test using numerical analysis.

5.5.2 Relationship between concentration and diffusion coefficient

Chatterji had suggested the diffusion coefficient model that is expressed similar with Kohlrausch's rule which is used to explain conductivity. Kohlrausch's rule is expressed by Eq. (5.24).

$$D = D_{ref,0}\left(1 - K\sqrt{c_{sol}}\right) \tag{5.24}$$

where, $D_{ref,0}$ is reference diffusion coefficient, K is experimental constant, c_{sol} is concentration in source solution. Tang had reported that it is difficult to apply Kohlrausch's rule to explain change of diffusion coefficient with concentration change since the experimental constant K is changed with concentration in source solution. Instead, Tang had proposed a new diffusion coefficient model that can predict change of steady-state migration coefficient with concentration change incorporating friction coefficient.

$$D_{ssm} = \theta \frac{2c_{molar} + c_0}{f\left(1 + \beta_v\right)c_{molar} + c_0} \tag{5.25}$$

where, c_{molar} is a molar concentration, c_0 is a solvent concentration and f is a friction coefficient. Eq. (5.25) was fit with the test results by Zhang fairly well. But, since the proposed model was developed to predict the migration coefficient change in steady-state migration test, it was difficult to apply the diffusion coefficient obtained from non-steady-state diffusion test. So, in this analysis, the equations obtained from regression analysis of validation test results and Zhang's results were used to predict change of diffusion coefficient with concentration change in source solution.

5.5.3 Regression analysis

Regression analysis equation obtained from Zhang's test results was shown in Fig. 5.10. The regression analysis equation in figure of power law fit with the Zhang's test results fairly well. So, the power law was adopted to calculate regression analysis equation of validation test results. The regression analysis equations were obtained as Eq. (5.26) and Eq. (5.27) from results of validation test. Fig. 5.11 shows the regression analysis equation.

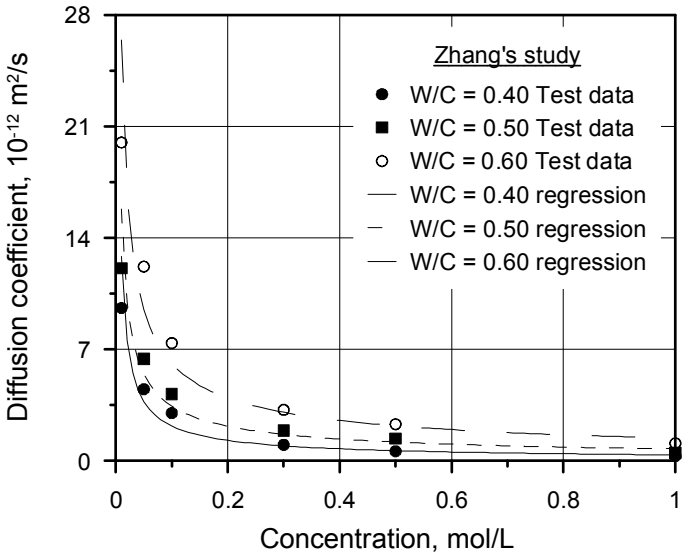

Figure 5.10 Regression analysis equation obtained from results of Zhang's study

a. W/C = 0.45

$$D_{con} = 144.59 \cdot c^{-0.955}, \ R^2 = 1 \tag{5.26}$$

b. W.C = 0.60

$$D_{con} = 246.40 \cdot c^{-0.966}, \ R^2 = 1 \tag{5.27}$$

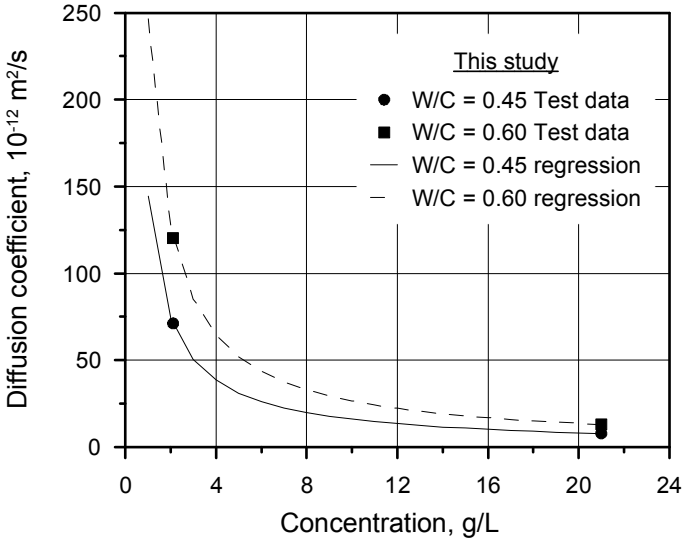

Figure 5.11 Regression analysis equation obtained from results of validation test for mortar specimens

5.5.4 Governing equation, initial and boundary conditions

The governing equation was expressed as Eq. (5.28). The regression analysis equation was incorporated as diffusion coefficient in the governing equation.

$$\frac{\partial c}{\partial t} = \frac{\partial c}{\partial t}\left(D_{con} \frac{\partial c}{\partial x} \right) \tag{5.28}$$

The initial conditions were expressed as Eq. (5.29) and (5.30).

$$c = c_{ini} \qquad in\ NaCl\ solution, \quad t = 0 \tag{5.29}$$

$$c = 0 \qquad in\ concrete, \qquad t = 0 \tag{5.30}$$

The boundary conditions were expressed as Eq. (5.31) and (5.32).

$$\left.\frac{\partial c}{\partial x}\right|_{x=0} = 0 \tag{5.31}$$

$$\left.\frac{\partial c}{\partial x}\right|_{x=end} = 0 \tag{5.32}$$

5.5.5 Results and discussions

Fig. 5.12 and 5.13 show concentration changes in source solution obtained from numerical analysis and analytical solution and test results of validation test. It can be shown that the concentration changes obtained from numerical analysis was similar with that of analytical solution.

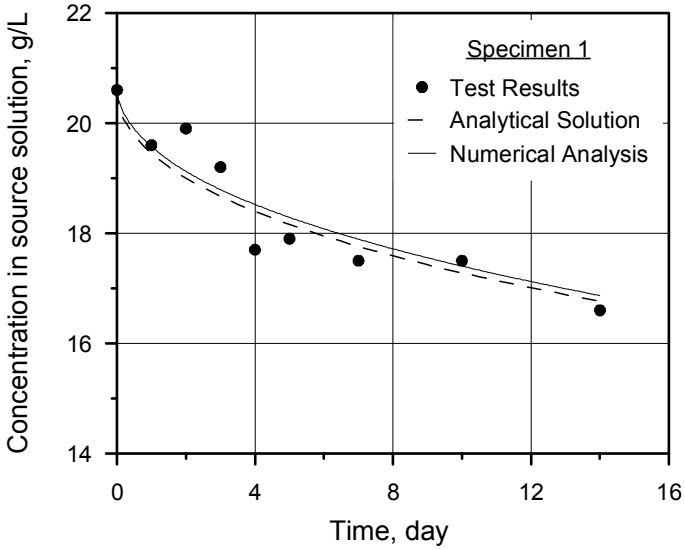

Figure 5.12 Concentration change in source solution obtained from numerical analysis for W/C = 0.45 mortar specimen 1

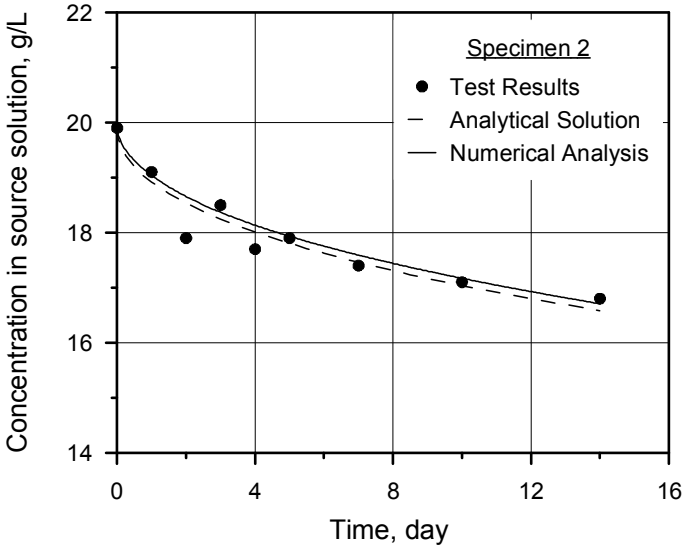

Figure 5.13 Concentration change in source solution obtained from numerical analysis for W/C = 0.45 mortar specimen 2

Table 5.6 and Table 5.7 show the results of numerical analysis. The diffusion coefficients were calculated using initial and final concentration of test. Average diffusion coefficient was calculated using concentration profiles in source solution obtained from numerical analysis. The arithmetic mean diffusion coefficient was calculated as average diffusion coefficient that was expressed in Fig. 5.14.

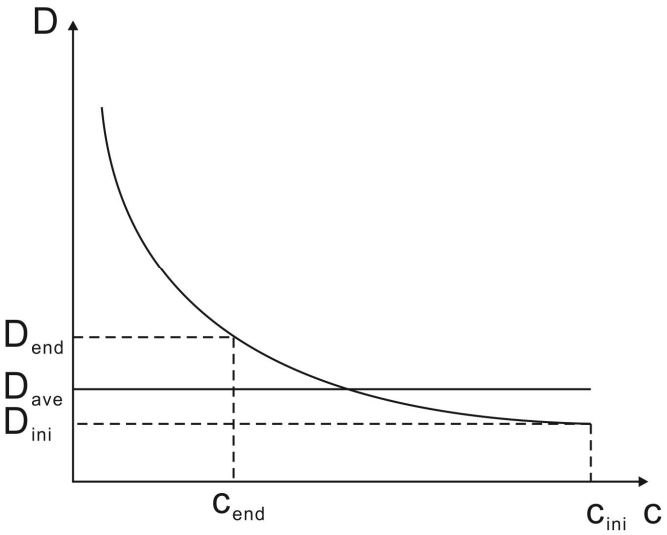

Figure 5.14 Calculation method of average diffusion coefficient with concentration

Table 5.6 Diffusion coefficient of mortar(W/C=0.45) obtained from numerical analysis

	D_{ST}	D_{con}		
Concentration	-	Initial	End	Average
Specimen 1	7.0	5.8	7.3	6.5
Specimen 2	5.4	4.3	5.3	4.8
Specimen 3	7.8	6.4	7.8	7.1
Specimen 4	7.4	6.0	7.5	6.7
Specimen 5	7.3	6.0	7.4	6.7
Specimen 6	9.8	8.1	10.1	9.1
Specimen 7	9.6	8.0	10.0	8.9
Specimen 8	8.6	7.1	8.9	7.9
Specimen 9	8.9	7.4	9.3	8.3
Specimen 10	9.0	7.3	9.1	8.2
Specimen 11	8.7	7.2	8.9	8.0
Specimen 12	5.2	4.2	5.3	4.7
Average	7.9	6.5	8.1	7.2

Table 5.7 Diffusion coefficient of mortar(W/C=0.60) obtained from numerical analysis

	D_{ST}	D_{con}		
Concentration	-	Initial	End	Average
Specimen 1	11.3	9.4	11.8	10.6
Specimen 2	17.0	14.2	18.2	16.1
Specimen 3	11.9	9.9	12.4	11.2
Specimen 4	16.4	13.7	17.6	15.5
Specimen 5	13.3	11.2	13.9	12.7
Specimen 6	12.0	10.0	12.6	11.3
Specimen 7	19.5	16.7	21.1	18.9
Specimen 8	8.5	7.0	8.6	7.9
Specimen 9	12.0	10.0	12.4	11.3
Specimen 10	11.6	9.7	12.1	11.0
Specimen 11	9.6	7.9	10.2	8.9
Average	13.0	10.9	13.7	12.3

From the results, it was shown that the diffusion coefficient at initial concentration was 15 % larger than that of short-term ponding test, but the average diffusion coefficient was only 5 % larger than that of short-term ponding test. This difference was very small in comparison with that the diffusion coefficient increased 7 – 10 times when concentration in source solution decreased 10 times. This result came from that diffusion coefficient

decreased according to power law as shown in Fig 5.10. So, the change of diffusion coefficient was small at the range of concentration change in short-term ponding test. Fig. 5.15 shows comparison between average diffusion coefficient obtained from numerical analysis and apparent diffusion coefficient obtained from short-term ponding test. The difference between two diffusion coefficients was shown as very small in the graph. From these results, it can be concluded that effect of concentration in source solution on diffusion coefficient can be neglected in range of short-term ponding test.

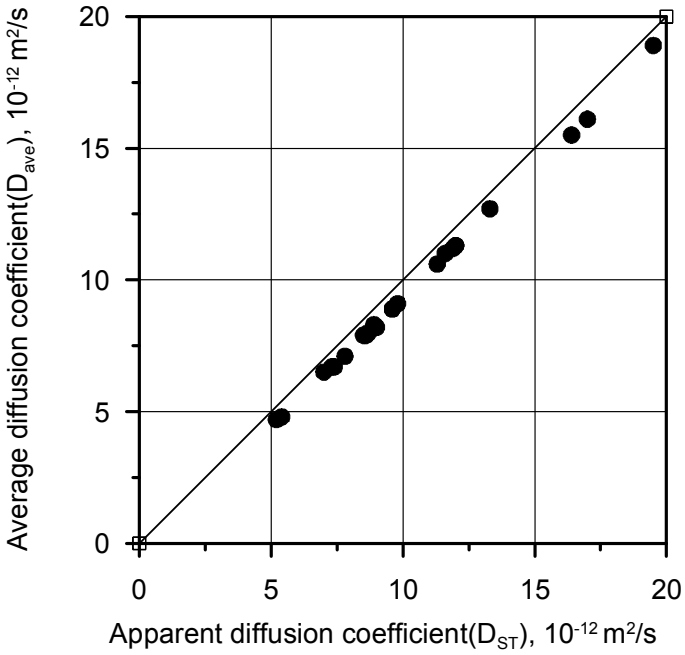

Figure 5.15 Comparison between average diffusion coefficient (D_{ave}) and apparent diffusion coefficient (D_{ST})

5.6 Verification of linear binding

5.6.1 General

In mathematical model developed in this thesis, the chloride binding was assumed to be linear to calculate analytical solution from governing equation. The assumption was supported by Tutti's research that the chloride binding was expressed similar with linear isotherm under 30 g/L chloride solution. But, in reality, the chloride binding has non-linear relationship with free concentration. So, the apparent diffusion coefficient obtained from validation test can be different from that of reality. The numerical analysis was performed to verify the assumption that chloride binding is linear isotherm. The inverse analysis was adopted to examine the binding isotherm of short-term ponding test using the measured concentration change in source solution of validation test.

5.6.2 Apparent diffusion coefficient

Apparent diffusion coefficient is a diffusion coefficient containing chloride binding effect and can be obtained non-state-state diffusion tests such as short-term ponding test. The apparent diffusion coefficient of short-term ponding test is expressed as Eq. (5.33).

$$D_{ST} = \frac{D_{ssd}}{\left(\theta + \frac{\partial c_b}{\partial c}\right)} \tag{5.33}$$

where, D_{ssd} is an effective diffusion coefficient, c_b is chloride binding. If chloride binding is linear with free concentration, the ratio $\partial c_b / \partial c$ between binding concentration and free concentration becomes a constant. But, if chloride binding is non-linear, the ratio $\partial c_b / \partial c$ between binding concentration and free concentration is changed with free concentration. So, it is important to know chloride binding isotherm to evaluate apparent diffusion coefficient.

5.6.3 Effective diffusion coefficient (D_{ssd})

Effective diffusion coefficient means a diffusion coefficient of Fick's first law and can be obtained from steady-state diffusion. Since chloride binding isn't contained in Fick's first law, the effective diffusion coefficient doesn't contain effect of chloride binding. Apparent diffusion coefficient can be expressed using effective diffusion coefficient and chloride binding isotherm as shown in Eq. (5.33). To obtain effective diffusion coefficient, steady-state diffusion test has to be performed, but some researchers have reported relationship between effective diffusion coefficient and apparent diffusion coefficient. Tang has suggested the relationship between the effective diffusion coefficient and apparent diffusion coefficient obtained from CTH test to calculate the effective diffusion coefficient. The relationship was expressed as Eq. (5.34).

$$D_{ssd} = \theta \cdot D_{nssm} \tag{5.34}$$

V. Baroghel-Bouny et al. has reported that the effective diffusion coefficient obtained from inverse analysis using chloride concentration profile of long-term immersion test showed similar results with effective diffusion coefficient obtained from Eq. (5.34). So, Eq. (5.34) was used to estimate effective diffusion coefficient in this study.

5.6.4 Inverse analysis

Inverse analysis is a kind of method that the experimental parameter is estimated by numerical analysis using test results. In this study, effective diffusion coefficient and the binding parameters of Freundlich isotherm were determined by inverse analysis. The governing equation was expressed as Eq. (5.35).

$$\frac{\partial c}{\partial t} = \frac{D_{ssd}}{\left(\theta + \frac{\partial c_b}{\partial c}\right)} \cdot \frac{\partial^2 c}{\partial x^2} \tag{5.35}$$

The binding isotherm was expressed as Eq. (5.36).

$$c_b = \alpha_{FD} \cdot c^{\beta_{FD}} \tag{5.36}$$

In governing equation, the apparent diffusion coefficient are consisted of three variables, D_{ssd}, α_{FD} and β_{FD}. Since there are no relationships between three variables, Monte Carlo Simulation was adopted to select

arbitrary value from proposed range of each variable. Trial-error method was adopted to determine optimum value of variables containing minimum error. The range of effective diffusion coefficient was determined using Eq. (5.34). The ranges of binding parameters α_{FD}, β_{FD} in Freundlich isotherm were determined from the research suggested by V. Baroghel-Bouny et al and Tang.

5.6.5 Results and discussions

Table 5.8 - 5.10 show results of invers analysis using validation test data.

Table 5.8 Effective diffusion coefficient and binding coefficients of Freundlich isotherm for mortar(W/C = 0.45) by numerical analysis

	D_{ssd}	α_{FD}	β_{FD}
Specimen 1	1.05	11.9	0.953
Specimen 2	3.63	1.62	0.899
Specimen 3	3.69	3.15	0.842
Specimen 4	3.89	2.28	0.905
Specimen 5	3.73	2.86	0.849
Specimen 6	3.9	3.98	0.807
Specimen 7	3.64	4.37	0.805
Specimen 8	3.74	4.06	0.747
Specimen 9	1.35	11.1	0.946
Specimen 10	3.96	5.23	0.621
Specimen 11	3.89	3.73	0.734
Specimen 12	2.62	3.7	0.724
Average	3.26	4.83	0.82

Table 5.9 Effective diffusion coefficient and binding coefficients of Freundlich isotherm for mortar(W/C = 0.60) by numerical analysis

	D_{ssd}	α_{FD}	β_{FD}
Specimen 1	5.04	2.23	0.998
Specimen 2	5.78	5.12	0.767
Specimen 3	5.52	6.60	0.502
Specimen 4	5.88	4.68	0.782
Specimen 5	5.95	2.98	0.876
Specimen 6	5.07	7.20	0.510
Specimen 7	5.36	4.18	0.942
Specimen 8	3.75	4.19	0.750
Specimen 9	5.85	4.42	0.667
Specimen 10	5.00	4.47	0.734
Specimen 11	4.14	6.14	0.583
Average	5.21	4.75	0.74

Table 5.10 Effective diffusion coefficient and binding coefficients of Freundlich isotherm for NC by numerical analysis

	D_{ssd}	α_{FD}	B_{FD}
Specimen 1	1.09	1.81	0.95
Specimen 2	2.88	1.81	0.99
Specimen 3	2.86	1.88	0.99
Specimen 4	1.92	5.43	0.83
Specimen 5	2.80	2.06	1.00
Specimen 6	2.91	5.23	0.55
Specimen 7	2.89	4.01	0.73
Specimen 8	2.94	3.91	0.75
Specimen 9	2.67	6.73	0.36
Specimen 10	2.73	2.81	0.98
Specimen 11	2.83	1.65	0.94
Average	2.59	4.58	0.82

In the Tables, β_{FD} means an exponent parameter of Freundlich isotherm. As β_{FD} approaches 1, the graph shows similar figure with linear isotherm. As shown in the tables, average β_{FD} of W/C = 0.45 mortar and NC was calculated as 0.82 and average β_{FD} of W/C = 0.60 mortar was calculated as 0.74. To verify linearity of binding isotherm, linear regression analysis was performed using data of Freundlich isotherm obtained from inverse analysis. Fig. 5.15 shows results of linear regression analysis of

Freundlich isotherm incorporating exponent coefficient obtained from inverse analysis. In this linear regression equation, y-intercept was fixed to zero. It can be shown that linear regression equations were well fitted with Freundlich isotherm at β_{FD} = 0.82 and 0.74. Eq. (5.37) and Eq. (5.38) show regression equation and R^2 of each specimen.

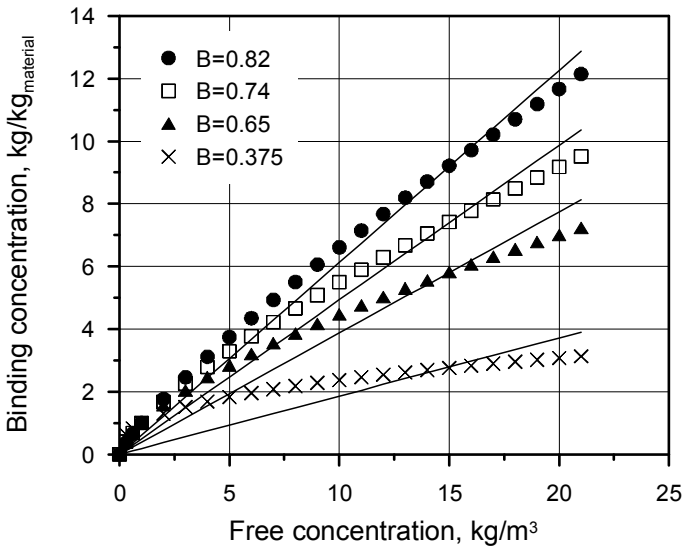

Figure 5.16 Linear regression analysis using data of Freundlich isotherm obtained from inverse anaylsis

$$c_b = 0.6125 \cdot \alpha \cdot c \quad R^2 = 0.985 \tag{5.37}$$

$$c_b = 0.4932 \cdot \alpha \cdot c \quad R^2 = 0.964 \tag{5.38}$$

From results of regression analysis for Freundlich isotherm, it can be concluded that chloride binding isotherm in short-term ponding test incorporating 21 g/L NaCl solution can be assumed to be linear. Fig. 5.17-

5.19 show concentration changes in source solution obtained from numerical analysis, analytical solution and test results of short-term ponding test. The figures express that the concentration curve obtained from numerical analysis and concentration curve obtained from analysis solution show similar results.

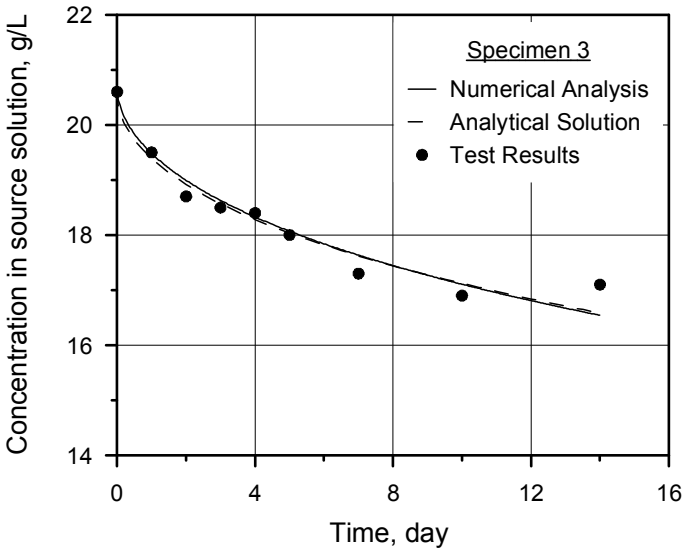

Figure 5.17 Concentration changes in source solution obtained from numerical analysis for W/C = 0.45 mortar

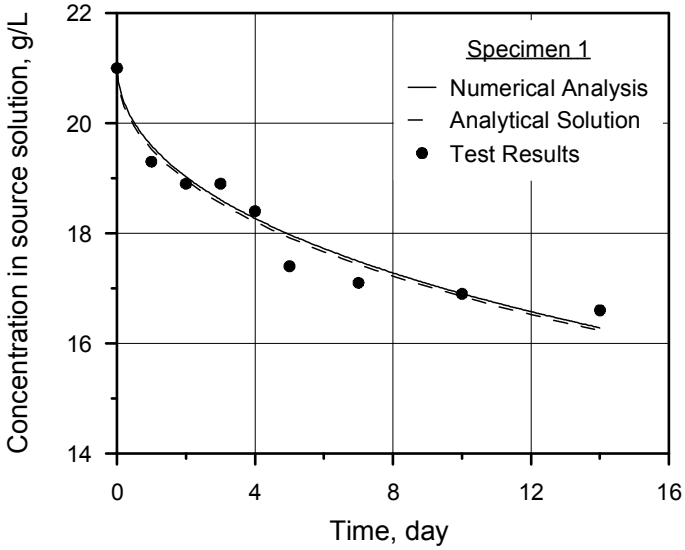

Figure 5.18 Concentration changes in source solution obtained from numerical analysis for W/C = 0.60 mortar

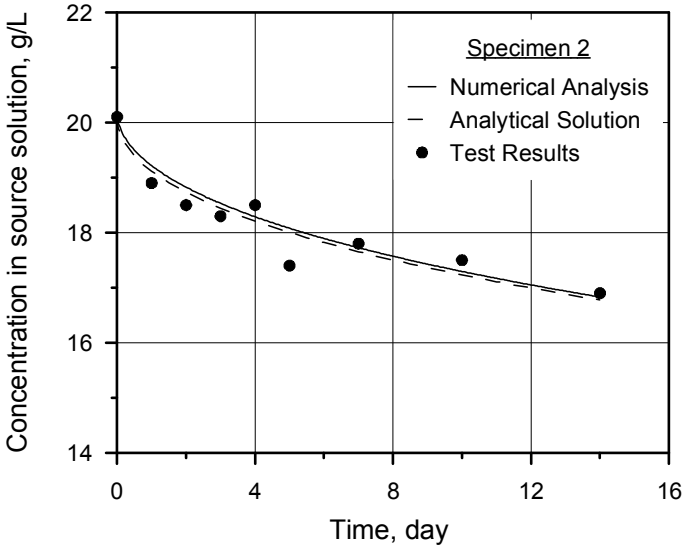

Figure 5.19 Concentration changes in source solution obtained from numerical analysis for NC

6. Conclusions and Recommendations

6.1 Conclusions

In this study, a short-term ponding test and mathematical model were developed to evaluate the chloride ion diffusion coefficient of concrete structures exposed to chloride environments. It was found that the short-term ponding test overcomes a weak point of the long-term immersion test with regard to test period, and enables simulation of the penetration mechanism in real concrete structures. This simulation is distorted in the electrical migration-diffusion test. In the mathematical model, Fick's 2nd law is incorporated as a governing equation, and the chloride ion concentration change in the source solution is employed as a boundary condition, to obtain an analytical solution. Since the diffusion coefficient obtained from the short-term ponding test has the same meaning as that of the long-term immersion test, it is expected that the diffusion coefficient can be used in design methods based on the long-term immersion test.

A series of tests was performed to validate the mathematical model and test method proposed in this study. The short-term ponding test showed that the specimen with a larger W/C ratio showed a greater diffusion coefficient, and that a decrease in concentration of the source solution led to an increase in the diffusion coefficient. The short-term ponding test also showed that high strength concrete showed a lower diffusion coefficient. It was also suggested that in using the short-term ponding test, at least seven days and more than

five measurements are required to determine a diffusion coefficient. In addition, it was suggested that the specimen number by target uncertainty be employed, using the mean diffusion coefficient and standard deviation. From the analysis, it can be concluded that 10 ~ 20 % uncertainty is shown in the short-term ponding test, when ten specimens are used to determine the diffusion coefficient.

To compare our results with the existing standardized test methods, the long-term immersion test (NT Build 443) and CTH test (NT Build 492) were simultaneously performed. Both the long-term immersion test and short-term ponding test showed similar results, but the CTH test results significantly differed. This result came from a different chloride mechanism, and the difference in transport mechanism between ion diffusion and migration. This result indicated that the short-term ponding test is a time-efficient and realistic method that reflects the actual marine environment.

Numerical analysis was performed to verify assumptions in the mathematical model of the short-term ponding test. Pdepe function, a Matlab function, was used to calculate the chloride concentration in the source solution by time, solving the governing equation of the mathematical model. The effects of concrete age and concentration in the source solution on the diffusion coefficient in the short-term ponding test were also verified. The reference diffusion coefficients (28 days) for concrete age were calculated to be 5~10 % larger than the apparent diffusion coefficients, and the average diffusion coefficient during short-term ponding tests was calculated to be 1 % larger than the apparent diffusion coefficients. These results indicated that the effect of concrete age could be neglected in the short-term ponding test.

Diffusion coefficients for the initial concentration in the source solution were calculated to be 15 % smaller than the apparent diffusion coefficient, and the average diffusion coefficients during the short-term ponding test were calculated to be 10 % smaller than the apparent diffusion coefficients. These results indicated that the change of diffusion coefficient by concentration change in the source solution during testing should be considered. So, further experimental studies are needed to modify the apparent diffusion coefficient, considering the concentration in the source solution.

The assumption that chloride binding is linear with free chloride concentration was verified. Inverse analysis was adopted, to estimate the effective diffusion coefficient and Freundlich binding isotherm coefficients from concentration change in the source solution. The exponent coefficients of the Freundlich isotherm for W/C=0.45 mortar and NC were calculated as 0.82. The exponent coefficients of the Freundlich isotherm for W/C=0.60 mortar was calculated as 0.74. It can be shown by linear regression analysis that the chloride binding isotherm in the short-term ponding test can be assumed to be linear. This result indicated that the linear binding assumption of the mathematical model is reasonable, in the case of incorporating 21 g/L chloride solution.

6.2 Recommendations

The following engineering contributions are presented, as well as recommendations for future studies, to strengthen the applicability of the short-term ponding test.

The short-term ponding test developed in this study can be applied to the durability design of concrete structures exposed to chloride environments. The diffusion coefficient obtained from the short-term ponding test can be adopted in durability design methods, such as ACI Life 365 and Duracrete, to predict the chloride concentration in concrete by time. From the prediction of chloride penetration rate in concrete, the concrete cover depth and kinds of binder of concrete can be determined for a concrete structure. Moreover, the short-term ponding test could be adopted in other chloride environments, such as concrete exposed to $CaCl_2$ solution in winter. When $CaCl_2$ is used to prevent roadways from being frozen, chloride ion penetrates into concrete from $CaCl_2$ solution. So, the chloride penetration into concrete needs to be predicted in the case of $CaCl_2$ is used on roadways. The diffusion coefficient for $CaCl_2$ solution can be determined by using only $CaCl_2$ solution as the source solution.

Also, the mathematical theory in the short-term ponding test can be adopted in radioactivity penetration into concrete in disposal sites of radioactivity waste, or the mass transfer of volatile organic compounds through geomembranes. Because the basic theory of chloride penetration in concrete is similar to those of these penetration mechanisms, the mathematical model of the short-term ponding test can be used to evaluate these penetration

rates to determine the depth of disposal sites of radioactivity waste, or the depth of geomembranes to prevent the penetration of volatile organic compounds in a waste disposal site.

In this study, validation tests for verification of the short-term ponding test were performed. So, it can be shown that the diffusion coefficient can be determined by the short-term ponding test. But, additional tests and statistical analyses need to be performed, to standardize for various kinds of specimen. From additional tests, the resolution by kinds of specimen, minimum number of specimen to determine diffusion coefficient, test duration needed to estimate the diffusion coefficient, and new measurement method of the source solution have to be presented, to standardize the short-term ponding test.

To apply different chloride environments with seawater, such as $CaCl_2$ solution, research is needed on the effect of cation in penetration mechanisms, such as the reaction between cement hydrate in concrete, and cation in source solution. Some researchers have presented that chloride binding is changed with the cation of chloride solution, and that pore structures are changed by the reaction between cations. So, the chloride binding isotherms of other cations other than Na^+ have to be verified in the short-term ponding test.

Non-equilibrium chloride binding needs to be verified in the short-term ponding test. In former researches, chloride binding with cement hydrate takes 7 ~ 10 days, due to the limitation of mass transfer between the pore solution and cement hydrate. Since it was shown that the diffusion coefficient could be determined in seven days by the short-term ponding test, non-equilibrium chloride binding has to be verified by numerical analysis.

References

AASHTO T 259, (1980). Standard Method of Test for Resistance of Concrete to Chloride Ion Penetration, Standard Specification for Transport Materials and Methods of sampling and Testing, American Association of State Highway Transportation Officers

AASHTO T 277, (2005). Standard Method of Test for Electrical Indicate of Concrete's Ability to Resist Chloride Ion Penetration, Standard Specification for Transport Materials and Methods Sampling and Testing, American Association of State Highway Transportation Officers.

Akita, H. and Fujiwara, T. (1995). "Water and salt movement within mortar partially submerged in salty water," Proceedings of the international Conference on Concrete under Severe Conditions, August, Sapporo, Japan, E & FN Spon, London

Andrade, C. and Page, C. L. (1986). "Pore solution chemistry and corrosion in hydrated cement systems containing chloride salts: a study of cation specific effects," British Corrosion Journal, Vol. 21, pp. 49-53

Andrade, C. (1993). "Calculation of chloride diffusion coefficient in concrete from ionic migration measurements," Cement and Concrete Research, Vol. 237 pp.24-42

Arsenault, J., Bigas, J. P., Ollivier, J. P. (1995) Determination of chloride diffusion coefficient using two different steady state methods: Influence of concentration gradient, Proc. RILEM Intl. Workshop on Chloride Penetration into Concr., St. Rémy-lès-Chevreuse, French, pp. 150-160

Arya, C., Buenfeld, N. R., Newman, J. B. (1987). "Assessment of simple methods of determining the free chloride ion content of cement paste," Cement and Concrete Research, Vol. 17, pp. 907-918

Arya, C., and Newman, J. B. (1990). "An assessment of four methods of determining the free chloride content of concrete," Materials and Structures, Vol. 23, pp. 319-330

ASTM C 1202, (2005). Standard Test Method for Electrical Indication of Concrete's Ability to Resist Chloride Ion Penetration, Annual Book of ASTM Standards, American Society for Testing and Materials.

Baroghel-Bouny, V., Bellin, P., Maultzsch, M., Henry, D. (2007). "AgNO3 spray test: advantages, weaknesses, and various applications to quantify chloride ingress into concrete. Part 1: non-steady-state diffusion tests in laboratory and exposure to natural conditions," Materials and Structures Vol. 40, pp. 759-781

Baroghel-Bouny, V., Bellin, P., Maultzsch, M., Henry, D. (2007). “AgNO3 spray test: advantages, weaknesses, and various applications to quantify chloride ingress into concrete. Part 2: Non-steady-state migration test and chloride diffusion coefficients,” Materials and Structures Vol. 40, pp. 783-799

Baroghel-Bouny, V., Wang, X., Thiery, M., Saillio, M., Barberon, F. (2012). “Prediction of chloride binding isotherms of cementitious materials by analytical model or numerical inverse analysis,” Cement and Concrete Research, Vol. 42, pp. 1207-1224

Baron, J. and Ollivier, J. P. (1992). La durabilité des bétons: Presses de l’École Nationale des Ponts et Chaussées

Bentz, E. C. and Thomas, M. D. A. (2008). Life-365 Service Life Prediction Model and Computer Program for Predicting the Service Life and Life-Cycle Costs of Reinforced Concrete Exposed to Chlorides, January 8

Bigas, J. P. (1994). Diffusion of chloride ions through mortars, Doctoral thesis, INSA-Genie Civil, LMDC, INSA de Toulous, France (in French)

Blunk, G., Gunkel, P., Smolczyk, H. G. (1986). “On the distribution of chloride between the hardening cement paste and its pore solution,” Proceedings of the 8th International Congress on the Chemistry of Cement, Brazil, Vol. 5 pp. 85-89

Bobby, A., Bentz, E., Thomas, M. D. A., Hooton, R. D. (1999). “An overview and sensitivity study of a multimechanistic chloride transport model,” Cement and Concrete Research, Vol. 29, pp. 827-837

Buenfeld, N. R. and Newman, J. B. (1986). “The development and stability of surface layers on concrete exposed to sea-water,” Cement and Concrete Research Vol. 16 pp. 721–732

Byfors, K. (1990). “Chloride-initiated Reinforcement Corrosion – Chloride binding”, Swedish Cement and Concrete Research Institute (CBI), Stockholm, CBI Report 1:90

Castellote, M., Andrade, C., Alonso, C. (1999). “Chloride-binding isotherms in concrete submitted to non-steady-state migration experiments,” Cement and Concrete Research Vol. 29 pp. 1799–1806

Castellote, M., Andrade, C., Alonso, C. (2001). “Measurement of the steady and non-steady-state chloride diffusion coefficients in a migration test by means of monitoring the conductivity in the anolyte chamber. Comparison with natural diffusion test,” Cement and Concrete Research Vol. 31, pp. 1411–1420

Chatterji, S. (1994). “Transportation of ions through cement based materials Part 1: Fundamental equations and basic measurement techniques,” Cement and Concrete Research, Vol. 24, pp. 907–912

Christensen, B. J., Coverdale, R. T., Olson, R. A., Ford, S. J., Garboczi, E. J., Jennings, H. M., Mason, T. O. (1994). “Impedance spectroscopy of hydrating cement-based materials: measurement, interpretation, and application,” Journal of the American Ceramic Society, Vol. 77 pp. 2789-2804

Delarave, A., Pigeon, J. M., Ollivier, J. P., Samson, E. (1995). “Diffusion of chloride ions in high performance mortar,” submitted to the ACI Fall Convention, Montreal

DuraCrete, (1998). Modeling of Degradation, EU-Project (Brite EuRam III) N0. BE95-1347, Probabilistic Performance based Durability Design of Concrete Structures, Report, Vol. 4-5

Eglinton, M. (1998). Resistance of concrete to destructive agencies. In: Hewlett P, Editor, Lea’s chemistry of cement and concrete, London: Arnold, pp. 299–340.

Juel, I. (2002) Mineralogical and thermodynamic processes by sulfate and seawater attach of Danish concrete, University of Copenhagen

Kim, K. H. (2003) Service life prediction of concrete structures subjected to chloride penetration using stochastic finite element method, Seoul National University

Mehta, P. K. (1990). Concrete in the marine environment (Modern Concrete Technology, 1st ed., Boca Raton: CRC Press

Mangat, P. S. and Molloy, B. T. (1995), “Chloride binding in concrete containing PFA, gbs or silica fume under seawater exposure,” Magazine of Concrete Research, Vol. 47, pp, 129-141

Mather, B. (1964). Effects of sea water on concrete. Highway Research Record: Highway Research Board, pp. 33-42

MacDonald, K. A. and Northwood, D. O. (1995). “Experimental measurements of chloride ion diffusion rates using a two-compartment diffusion cell: Effects of material and test variables,” Cement and Concrete Research, Vol. 25, pp. 1407–1416

NT Build 355, (1997). Concrete, Mortar and Cement Based Repair Materials: Chloride Diffusion Coefficient From Migration Cell Experiments, Nordtest, Finland.

NT Build 443, (1995). Concrete, Hardened: Accelerated Chloride Penetration, Nordtest, Finland.

NT Build 492, (1999). Concrete, Mortar and Cement-Based Repair Materials: Chloride Migration Coefficient from Non-Steady-State Migration Experiments, Nordtest, Finland.

Page, C. L., Short, N. R., Tarras, A. E. (1981). “Diffusion of chloride ions in hardened cement, pastes,” Cement and Concrete Research, Vol. 11, pp.395-406

Pereira, C. J. and Hegedus, L. L. (1984). “Diffusion and reaction of chloride ions in porous concrete,” Proceedings of the 8th International Symposium on Chemical Reaction Engineering, Edinburg, Scotland, Publication Series No. 87 pp. 427-438

Poursaee, A., Laurent, A., Hansson, C. M. (2010). “Corrosion of steel bars in OPC mortar exposed to NaCl, $MgCl_2$ and $CaCl_2$: Macro- and micro-cell corrosion perspective,” Cement and Concrete Research, Vol. 40, pp. 426-430

Ramachandran, V. S., Seeley, R. C., Polomark, G. M. (1984). “Free and combined chloride in hydrating cement and cement components,” Materials and Structures, Vol. 17, pp. 285-289

Richartz, W. (1969). “The combining of chloride in the hardening of cement,” Zement-Kalk-Gips, Vol. 22, pp. 447-456

Samson, E., Lemaire, G., Marchand, J., Beaudion, J. J. (1999). Modeling chemical activity effects in strong ionic solutions. Computational Materials Science Vol. 15 pp. 285-294

Sandberg, P. and Larsson, J. (1993). “Chloride binding in cement pastes in equilibrium with synthetic pore solutions as a function of [Cl] and [OH],” in “chloride penetration in concrete structures – Nordic Miniseminar” ed. By L. O. Nilsson, Division of Building Materials, Chalmers University of Technology, Publication P-93:1, pp. 98-107

Santhanam, M. (2011). Magnesium attack in marine environments. RILEM TC211-PAE concrete durability: aspects of degradation in aggressive aqueous environments, pp. 14-20

Scrivener, K. L. and Young, J. G. (1997). Mechanisms of chemical degradation of cement-based systems, 1st ed., New York: E & FN Spon

Seo, B. R., Moon, S., Nam, K., Kim, J. Y. (2003). Estimation of mass transfer parameters of volatile organic compounds through the geomembrane using an analytical solution. In: 9th International waste management and landfill symposium, Sardinia, Italy, pp. 479-480

Sibbick, T., Fenn, D., Crammond, N. (2003). “The occurrence of thaumasite as a product of seawater attack,” Cement and Concrete Composite, Vol. 25, pp. 1059–66

Spiesz, P., Ballari, M. M., Brouwers, H. J. H. (2012). RCM: A new model accounting for the non-linear chloride binding isotherm and the non-equilibrium conditions between the free- and bound- chloride concentrations. Construction and Building Materials, Vol. 27, pp.293-304

Spiesz, P. (2012). “Influence of the applied voltage on the Rapid Chloride Migration (RCM) test,” Cement and Concrete Research, Vol. 42, pp. 1072-1082

Stanish, K. D. (2002). The migration of chloride ions in concrete. PhD thesis, University of Toronto, Canada

Stanish, K. D., Hooton, R. D., Thomas, M. D. A. (1997) Testing the Chloride Penetration Resistance of Concrete: A Literature Review, University of Toronto, Canada

Stanish, K. and Thomas, M. (2003). “The use of bulk diffusion tests to establish time-dependent concrete chloride diffusion coefficients,” Cement and Concrete Research, Vol. 33, pp. 55-62

Streicher, P. E. and Alexander, M. G. (1995). “A chloride conduction test for concrete,” Cement and Concrete Research Vol. 25 pp.1284-1294

Tang, L. and Nilsson, L.-O. (1992). “Rapid estimation of the chloride diffusivity in concrete by applying an electrical field,” ACI Material Journal, Vol. 89, pp. 49-53

Tang, L. (1996). Chloride Transport in Concrete – Measurement and Prediction, Division of Building Materials, Doctoral thesis, Publication P-96:6, Dept. of Building Materials, Chalmers University of Technology, Goteborg, Sweden.

Tang, L. (1996). “Electrically accelerated methods for determining chloride diffusivity in concrete – current development,” Magazine of Concrete Research, Vol. 48, pp. 173-179

Tang, L. (1999). “Concentration dependence of diffusion and migration of chloride ions Part 1. Theoretical considerations,” Cement and Concrete Research, Vol. 29, pp. 1463-1468

Tang, L. (1999). “Concentration dependence of diffusion and migration of chloride ions Part 2. Experimental evaluations,” Cement and Concrete Research, Vol. 29, pp. 1469-1474

Tang, L. and Sorensen, H. E. (2001). “Precision of the Nordic test methods for measuring the chloride diffusion/migration coefficients of concrete,” Materials and Structures, Vol. 34, pp. 479-485

Theissing, E. M., Hest-Wardenier, P. V., Wind, G. D. (1978). “The combining of sodium chloride and calcium chloride by a number of different hardened cement pastes,” Cement and Concrete Research, Vol. 8 pp. 683-692

Tritthart, J. (1989). “Chloride binding in cement: I. Investigations to determine the composition of porewater in hardened cement,” Cement and Concrete Resarch, Vol. 19, pp. 586-594

Tritthart, J. (1989), “Chloride binding in cement: II. The influence of the hydroxide concentration in the pore solution of hardened cement paste on chloride binding,” Cement and Concrete Research, Vol. 19, pp. 683-691

Tuutti, K. (1982). “Corrosion of steel in concrete,” Swedich Cement and Concrete Research Institute (CBI), Stockholm, Report Fo 4.82

Xu, A. (1990). “The structure and some and some physical properties of cement mortar with fly ash,” Licentiate thesis, Dept. of Building Materials, Chalmers University of Technology, Goteborg, Sweden, Publication 90:9

Weerdt, K. D., Justnes, H., Geiker, M. R. (2014). “Changes in the phase assemblage of concrete exposed to sea water,” Cement & Concrete Composites, Vol. 47, pp. 53-63

Yuan, Q. (2009). Fundamental studies on test methods for the transport of chloride ions in cementitious materials. PhD thesis, University of Ghent, Belgium

Zhang, T. (1997) Chloride diffusivity in concrete and its measurement from steady state migration testing, Doctoral thesis, 1997:132, Trondheim University of Sci. & Techn., Norway

Zhang, T. and Gjørv, O. E. (2005). "Effect of chloride source concentration on chloride diffusivity in concrete," ACI Material Journal, Vol. 102, pp. 295-298

국문초록

단기 침지 실험(Short-Term Ponding Test)를 이용한 시멘트 계 재료 내부로의 염소이온 침투 평가

박병선

최근 해양환경에서는 많은 콘크리트 구조물이 건설되고 있다. 이러한 구조물에서는 확산 등에 의해 해수로부터 염소이온이 침투가 발생하는데, 콘크리트 내부로 침투한 염소이온은 철근의 부식을 야기한다. 다라서 목표 수명 동안 콘크리트 구조물의 내구성능을 확보하기 위해서는 염소이온의 침투 속도를 예측할 수 있어야 한다. 염소이온 확산계수는 염소이온의 침투 속도를 평가하는 중요한 인자로, 콘크리트의 염소이온 확산계수를 산정하기 위한 다양한 실험 방법이 개발되어 왔다. 하지만 대부분의 실험 방법은 너무 오랜 시간이 소요되거나, 실제 구조물에서 발생하는 염소이온의 침투 메커니즘을 제대로 반영하지 못한다는 문제점이 존재한다. 따라서 본 논문에서는 이러한 문제점을 해결하면서 염소이온 확산계수를 산정할 수 있는 새로운 실험 방법을 제안하였다 개발한 실험 방법은 외부 용액의 농도 변화를 이용하여 확산계수를 산정하는 실험 방법으로 short-term ponding test로 명명할 수 있다. 개발한 실험 방법과 수학적 모델을 검증하기 위한 실험을

수행하여 개발한 실험 방법을 통하여 콘크리트의 확산계수를 산정할 수 있는 것을 확인할 수 있었다. 또한 개발한 실험 방법을 통해 얻은 확산계수를 기존에 사용되고 있는 장기 침지 시험, CTH 시험에 의한 확산계수와 비교 분석하였다. 개발한 실험 방법에 의한 확산계수는 장기 침지 시험에 의한 확산계수와 유사한 결과를 보였으나, CTH 시험에 의한 확산계수와는 다른 결과를 보였다. 개발한 실험 방법의 수학적 모델에서 가정한 사항을 검증하기 위해 수치해석을 수행하였다. 수치해석에는 Matlab 내장함수의 하나인 Pdepe 함수를 이용하였으며, 콘크리트의 재령에 의한 확산계수 변화, 외부 용액의 농도 변화에 의한 확산계수 변화를 알아보았다. 해설 결과 short-term ponding test를 수행하는 동안 발생하는 재령 및 외부 용액의 농도 변화는 확산계수에 큰 영향을 미치지 않는 것을 확인할 수 있었다. 또한 역해석을 통해 수학적 모델에서 염소이온의 구속 모델을 선형 구속 모델으로 가정한 것이 타당하다는 것을 확인할 수 있었다.

주요어: 염소이온, 확산계수, 내구성 설계, 수치해석, short-term ponding test

학번: 2008-21030